IN-44585

238P.

NASA Contractor Report 179551

The Mathematical Modeling of Rapid Solidification Processing

Ernesto Gutierrez-Miravete

Massachusetts Institute of Technology
Cambridge, Massachusetts

November 1986

NASA

National Aeronautics and
Space Administration

TABLE OF CONTENTS

NOTE: The figures have been numbered according to the section

in which they appear. However, when mentioned in their sections,

they are described by the last digit only. The same convention

has been followed regarding tables, plates and equations.

                              iii

LIST OF SYMBOLS

Variable	Meaning	Place
a	atomic diameter	Eqn(2.2.2)
A	surface area of sample	Eqn(3.2.1)
A_s	dimensionless variable in stability equation	Eqn(2.6.4e)
$\underline{A}$	square matrix in the discrete formulation of Stefan problem	Eqn(3A.2.15)
B	coefficient for cooling rate (ideal cooling)	Eqn(3.3.1)
B'	coefficient for freezing rate (ideal cooling)	Eqn(3.3.2)
B_1	coefficient for dendrite/cell spacings	Eqn(2A.1.1)
B_3	coefficient for interlamellar spacings in eutectics	Eqn(2A.1.3)
C	concentration of solute (binary system)	Eqn(3A.1.15)
C_{eff}	effective specific heat (alloys)	Eqn(3A.2.9)
C_o	concentration fluctuation amplitude	Eqn(2.6.2)
C_p	specific heat	Eqn(2.5.1)
$\overline{C}_p$	average specific heat of solid and liquid	Eqn(2.2.1)
C_s , C_l	concentration in solid and liquid phases	Eqn(2.5.3,4)
C_s^*	concentration in the solid side of solidification interface	Eqn(2.5.3)

iv

Variable	Meaning	Place
C_∞	concentration in bulk liquid	Eqn(2.5.$\underline{3}$)
d	particle diameter (sample size)	Eqn(2.2.$\underline{2}$)
D	diffusion coefficient	Eqn(3A.1.$\underline{15}$)
D_1	diffusion coefficient in liquid	Eqn(2.2.$\underline{2}$)
D_{eff}	effective rate of deformation	Eqn(3A.1.$\underline{10b}$)
D_{ij} , $\underline{D}$	rate of deformation tensor	Eqn(3A.1.$\underline{18}$)
$D(\ )/Dt$	substantial (material) derivative $= \partial(\ )/\partial t + \nabla(\ )\cdot \underline{v}$	Eqn(3A.1.$\underline{1}$)
E	enthalpy	Eqn(2.4.$\underline{3a}$)
E_f	latent heat of fusion (volume basis)	Eqn(3.3.1.$\underline{4}$)
$\underline{E}^n$	vector of discrete enthalpy values at the nth time step	Eqn(3A.2.$\underline{15}$)
f	function relating enthalpy and temperature	Eqn(3A.2.$\underline{12}$)
F	function giving the location of the solidification interface	Eqn(2.6.$\underline{3}$)
f_s	fraction solidified	Fig(2.4.$\underline{1}$)
F_o	interface shape fluctuation amplitude	Eqn(2.6.$\underline{3}$)
$\underline{f}$	vector of external forces	Eqn(3A.1.$\underline{4}$)
g	function for boundary conditions in mass transfer	Eqn(3A.1.$\underline{25}$)
G_c	effective concentration gradient in liquid	Eqn(2.6.$\underline{4c}$)
G_1	temperature gradient in liquid	Eqn(2.6.$\underline{4b}$)
h	heat transfer coefficient	Eqn(3.2.$\underline{1}$)

Variable	Meaning	Place
H	splat thickness (continuous processes)	Eqn(3.2.9)
H_f	final ribbon thickness (PFMS)	Fig(3.3.1.2)
H_1	fluid film thickness (PFMS)	Eqn(3.3.1.5)
H_1'	slope of downstream meniscus (PFMS)	Eqn(3A.3.23)
H_1''	curvature of downstream meniscus	Eqn(3A.3.23)
H_o	nozzle-wheel gap (PFMS)	Fig(3.3.1.2)
I_v	nucleation rate	Eqn(2.3.1)
$\underline{I}$	identity tensor	Eqn(3A.1.9)
$\underline{j}$	mass flux vector	Sec(3A.1)
k	equilibrium partition ratio	Sec(2.5)
K	thermal conductivity	Eqn(2.4.3a)
k_B	Boltzmann's constant	Eqn(2.2.2)
k_m	mass transfer coefficient	Eqn(3A.1.26)
K_s, K_1, K_m	thermal conductivities of solid, liquid and mold	Sec(3A.2)
L	latent heat of fusion	Eqn(2.2.1)
L_p	melt puddle length (PFMS)	Fig(3.3.1.11)
m	exponent to obtain solidified thickness from f_s	Eqn(3.2.8)
m_S, m_L	slopes of solidus and liquidus curves in phase diagram	Eqn(2.5.5) & (2.6.4a)
n	exponent in equation for dendrite/cell spacings	Eqn(2A.1.1)

Variable	Meaning	Place
$\underline{n}$	normal vector	Eqn(3A.1.$\underline{4}$)
N_A	Avogadro's number	Eqn(2.3.$\underline{3}$)
N_v^o	number of atoms per unit volume	Eqn(2.3.$\underline{2}$)
p	pressure	Sec(3A.1)
P	pressure	Eqn(3.3.1.$\underline{2}$)
P_σ	capillary pressure	Eqn(3A.3.$\underline{19}$)
$\underline{q}$	heat flux vector	Eqn(3A.1.$\underline{8}$)
Q	volumetric flow rate	Eqn(3.3.1.$\underline{1a}$)
Q_s, Q_l	flow rates in solid and liquid (PFMS)	Eqn(3.3.1.$\underline{1a}$)
$\dot{Q}$	rate of internal heat generation ($= r_h$)	Eqn(3A.1.$\underline{5}$)
r	parameter in stability equation	Eqn(2.6.$\underline{4f}$)
R	growth rate	Eqn(2.3.$\underline{1}$)
r_c	rate of internal mass generation	Eqn(3A.1.$\underline{15}$)
r_h	rate of internal heat generation	Eqn(2.4.$\underline{3a}$)
$r*$	radius of critical nucleus	Eqn(2.2.$\underline{2}$)
R_o	coefficient in exponential law for growth rate	Eqn(2.4.$\underline{1}$)
R_o'	coefficient in linear law for growth rate	Eqn(2.4.$\underline{2}$)
S	source term in transport equation	Eqn(4A.1.$\underline{1}$)
$S(A_s,k)$	Sekerka's stability function	Eqn(2.6.$\underline{4a}$)
S_{eff}	effective deviatoric stress	Eqn(3A.1.1.$\underline{10a}$)
t	time	Eqn(2.3.$\underline{1}$)

Variable	Meaning	Place
T	temperature	Eqn(2.3.$\underline{2}$)
t_c	critical time for the start of crystallization from melt	Eqn(2.3.$\underline{5}$)
$\underline{t}$	tangent vector	Eqn(3A.1.$\underline{16}$)
T_f	temperature of fusion	Eqn(2.3.$\underline{2}$)
T_h	temperature of hypercooling	Fig(2.4.$\underline{1}$)
T_N	temperature of nucleation	Eqn(2.2.$\underline{1}$)
T_o	temperature fluctuation amplitude	Eqn(2.6.$\underline{1}$)
T_p	pouring temperature	Eqn(3.2.$\underline{4a}$)
T_S, T_L	temperatures of solidus and liquidus lines (phase diagram)	Eqn(2.2.$\underline{1}$)
T_x	temperature at location x (continuous processes)	Eqn(3.2.$\underline{9}$)
T^*	maximum recalescence temperature	Sec(2.5)
T_∞	temperature in bulk of heat sink	Eqn(3.2.$\underline{1}$)
$\dot{T}$	cooling rate	Eqn(2.2.$\underline{2}$)
$\overline{T}$	average cross-sectional cooling rate (PFMS)	Eqn(3.3.1.$\underline{7}$)
$\dot{T}_e$	effective cooling rate at the solidification interface (PFMS)	Eqn(3.3.1.$\underline{8}$)
$\underline{\underline{T}}$	stress tensor	Eqn(3A.1.$\underline{4}$)
u	temperature	Sec(3A)&(4A)
U	internal energy	Eqn(3A.1.$\underline{5}$)
u_1, u_2	boundary temperatures	Eqn(3A.2.$\underline{5}$)
u_f	temperature of fusion	Eqn(3A.2.$\underline{3}$)

Variable	Meaning	Place
u_s, u_l, u_m	temperatures in solid, liquid and mold	Sec(3A.2)
u_S, u_L	temperatures of solidus and liquidus lines (phase diagram)	Sec(3A.2)
$\underline{u}^n$	vector of discrete temperatures for the nth time step	Eqn(3A.2.15)
V	volume of sample	Eqn(3.2.1)
$\underline{v}$	velocity vector	Sec(3A.1)
v_x, v_y	x- and y- components of $\underline{v}$	Eqn(3A.1.28)
V_x	x- component of velocity	Eqn(3.3.1.1a)
V_o	reference velocity	Eqn(3A.1.32)
V_{r_x}	x- component of roll velocity (PFMS)	Eqn(3.3.1.5)
$\bar{V}_x$	average cross-sectional velocity (PFMS)	Eqn(3.3.1.6)
$\underline{V}$	velocity vector	Eqn(3.3.1.1)
w	ribbon (& slot) width (PFMS)	Eqn(3.3.1.1a)
x	rectangular Cartesian coordinate	Eqn(2.6.1)
X	location of solidification interface in Stefan problem	Sec(3A.2)
X_c	fraction of sample that has crystallized	Eqn(2.3.1)
y	rectangular Cartesian coordinate	Eqn(2.6.1)
y_g	maximum sample thickness that can transform into glass	Eqn(2.3.5)
y_s	solidified thickness	Fig(3.3.1.2)
z	solidified thickness (Newtonian)	Eqn(3.2.8)

Variable	Meaning	Place
z	sample half thickness	Eqn(3.2.7)
α	thermal diffusivity	Eqn(2.3.5)
Γ	diffusion coefficient for generalized transported quantity	Eqn(4A.1.1)
η	coefficient in deviatoric stress for power law fluid	Eqn(3A.1.10)
θ	nozzle-melt downstream contact angle (PFMS)	Eqn(3A.3.24a)
$\varkappa$	slip coefficient	Eqn(3A.1.17)
λ	parameter in solution of Stefan problem	Eqn(3A.2.6d)
λ_s	secondary dendrite arm/cell spacing	Eqn(3.3.1.9)
Λ	temporal frequency of perturbations	Eqn(2.6.1)
μ	viscosity	Eqn(2.3.4)
ν	jump frequency of atoms	Eqn(2.3.2)
ρ	density	Eqn(2.6.4a)
σ	surface tension	Eqn(2.2.2)
τ_c	critical delay time required for nonequilibrium phase formation	Eqn(2.4.4)
ϕ	arbitrary function	Eqn(3A.2.14)
Φ	scalar, vector or tensor function of time and position	Eqn(3A.1.1)
ψ	stream function	Fig(3.3.1.4)
ω_x, ω_y	spatial frequency of perturbations	Eqn(2.6.1)

Variable	Meaning	Place
Ω	atomic volume	Eqn(2.2.2)
$\mathcal{H}$	mean curvature of interface	Eqn(3A.1.19)
Q	flow rate per unit width (PFMS)	Fig(3.3.1.10)
ϕ	general transportable quantity	Eqn(4A.1.1)
$\Delta x, \Delta y$	step-lengths in x and y direction	Eqn(3.3.1.6)

Chapter 1

INTRODUCTION

The main objective of the work reported in this thesis has been the application of fundamental concepts of continuum mechanics and numerical analysis for the quantitative description of some commonly used methods of Rapid Solidification Technology (RST). Although time limitations have restricted us to the description of only one process in detail (namely , the Planar Flow Melt Spinning (PFMS) system), we believe that the information presented should allow the use of the same methods for the description of any other Rapid Solidification Processing (RSP) system.

In this first chapter we present some background information about RST . After defining RSP , we comment on the merits of the mathematical approach to the study of RST. Then, the significant changes in structure and properties produced by rapid solidification are briefly discussed. A comment is also included regarding the essential process requirements for the achievement of large cooling and freezing rates. Furthermore, for the sake of motivation and completeness we briefly review important facts concerning the actual and possible applications of rapidly solidified materials. We conclude the chapter with a summary description of what the reader can expect to find in succeeding chapters.

1.1.- Definition of RSP and the Merits of Mathematical Modeling.

RSP is the name given to a wide array of materials processing operations in which the intended purpose is the production of solid materials directly from their melts by imposing relatively large cooling and freezing rates on the molten samples. Although the boundary between conventional casting operations and RSP is not clear-cut there seems to be agreement in calling RSP solidification processes in which the cooling rates are greater than say 10^2 ^{o}C/s and the freezing rates larger than about 1 cm/s .

The explicit purpose of RSP is to exploit the structure-properties correlation so as to be able to obtain products with desirable metallurgical characteristics in a reproducible fashion. Because of the peculiar features of RSP systems, the performance of suitable measurements, relatively straightforward in other casting systems, becomes very difficult at best. Researchers have resorted again and again to more unorthodox approaches in an attempt to reveal the fundamentals of RS processes. Mathematical modeling has been one of such approaches ever since the inception of RST.

The mathematical modeling approach is in reality an attempt to make the study of RSP systems an interdisciplinary enterprise. When modeling, one combines the results of actual experiments with basic principles of continuum mechanics and concepts of numerical analysis to produce quantitative representations of the processes

under study. The explicit objectives of the approach are:

(i) To gain an improved insight into the complex behavior of

RSP systems,

(ii) to establish a quantitative framework for the rational

design and control of RST devices, and

(iii) to demonstrate the applicability of some very basic

principles of physics to the description of complicated,

real-life RSP systems.

1.2.- The Effects of RSP on the Structure of Materials.

The structures of rapidly solidified materials have been found

to be markedly different to those of samples of the same materials

processed in more conventional ways. There is ample evidence

supporting the structure and property modifications resulting from

RSP . Reference could be made to the review by Jones (1984) and to

the proceedings of the various international conferences on the

subject (see the References at the end of the report). The interest

generated by these discoveries is such that an international journal

has just appeared specifically devoted to RS research.

According to Grant (1983b), the following effects of RS are

the main reason for the increased attention metallurgists are

paying to RST :

(i) Much reduced extent of segregation. The large cooling and

freezing rates during RS do not allow time for the separation

3

and/or growth of segregated phases. As a consequence of this, multiphase rapidly solidified materials usually contain the second phases in the form of a homogeneous dispersion of very fine particles.

(ii) Decreased size of microstructural features. Again , due to the high cooling rates involved, grains, cells and/or dendrites are usually much smaller than those found in samples produced by more conventional methods.

(iii) The possibility of producing new phases or entirely new materials. It has been found that RS may prevent the formation of some phases commonly observed in conventionally processed stock. Instead, new, previously unknown metastable phases can appear. Moreover, the effect of RS can be so drastic as to entirely prevent the formation of any crystalline phases, thus resulting in metallic glasses.

1.3.- Requirements for Rapid Solidification.

There is one most important requirement that must be satisfied if one wishes to induce large cooling and freezing rates in molten samples. The requirement is the rapid formation of a thin layer of melt in good thermal contact with a heat absorbing medium. Rapidly solidified structures can also be obtained in bulk samples, however, if one is careful enough to eliminate all nucleating agents. Since,

in practice, such agents are almost always present, the requirement of rapidly forming thin liquid layers is really essential. Jones (1982) has suggested that by imposing any of the following on molten samples, rapid solidification can be obtained:

(i)   A high undercooling prior to solidification. Unfortunately, this is only possible by the avoidance of nucleating agents.

(ii)   A high withdrawal velocity of the sample through a steep temperature gradient. This is what is usually done during steady state continuous casting of rapidly solidified materials.

(iii) A high cooling rate during solidification. This is usually the case during the solidification of the smaller droplets produced by atomization.

From the above we can conclude that, in most cases of practical interest, a small sample size is required along at least one spatial dimension to be able to achieve the benefits of rapid solidification.

1.4.-   Properties and Applications of Rapidly Solidified Materials.

Unexpected properties or combinations of them have been found in rapidly solidified materials. For example, metallic glasses tend to combine good ductility with high mechanical strength . Also, glasses with high corrosion resistance or with good catalizing properties have been found. Rapidly solidified stainless steels have been shown to be very resistant to high temperature oxidation. Useful electric

and magnetic properties are currently under study. The effects of RS on specific alloy systems are also being investigated. For example new alloys have been prepared by combining aluminum with unusual alloying elements (such as Li), resulting in improvements in thermal stability and mechanical properties. Property changes have also been reported in the cases of iron-base alloys and superalloys. These examples, together with the promise of more to come, have stimulated the current interest in RST .

In the last few pages we have presented a summary description of what we believe is important background information about RST. At best, the information presented should enable the reader to understand those aspects of RST to which frequent reference is made in subsequent chapters without having to resort to the bibliography. Thus , we have presented a definition of the field and of the role played by mathematical models, followed by comments on the effects of RST on materials and the requirements for the achievement of high cooling and freezing rates.

In the following chapters we take the discussion into the basic aspects of the modeling of rapid solidification phenomena (Ch. 2), then into the detailed description of the use of mathematical modeling techniques for the study of RSP systems (Ch. 3). We conclude the report with a summary description of our results , a series of suggestions for further work (Ch. 4) and the FORTRAN listings of the computer programs which have produced the bulk of the results reported (Ch. 5). Several appendices have also been

included both in order to avoid interrupting the continuity of the main text and to help in making the monograph more self-contained.

We close this chapter now with a comment. Our work constitutes one more contribution to the rather long history of RS research at MIT . For the past two decades, young researchers have developed RS processes and have probed the characteristics of the resulting products. Mention should be made of , among others , the thesis reports by Ruhl(1967), Strachan(1967), Lebo(1971), Jansen(1971), Domalavage(1980), Lynch(1982), Libera(1983), Segal(1983), Ashdown (1984) and Speck(1985). To them , I am sincerely indebted. Our work, however, has a slant in a different, relatively new direction. We have not performed any experiments; however, we hope to have demonstrated by the end of this report, that the mathematical modeling approach is indeed a legitimate, alternative way of looking at RSP problems. We believe that the development and optimization of RST will require a strongly interdisciplinary approach and we hope that our work will be regarded as an example of the way mathematical models can contribute to the understanding of RSP.

Chapter   2

THE MODELING OF RAPID SOLIDIFICATION PHENOMENA

In this chapter we undertake a more detailed description of some fundamental features of rapid solidification. Starting with a discussion of the effects of RS on the structure of materials we proceed to present summary reviews on the maximum undercoolings achievable in metallic melts, on the likelihood of forming metallic glasses and on the solidification of undercooled melts. A comment on the problem of morphological stability is also included.

The attention we devote in this chapter to the undercooling phenomenon is due to its apparent importance in many RS systems. Even though our model of the PFMS process, presented in Ch. 3 , does not take into account undercooling effects, because the available evidence seems to indicate this is indeed a good assumption , these effects can be very significant in other RS systems. The prospective modeler should be aware of that, and should also be able to take such effects into account in his/her calculations, if the need arises. The information presented below should provide enough background to be able to follow unaided the current literature on the subject .

2.1.- More on the Effects of RSP .

The effects produced by rapid solidification can be classified into two main groups: constitutional and microstructural . These in turn can be subdivided as follows;

(a)   Constitutional effects

(i)   Metallic glass formation. Metallic glasses can be formed when the rate of solidification is faster than the rate required for the formation of crystalline material at the solidification interface. Metallic glasses can be formed between: (1) metals and metalloids, (2) transition metal-transition metal, and (3)group II metals − B subgroup solutes . The kinetic conditions for metallic glass formation are discussed in Sec(2.3) below.

(ii)   Formation of non-equilibrium crystalline phases. It may well happen that the rate of solidification is faster than that required for the formation of the equilibrium crystalline phase. In this case non-equilibrium crystalline phases can appear. These phases can form between: (1) noble and B- subgroup metals, (2) B-subgroup − B-subgroup metals, and (3) transition-transition metals. The conditions required for the formation of non-equilibrium crystalline phases are described in Sec(2.4) below.

(iii) Solid solubility extensions. Many systems have been found in which RS produces significant solid solubility extension. This phenomenon was indeed the first indication of the effects of RS. In Sec(2.5) we discuss solute redistribution during RSP.

(b)   Microstructural effects

(i)   Grain structure and size. Equiaxed grains, cells and
dendrites have all been observed in rapidly solidified specimens.
However, in all cases the sizes involved are much smaller than
those that can be obtained by conventional processes. In Sec(2.2)
we review the thermal conditions required for the production of
microcrystalline structures from the melt and in Sec(2.6) we
briefly describe the main features of the problem of morphological
stability during RS .

(ii)   Formation of lattice defects. Few heavily dislocated
specimens have been found as a result of RS. Few twins and some
stacking faults have also been observed. On the other hand,
considerable vacancy supersaturations have been found.

The presence of some or all of these effects in rapidly solidified
materials accounts for their unexpected properties. In the sequel
we present a summary description of the phenomena which produce
such effects.

2.2.-   On the Maximum Attainable Undercooling During RSP.

Since the solidification structures of heavily undercooled
samples are usually composed of very finely grained material it
has been natural to ask about the maximum possible undercooling
a given sample can achieve prior to solidification. The problem

10

has been studied by Hirth(1978) using concepts from nucleation theory. It is well known that, given sufficient undercooling prior to solidification, nucleation and growth can proceed to complete solidification without the solid-liquid interface ever reaching the solidus temperature . A sample in this condition is said to be hypercooled. The condition for hypercooling can be derived from thermodynamics and it is

$$\overline{C}_p \, ((T_L - T_N) + (T_S - T_L)) \quad \geqslant \quad L \qquad (1)$$

where all the symbols are defined in the List of Symbols. We note that Eqn(1) is only valid for the situation in which the temperature is uniform across the sample (Newtonian cooling), however , despite this limitation it constitutes an useful estimate. It should also be mentioned that under hypercooled conditions, the rate controlling step of the solidification process are the atomic jumps across the solid-liquid interface.

The maximum attainable undercooling is, obviously, the one corresponding to homogeneous nucleation. An index of merit can then be defined for the achievement of nucleation control. If the formation of one nucleus per sample constitutes a suitable definition of the critical condition for the production of homogeneous microcrystalline structures, the use of homogeneous nucleation theory leads to the following expression for the maximum attainable undercooling,

$$T_L - T_N = \left(\frac{16 \pi \sigma^3 \Omega^2 T_L^2}{3 k_B T_N L^2 \ln(10^{-3} d^3 (r^*/a)^2 (a/\Omega) D_1 (T_L - T_N)/\dot{T})} \right)^{1/2}$$

$$(2)$$

Since there are only small differences in the nucleation behavior of single and multicomponent systems, Eqn(2) can be used to estimate maximum undercoolings in both cases. For a given material and sample size , Eqn(1) can be used to estimate the minimum undercooling required for hypercooling. Afterwards, Eqn(2) can be used to compute the minimum cooling rate required for the production of homogeneous microcrystalline structures.

Hirth has been able to obtain reasonable estimates of critical cooling rates for various alloy systems. His final advice is , however, that more attention be paid to the role of impurities and other heterogeneities in promoting nucleation, thus preventing the attainment of the maximum undercooling.

2.3.- Metallic Glasses.

When the cooling rates during RSP are sufficiently large , metallic glasses can be formed instead of the usual crystalline phases. The formulation of the critical conditions for metallic glass formation has been worked out by Uhlmann(1983).

From the Johnson-Mehl-Avrami theory of phase transformation kinetics, the relationship between the fraction of new phase formed, X_c and the time t is

$$X_c \cong (1/3) \pi I_v R^3 t^4 \tag{1}$$

The nucleation rate I_v can be estimated from homogeneous nucleation theory and is

$$I_v \cong N_v^o \nu \exp\left(-\frac{1.024}{(T/T_f)^3((T_f - T)/T_f)^2}\right) \tag{2}$$

The growth rate can be estimated from crystal growth kinetics to be

$$R \cong 0.2 \left((T_f - T)/T_f\right) \nu a\left(1 - \exp\left(-\frac{L((T_f - T)/T_f)}{k_B N_A T}\right)\right)$$

$$\tag{3}$$

Finally, the jump frequency ν, can be related to the viscosity of the melt through the Stokes-Einstein relationship, i.e.

$$\nu \cong \frac{k_B T}{3 \pi a^3 \mu} \tag{4}$$

Equations (1)-(4) above can now be used to construct temperature-time-transformation diagrams for the prediction of the critical conditions for metallic glass formation. The procedure used for the construction of such diagrams is as follows:

(i) First , an arbitrarily small fraction crystallized (say $X_c^* = 10^{-6}$) is selected and a temperature (below the solidus) is chosen.

(ii) From Eqns(1)-(4) the time required for fraction X_c^* to form is calculated . The pair T , t is plotted on a scale of T vs. log t .

(iii) Steps (i) and (ii) above are repeated for different T's (but the same X_c^*) to obtain the complete T-T-T diagram.

Figure(1) shows the result of one such calculation for various metallic systems. Based on the same ideas, Uhlmann estimated the maximum thickness of sample that can be transformed into glass by rapid cooling to be

$$y_g \cong (\alpha \, t_c)^{1/2} \qquad (5)$$

where t_c is shown in Fig.(1) for the case of AuGeSi.

Other factors that have been found to influence the formation of metallic glasses are , heterogeneous nucleants and nucleation transients . For a discussion of these factors the reader shoul see the paper by Uhlmann mentioned above.
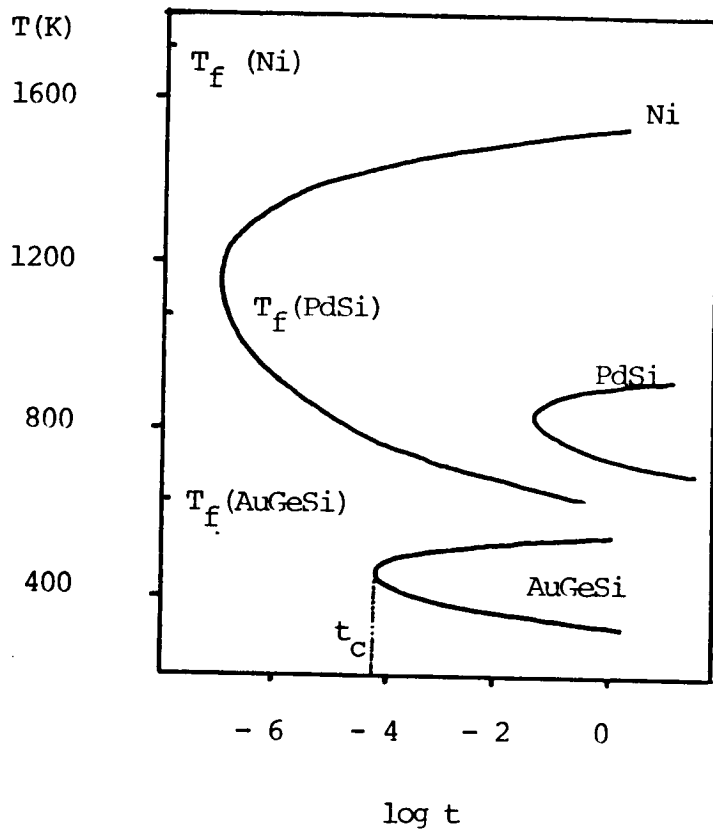
Fig(2.3.1).- Temperature-time-transformation (T-T-T) diagrams for the crystallization of several metals from their undercooled melts. Here $X_c^* = 10^{-6}$. From Davies(1976).

2.4.- Solidification of Undercooled Melts.

When a melt sample which has been undercooled starts to solidify, the latent heat of solidification is released very rapidly at the solid-liquid interface. The sudden release of this latent heat is so fast that the outer surface of the sample may well be unable to dissipate this energy. The liberated heat has to be retained in the melt thus producing the phenomenon known as recalescence. During recalescence , the temperature of the solidification interface rises quickly and can even reach the equilibrium value.

The solution of the coupled heat transfer – crystal growth problem is not a simple task. Solution procedures usually start by assuming a particular expression for the crystal growth rate as a function of the interface temperature. The heat transfer problem is handled essentially in the same way as the usual Stefan problem (see Sec(3A.2)). However , instead of the fixed , equilibrium freezing temperature found in the classical Stefan problem, here the interface temperature is variable.

Two growth rate – interface temperature relationships have been the most popular, namely , the exponential law

$$R = R_o (1 - \exp(L(T - T_f)/T T_f)) \qquad (1)$$

and the linear law

$$R = R_o' (T - T_f) \qquad (2)$$

16

The solidification problem is described by the equations of the classical Stefan problem in the weak (enthalpy) formulation (see Sec(3A.2)),

$$\partial E / \partial t \quad = \quad \text{div}(K \text{ grad } T) \ + \ r_h \qquad (3a)$$

$$E \quad = \quad f (T) \qquad (3b)$$

However, instead of assuming the solid-liquid interface temperature to be given by equilibrium considerations, it is assumed to be dependent on the crystal growth rate according to either Eqn(1) or Eqn(2) above .

The mathematical problem represented by either Eqns(1) and (3) or (2) and (3) must be solved to obtain the temperature field inside the sample, the freezing rate and the interface temperature. Various methods have been proposed for the solution of this problem.

Boswell(1979) used a front-tracking technique (Sec(3A.2))to solve Eqns(1) and (3) for the case of a pure metal solidifying against a metal chill. An iterative method was used to compute the interface temperature. Although no details were given, he presented a plot describing the effects of the heat transfer coefficient, of the splat-chill interface temperature at the start of freezing and of the materials properties.

17

Levi and Mehrabian(1982) performed a detailed analysis of the rapid solidification phenomena taking place during the freezing of undercooled pure metal droplets. They solved Eqns(1) and (3) and (2) and (3) in a suitable coordinate system using appropriate boundary conditions. The most important parameters in their calculations were the droplet diameter, the heat transfer coefficient, the droplet surface temperature at the onset of nucleation, and the kinetic growth coefficients R_o and R_o' in Eqns(1) and (2).

Two heat transfer models were used by Levi and Mehrabian. The simplest one assumed negligible temperature gradients inside the droplet (Newtonian model). In the other model , this restriction was relaxed. An implicit finite difference method was used to solve the equations for this latter case. Although somewhat similar results were obtained from both models, the one based on non-Newtonian cooling provided more detailed information. The results of their calculations were conveniently summarized in the form of dimensionless enthalpy-temperature curves. The cooling and freezing paths of individual droplets can be easily followed in such diagrams. One example of such plots is included in Fig(1). We will describe now how to read this diagram.

At the lower limit of slow cooling rates, the freezing path followed by the droplets is close to the equilibrium freezing path. In this case, when the droplet reaches the equilibrium freezing temperature T_f , solidification at constant temperature starts and continues until the entire latent heat has been withdrawn (
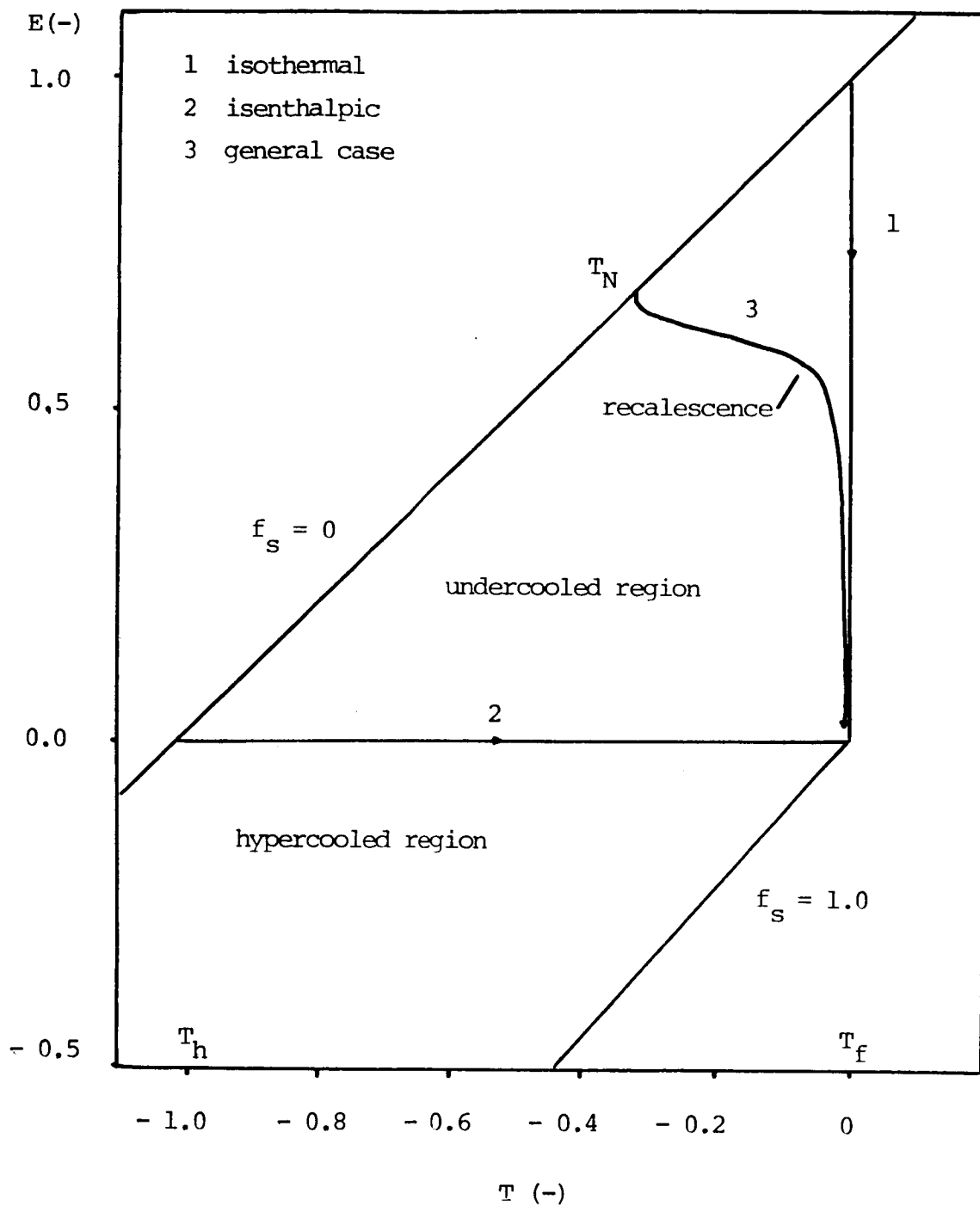
Fig(2.4.1).- Dimensionless enthalpy-temperature diagram showing the various possible freezing paths of undercooled melts. From Mehrabian(1982).

and the dimensionless enthalpy is equal to zero). This solidification

mode is called isothermal for obvious reasons.

At high cooling rates the other extreme possibility appears.

Namely , during cooling, an amount of energy at least equal to the

latent heat of fusion is withdrawn without nucleation taking place.

Once this is done the system can solidify without having to extract

any more heat from the sample. This is the so called isenthalpic

(or adiabatic) solidification mode.

A much more common occurrence is the intermediate case where

solidification starts below the equilibrium freezing point but

before the entire latent heat of solidification has been released.

Since nucleation is accompanied by the liberation of a certain

amount of heat, the droplet temperature will tend to rise until

the equilibrium melting point is almost reached. Solidification

can then proceed according to the isothermal mode. This self-

heating process is known as recalescence.

Two distinct solidification regimes can thus be observed in

this the more general case. First, during recalescence, the

solidification interface moves rapidly into the liquid. The latent

heat is released so quickly that the external cooling is unable

to extract it thus resulting in the heating up of the droplet.

However, afterwards, when the droplet temperature has reached a

value close to the equilibrium melting point, the subsequent

freezing depends mainly on the rate of heat extraction through the

outer droplet surface .

As expected, the microstructures of the products formed during the two freezing stages in the general case, are markedly different. A detailed review of the subject ,including many photomicrographs, has prepared by Mehrabian.

More recently, Crowley(1984) studied the process of pulsed laser annealing. The large heating and cooling rates produced by this process induce undercooling. She proposed a fixed domain method with partial front tracking for the solution of this problem. The formulation is again identical to that of the conventional Stefan problem except for the allowance of a variable solidification interface temperature. Crowley produced a consistent and stable algorithm free of oscillations. Her technique certainly warrants attention from people studying the solidification of undercooled melts.

In a related study, Dantzig and Davis(1978) used the same basic set of equations in combination with alternative mathematical methods (matched asymptotic expansions with embedding) to analyze the conditions for non-equilibrium phase formation during RSP. They introduced the concept of the delay time as the time that must elapse between the attainment of the equilibrium melting point and the moment when the melt transforms into the equilibrium product. By comparing the delay time with the times required for non-equilibrium products to form, they derived a criterion for the formation of the latter. The basis for comparison was the difference in rates of the process of interfacial attachment and the process of

heat conduction. The exponential law for crystal growth (Eqn(1)),
was solved simultaneously with the equations of the classical
Stefan problem modified by the presence of the delay time in the
Stefan condition.

The conclusion reached by Dantzig and Davis was that, if the
kinetic processes of atomic attachment at the solidification
interface are slow compared to the cooling rate, the expected
equilibrium crystalline phase may never form. Instead, a super-
cooled layer of fluid will grow from the chill until it reaches
macroscopic dimensions. The critical delay time separating
equilibrium from non-equilibrium products was calculated to be

$$\tau_c \simeq - (T_N / \dot{T}) \qquad (4)$$

Equation (4) shows the expected result, that low nucleation
temperatures and high cooling rates facilitate the formation of
non-equilibrium products.

Clyne(1984) has presented a review of the numerical treatment
of RS processes in which undercooling is an important consideration
and his paper can be consulted for additional information.

2.5.-   Solute Redistribution During RS .

The phenomenon of solute redistribution during RS is still the

subject of active research. Although many aspects of it are still obscure, important insight was gained from the model proposed by Kattamis (see e.g. Flemings(1981)). This model suggests that the freezing of undercooled alloys takes place according to the following three stages:

(i) Recalescence up to the solidus temperature T_S ,

(ii) recalescence from T_S up to the maximum recalescence temperature $T*$, and

(iii) cooling from $T*$.

In the model it is also assumed that the diffusion of solute is negligible during stage (i) but not during (ii). The segregation during stage (iii) is described by the Scheil equation. Next we present a brief summary of the equations of this model.

For stage (i) above, a heat balance can be written as

$$d\ f_s/d\ T\ =\ C_p/L \tag{1}$$

so that the fraction solidified once the solidus temperature is reached during recalescence, f_s^i , is

$$f_s^i\ =\ (C_p/L)(T_S\ -\ T_N) \tag{2} .$$

Since diffusion is neglected during this stage, the solute concentration in the solid forming between T_N and T_S is

$$C_s\ =\ C_\infty\ =\ C_s^* \tag{3}$$

For stage (ii), a solute balance can be written as

$$d \, f_s/d \, C_1 \quad = \quad (1 - f_s)/(C_1 - C_s^*) \qquad (4)$$

Moreover, from the phase diagram, the slope of the solidus curve
is given as

$$m_S \quad = \quad d \, T/d \, C_s^* \qquad (5)$$

The combination of Eqns(4) and (5) leads to

$$d \, f_s/d \, C_s^* \quad = \quad (C_p/L) \, m_S \qquad (6)$$

which can be integrated between f_s^i and f_s to give

$$C_s^* \quad = \quad C_\infty \quad + \quad (L/m_S \, C_p)(f_s - f_s^i) \qquad (7)$$

Substituting now Eqn(7) into Eqn(4) and assuming that $f_s \cong f_s^i$ and that $(1 - f_s) \cong$ constant , leads to

$$(C_1 - C_\infty)(f_s - 1) \quad - \quad (f_s - f_s^i)^2 \, (\, L/(2 \, m_S \, C_p)) \quad = \quad 0 \qquad (8)$$

Now, since $C_s^* = k \, C_1$ when $T = T^*$, form the assumption
of local equilibrium at the solidification interface, the combina-
tion of Eqns(7) and (8) allows us to compute the fraction

solidified when the maximum recalescence temperature is reached, f_s^{ii} .

Finally , stage (iii) is assumed to take place according to the Scheil equation modified by the fact that the initial state is given by $f_s = f_s^{ii}$. The resulting expression is

$$C_s^* = C_s^{*ii}(1 - ((f_s - f_s^{ii})/(1 - f_s^{ii})))^{k - 1} \qquad (9)$$

Where C_s^{*ii} is the solute concentration in the solid side of the solidification interface corresponding to the maximum recalescence temperature T^* . Because of the assumed negligible diffusion in the solid, all the interfacial concentrations mentioned above are basically equal to the final concentrations inside the solid, i.e. $C_s = C_s^*$.

The model described above provided the first quantitative explanation for the frequently observed solute rich cores of dendrites found in samples produced by solidification of under-cooled melts. The model has been refined and alternative stages have been proposed. The thesis by Chu(1983) contains a detailed description of the state of the art in this area and it should be consulted for further information.

2.6.- Morphological Stability During RS .

Since material properties are the main concern of the metallurgist and because these properties are strongly related to the microstructure, the prediction of the relationship between the process parameters and the resulting microstructure has long been an important consideration. This has also been the case in RS research. The main question to be answered is if the solid-liquid interface will grow in a planar fashion without micro-segregation or will it break up into cells or dendrites, resulting in segregated, multiphase structures.

The principle of constitutional supercooling provides a useful guide to ascertain the growth conditions resulting in solidification interface shape instability during alloy solidification. However, research on RS has shown that the constitutional supercooling principle produces entirely erroneous predictions in the extreme case of large freezing rates. This deficiency has been removed by the introduction of the theory of morphological stability (see e.g. Coriell and Sekerka(1980) or Cahn et al.(1980)).

The theory of morphological stability is based on a kinetic analysis of the spatial and temporal behavior of perturbations formed on the solidification interface. The starting point for the analysis is the governing equations for heat and mass transfer (see Sec(3A.1)). A perturbation-type linear stability analysis is employed to derive the conditions for stability. The simplest

model adopted for study is the directional solidification of a binary alloy under a constant growth velocity and under local equilibrium conditions at the solid-liquid interface.

The governing equations for heat and mass transfer must account for the latent heat released during solidification and thus they are basically the same as those of the Stefan problem for alloy solidification (Sec(3A.2)), except for the incorporation of interface curvature effects in the boundary conditions. First, the temperature field , the concentration field and the interface shape are written as the product of a constant term and a perturbed part, i.e.

$$T = T_o \exp(\Lambda t + i(\omega_x x + \omega_y y)) \tag{1}$$

$$C = C_o \exp(\Lambda t + i(\omega_x x + \omega_y y)) \tag{2}$$

$$F = F_o \exp(\Lambda t + i(\omega_x x + \omega_y y)) \tag{3}$$

From the form of these expressions, it can be readily seen that the interface will become unstable whenever the real part of Λ is positive for any real values of ω_x and ω_y. It is possible to derive an equation for the quantity Λ as a function of the process parameters and the material properties by simply substituting Eqn(1)-(3) into the original governing equations. The use of appropriate boundary conditions leads finally to the desired

expression which will not be quoted here but can be found in the references given. The main feature of this equation is , however, that it is composed of three terms: a term involving thermal effects, another involving surface tension effects and the last one involving concentration effects. From the form of the equation it is seen that the thermal and surface tension effects tend to dampen the interface shape perturbations and are thus stabilizing. The concentration term , on the other hand, has always a de-stabilizing effect. When this last term is sufficiently large, the interface may become unstable and perturbations will grow.

The stability equation mentioned above can be simplified con-siderably if due account is taken of the extremely large thermal diffusivities of metallic melts by assuming it equal to infinity. Under this assumption the stability equation becomes,

$$2 \, K_1 \, G_1 \; + \; R \, L \, \rho \quad \geqq \quad (K_s + K_1) \; m_L \, G_c \, S(A_s, k) \tag{4a}$$

where
$$G_1 \quad = \quad (d \, T/d \, x)_1 \tag{4b}$$

$$G_c \quad = \quad R \, C \quad (k - 1)/D_1 \, k \tag{4c}$$

$$S(A_s, k) \quad = \quad 1 + (A_s/4k)(1 - r^2 + 2kr^2) - (3 \, A_s^{1/2} \, r/2) \tag{4d}$$

$$A_s \quad = \quad k \, T_f \; (\sigma/\rho \, L) \; R^2/D_1^2 \, m_L \, G_c \tag{4e}$$

and the quantity r must be obtained by solving

$$r^3 + (2k - 1)\, r - (2k/A_s^{1/2}) = 0 \qquad (4f)$$

Equations (4a)-(4f) provide a suitable representation of the stability behavior of metallic melts for a wide variety of process conditions. Two limiting cases exist, namely, for small growth velocities , the constitutional supercooling criterion is adequate and the stability limit is thus given by (Flemings(1974)),

$$G_1/R = -m_L\, C_s^*\, (1 - k)/k\, D_1 \qquad (5)$$

On the other hand, for large growth velocities, the absolute stability limit (obtained by making $A_s = 1$ in Eqn(4)), is a good approximation, i.e.

$$G_c/R = k\, T_f\, (\sigma/\rho\, L)\, m_L\, R/D_1 \qquad (6)$$

Equation (6) indicates that much greater stability can be expected at high freezing rates than that predicted from the constitutional supercooling criterion. At least three factors can explain this behavior. First, the capillary forces have a strongly stabilizing effect, particularly on the short wavelength

perturbations characteristic of high growth rates. Furthermore, the deviations from local equilibrium at the solidification interface and the peculiar temperature gradients resulting from the freezing of undercooled melts also have a stabilizing effect.

A convenient way of presenting the results of the calculations performed using Eqn(4) or (5) and (6) is by plotting the bulk liquid solute concentration against the growth velocity. The pairs of values of these quantities corresponding to the critical condition display the limit of stability. One such plot, for the case of the Al-Cu system is presented in Fig(1).

The theory of morphological stability has been extended to deal with other effects such as interfacial anisotropy, melt undercooling, nonlinearities , and deviations from local equilibrium at the solidification interface. For this latter case, a corresponding stability equation has been derived using ideas very similar to those described above. The analysis has provided useful insight about the important phenomena of solute partitioning and trapping during RS . The references should be consulted for details.

In this chapter we have reviewed several topics concerning the mathematical representation of rapid solidification phenomena. As can be inferred from the discussions on undercooling, metallic glasses and the freezing of undercooled melts, the fundamental processes of nucleation and growth played an important part in the description of such systems. However, when kinetic considerations

30
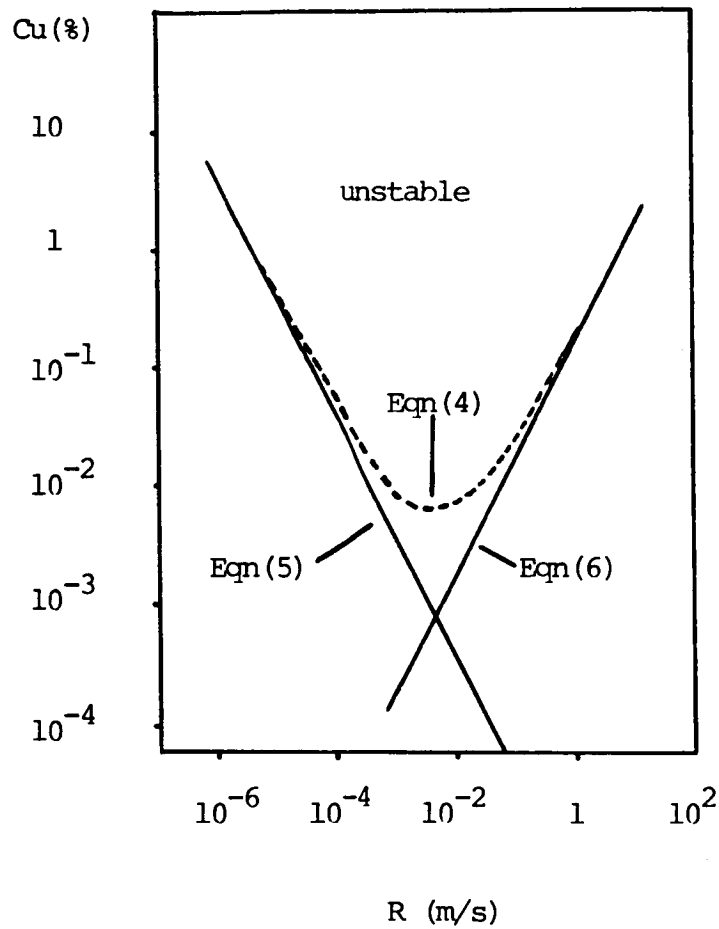
Fig(2.6.1).- Interface stability diagram for the directional solidification of Al-Cu alloys. Here $G_1 = 2 * 10^4$ K/m . From Coriell and Sekerka(1980).

of this type are tried for the description of the more complex

RSP systems found in practice, the mathematical problem becomes

very difficult. The non-constant growth rates, the poorly defined

boundary conditions and the existence of undetermined computational

domains, all contribute to the difficulties.

A very useful simplification is obtained when the kinetic

processes taking place at the solidification interface are assumed

to be so fast that they can be safely disregarded as the rate

controlling step of the overall process. Under these circumstances,

the macroscopic transport processes control the overall performance

of the system. In the following chapter we present some solutions

to the mathematical problem resulting from the neglect of the

atomic kinetic processes at the solidification interface. Only

one system (the PFMS) is dealt with in all detail and summary

comments are included for a few others.

Chapter 3

THE MATHEMATICAL MODELING OF RAPID SOLIDIFICATION PROCESSING

As mentioned at the end of the previous chapter, the solution

of problems in RST can be facilitated if the atomic kinetic

processes taking place at the solidification interface are

assumed to be so fast that they can safely be disregarded as the

controlling mechanism for the overall process. This is equivalent

to assuming that the rate controlling processes are of a macro-

scopic nature. It is indeed fortunate that the assumption of

infinitely fast interfacial processes is justified for substances

constituted by small molecules (such as metals) in many cases of

practical interest.

In this chapter we undertake the task of simulating mathemati-

cally the behavior of some important RSP systems using the

assumption of infinitely fast interfacial processes. For the sake

of organization, in the first section we attempt a classification

of RSP systems which is capable of including every existing (and

non-existing) rapid solidification technique. We then proceed to

the formulation of the simplest macroscopic heat transfer models,

based on the assumption of Newtonian cooling conditions. These

simple models can be very useful to obtain first order estimates

of cooling and freezing rates in actual RSP configurations.

Although the simple heat transfer models have been widely used, the interpretation of the subtle variations found from process to process requires models of greater accuracy.

In Sec(3.3) we describe the somewhat more sophisticated models resulting from the elimination of the assumption of Newtonian cooling. Since the details of these models are highly system-specific, only one RSP system is dealt with in all detail while the basic ideas required for the formulation of the models of other important systems are the subject of much briefer presentations. We focus our attention on the Planar Flow Melt Spinning System (PFMS) and present enough detail, that the extension of our methods to other RSP systems should be relatively straightforward .

To facilitate the reading we have decided to separate background information from that pertaining specifically to the modeling of RSP systems. However, for completeness , the background information has been put in appendices at the end .

3.1.- Rapid Solidification Processing Systems.

A large variety of devices have been constructed and used for the production of rapidly solidified materials. Most of them, however, have been designed having in mind the main requirement for obtaining high cooling and freezing rates, namely, the existence of a small section in at least one spatial direction.

Jones(1982) has proposed a classification of RSP systems based on some key features of the various processes. He considers RSP systems to be divided into: (i) Spray methods (involving the complete disruption of the continuity of the melt), (ii) chill methods (where the melt is thinned instead of being disrupted), and (iii) weld methods (where a high energy beam melts the surface of a bulk object). We believe that the classification presented in Table(1) below, which is based on Jones' , is more comprehensive and it is the one we will use in our discussion.

Actual, representative examples of all the categories listed in Table (1) can be found in Table (2) together with references where the actual devices are described. To aid in the reading of Table (2) , Fig(1) shows schematically some of the most important processes included in this table. Interestingly enough , most of the seemingly entirely different processes included in Table (2) have important features in common. The basic physical phenomena involved with the performance of RSP systems are described in Table (3). A glance at this table readily shows that the most important physical processes taking place during RSP operations are: (i) The fluid flow phenomena associated with the spreading, squeezing, thinning and breaking up of molten metal samples, and (ii) the energy transfer processes governing the cooling and the solidification of such samples.

It should be noted that even though very much the same physical processes are at work in all RSP systems, subtle differences in design can produce significant changes in the characteristics of

Table (3.1.1).-   Rapid Solidification Processing Systems

I)   Melt Fragmentation Processes

    a)   Fragmentation produced by moving solids

    b)   Fragmentation produced by moving fluids

II) Splatting Processes

    a)   Splatting to produce particulate material

    b)   Splatting to produce continuous material

III) Direct Quenching Without Fragmenting or Splatting

IV) Melting and Quenching of Thin Surface Layers

V)   Liquid Dynamic Compaction and Spray Deposition

Table (3.1.2).-   Some Examples of RSP Systems

Ia)   Melt Fragmentation Produced by Moving Solids

    1) Rotating Cup or Dish   Glickstein et al(1978)

    2) Rotating Perforated Cup   Daugherty(1964)

    3) Rotating Electrode Process   Champagne & Angers(1984)

    4) Impact Disintegration   Schmitt(1979)

    5) Vibrating Electrode   Ruthardt & Lierke(1981)

    6) Melt Drop Technique   Aldinger et al(1977)

    7) Twin Roll Technique   Singer et al(1980)

    8) Single Roll w/Serrated Surface   Carbonara et al(1982)

    9) Melt Extraction w/Serrated Wheel Pond et al(1976)

  10) Single Roll Atomization   Narasimha & Sekhar(1984)

Ib)   Melt Fragmentation Produced by Moving Fluids

    1) Water Atomization   Tallmadge(1978)

    2) Subsonic Gas Atomization   Beddow(1978)

    3) Ultrasonic Gas Atomization   Grant(1983a)

Table (3.1.2).- (contd.)

IIa)   Splatting for Particulates

    1) Gun-Ski jump Device   Duwez & Willens(1963)

    2) Piston and Anvil Device   Strachan(1967)

    3) Injection Chill Mold   Hinesley & Morris(1970)

    4) Isolated Droplets on Chill   Madejski(1976)

    5) Rotating Impactor   Predel(1978)

IIb)   Splatting for Ribbon or Sheet

    1) Chill Block Melt Spinning   Liebermann & Graham(1976)

    2) Centrifugal Melt Spinning   Chen & Miller(1976)

    3) Planar Flow Melt Spinning   Fiedler et al(1984)

    4) Melt Drag   Hubert et al(1973)

    5) Twin Roll Quenching   Murty & Adler(1982)

    6) Melt Extraction   Robertson et al(1978)

Table (3.1.2).- (contd.)

III)   Direct Quenching Without Fragmenting or Splatting

    1) Melt Extrusion   Shepelsky & Zhilkin(1968)

    2) Taylor Wire Process   Manfre et al(1974)

    3) Free Flight Melt Spinning   Kavesh(1976)

IV)   Melting and Quenching of Thin Surface Layers

    1) Laser Processing   Breinan & Kear(1983)

    2) Electron Beam Processing   Mawella(1984)

V)   Liquid Dynamic Compaction and Spray Deposition

    1) Liquid Dynamic Compaction   Singer & Evans(1983)

    2) Plasma Deposition   Apelian et al(1983)

(Ia.1)

(Ia.9)

(Ib.3)

(IIa.1)

(III.3)

(IIb.1)

(IV.1)

(V.1)
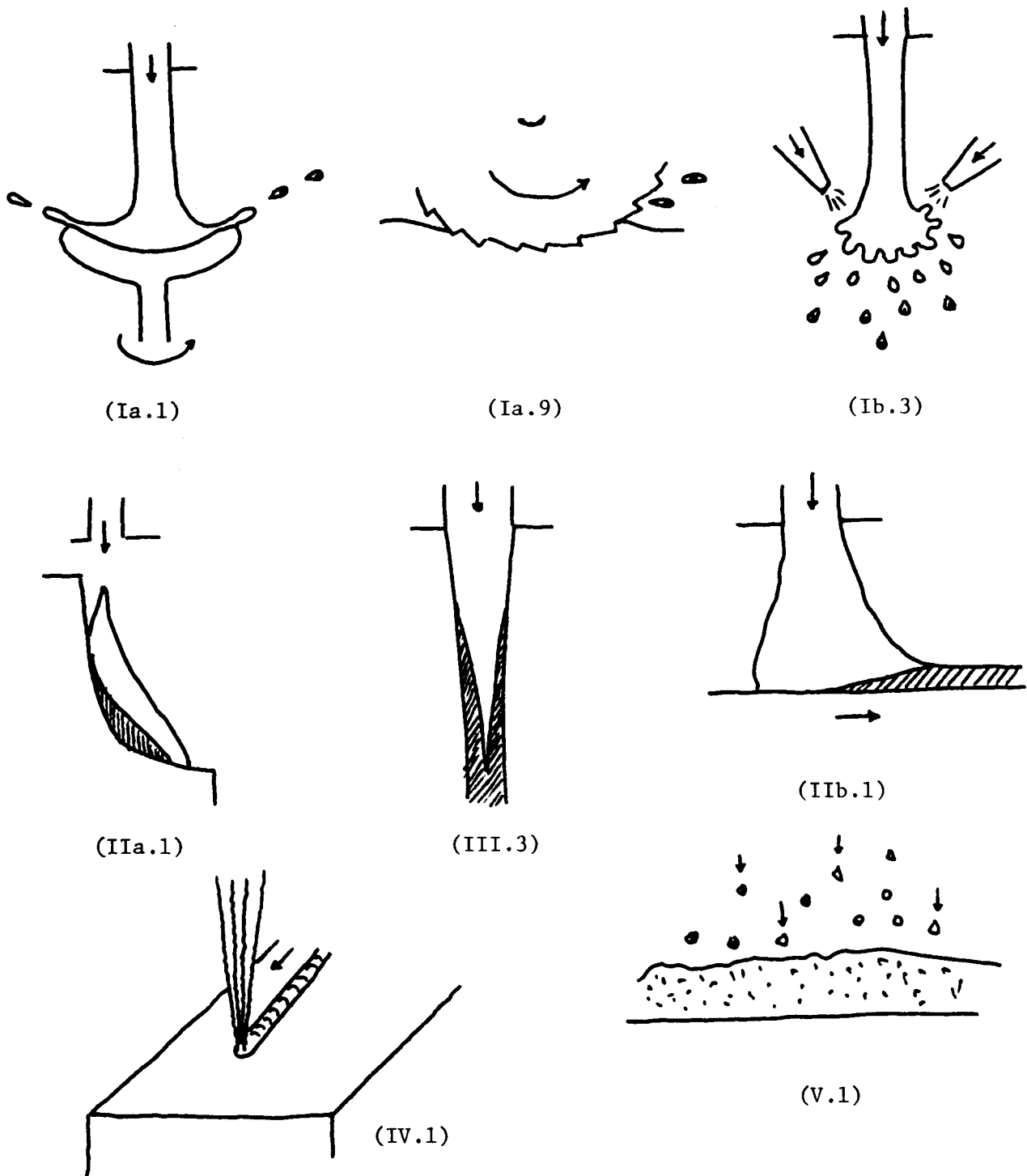
Fig(3.1.1).-   Schematic Representation of Some Typical RSP

Systems. See also Table(3.1.2).

Table (3.1.3).-   Basic Physical Processes During RSP

Ia)   Melt Fragmentation Produced by Moving Solids

   1) Fluid Flow Phenomena

      a) Impact and Spreading of Melt on Moving Solid

      b) Melt Thinning and Acceleration

      c) Melt Fragmentation Proper

         i) Direct Drop Formation

         ii) Ligament Formation

         iii) Film Formation

      d) Bursting of Melt by Impactor

      e) Capillary Wave Atomization

      f) Cavitation Inside Melt

      g) Shearing of Melt by Serrated Disk

   2) Heat Transfer Phenomena

      a) Cooling

      b) Freezing

Table (3.1.3).-   (contd.)

Ib)   Melt Fragmentation Produced by Moving Fluids

   1) Fluid Flow Phenomena

      a) Melt Thinning

      b) Growth of Disturbances on Melt Surface

      c) Formation and Tearing of Ligaments from Melt Sheet

      d) Growth of Disturbances on Surface of Ligaments

      e) Formation and Separation of Droplets

      f) Droplet Breakup

   2) Heat Transfer Phenomena

      a) Cooling

      b) Freezing

IIa)   Splatting for Particulates

   1) Fluid Flow Phenomena

      a) Impact and Spreading of Melt on Substrate

      b) Squeezing of Melt between Two Substrates

Table (3.1.<u>3</u>).-   (contd.)

2) Heat Transfer Phenomena

   a) Cooling

   b) Freezing

IIb)   Splatting for Ribbon or Sheet

1) Fluid Flow Phenomena

   a) Ejection of Melt from Nozzle

   b) Impact, Adhesion and Spreading of Melt on Moving Chill

   c) Impact, Adhesion , Spreading and Squeezing of Melt
      between Nozzle and Moving Chill

   d) Squeezing of Melt betwee Two Moving Chills

   e) Capillary Flows

2) Heat Transfer Phenomena

   a) Cooling

   b) Freezing

Table (3.1.3).- (contd.)

III) Direct Quenching Without Fragmenting or Splatting

    1) Fluid Flow Phenomena

        a) Stabilization of Liquid Metal Jet

        b) Velocity Relaxation in Melt Jet

    2) Heat Transfer Phenomena

        a) Cooling

        b) Freezing

IV)   Melting and Quenching of Thin Surface Layers

    1) Fluid Flow Phenomena

        a) Motion on Free Surfaces

        b) Surface Tension Driven Flows

        c) Natural and Forced Convection

    2) Heat Transfer Phenomena

        a) Cooling

        b) Freezing

Table (3.1.3).-   (contd.)

V)   Liquid Dynamic Compaction and Spray Deposition

1) Fluid Flow Phenomena

a) Impingement, Spreading and Mixing of Falling Droplets on
either Shallow Melt Pools, Mushy Surfaces or Solid Droplets

2) Heat Transfer Phenomena

a) Cooling

b) Freezing

the products of processing. The varying degrees of interaction between the fluid flow and the heat transfer phenomena in the various processes account for the observed differences in process performance. For example, although a molten jet is thinned during both gas atomization and melt spinning, complete breakup to form powder is the final objective in the first case, while the formation of a continuous ribbon is desired in the latter. It is, thus, the interplay between spreading and thinning rates on the one hand and cooling and freezing rates on the other that accounts for the wide variety of existing RSP systems .

As expected, the different techniques will produce rapidly solidified products with structures (and properties) peculiar to them and thus, widely different microstructures may be found in samples of the same material produced by different techniques. This complexity makes necessary a case by case study of the various processes.Fortunately, despite the idiosyncracies of the different RS techniques, the same fundamental principles of continuum mechanics are applicable to all of them. This fact provides the unifying feature for the mathematical modeling of RSP systems.

3.2.-   Mathematical Models for RSP Systems. Newtonian Cooling.

Mathematical models based on heat transfer considerations have

long been used to estimate the cooling and freezing rates obtained during RSP . Because of their inherent simplicity, lumped parameter models were almost always invariably adopted. The main assumption involved in all of these early models was the neglect of temperature differences across the sample thickness , i.e. Newtonian cooling conditions. Mathematical models of heat transfer and solidification based on the assumption of Newtonian cooling always lead to ordinary differential equations which are relatively easy to solve.

In this section we describe the formulation and the solution of mathematical models of RSP systems based on the assumption of Newtonian cooling. Because of their simplicity, the models can be very general. Furthermore, to avoid the drudgery of hand calculating the cooling and solidification rates we have included (in Ch. 5) a computer program capable of doing all the necessary computations.

In the description which follows we first present the formulation for the processes resulting in separated particles and then go on to describe the formulation for those processes resulting in ribbon, sheet or wire.

a) Lumped parameter models for discrete splats

Let A and V be , respectively, the splat surface in contact with the heat sink and the total volume of the sample (Fig(1)). An overall heat balance for the splat is composed of three separate

2 Z

(a)

2 Z

(b)

2 Z
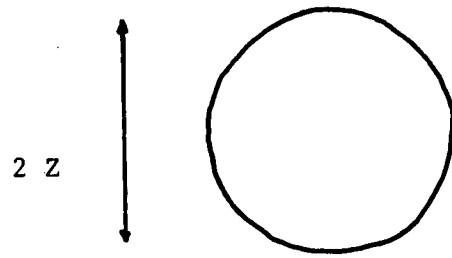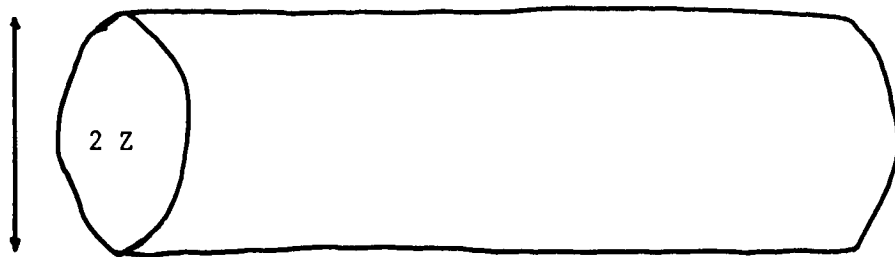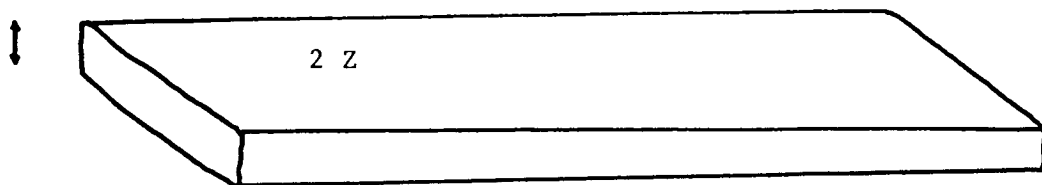
(c)

Fig(3.2.1).- Schematic representation of RSP systems used for heat transfer calculations according to the lumped parameter model. (a) Sphere , (b) cylinder, and (c) slab.

stages:

(i) Cooling of the melt down to the melting point

$$\rho \, V \, C_p \, dT/dt \quad = \quad - \, h \, (T - T_\infty) \, A \qquad\qquad (1),$$

(ii) solidification of the sample at constant temperature T_f

$$V \rho \, L \, df_s/dt \quad = \quad h \, (T_f - T_\infty) \, A \qquad\qquad (2),$$

and

(iii) cooling of the solidified sample

$$\rho \, V \, C_p \, dT/dt \quad = \quad - \, h \, (T - T_\infty) \, A \qquad\qquad (3).$$

Integrating Eqns(1)-(3) between suitable limits produces the following expressions for the temperature and the cooling and freezing rate;

For stage (i)

$$T \quad = \quad (T_p - T_\infty) \, \exp(- \, h \, A \, t/V \rho \, C_p) \quad + \quad T_\infty \qquad (4a)$$

$$dT/dt \quad = - \, (T_p - T_\infty)(h \, A/V \rho \, C_p) \, \exp(- \, h \, A \, t/V \rho \, C_p) \qquad (4b)$$

For stage (ii)

$$f_s \quad = \quad h \, A \, (T_f - T_\infty)(t - t_{ss})/V \rho \, L \qquad\qquad (5a)$$

$$df_s/dt = h A (T_f - T_\infty)/V \rho L \tag{5b}$$

And for stage (iii)

$$T = (T_f - T_\infty) \exp(- h A (t - t_{es})/V \rho C_p) + T_\infty \tag{6a}$$

$$dT/dt = - (T_f - T_\infty)(h A/V \rho C_p) \exp(- h A (t - t_{es})/V \rho C_p) \tag{6b}$$

In these expressions t_{ss} is the time for the start of freezing and t_{es} is the time for the end of solidification.

If we write Z for the radius of the sphere or of the cylinder or for the half-thickness of the slab in Fig(1), the following relationships hold,

$$A/V = 3/Z \qquad \text{for the sphere} \tag{7a}$$

$$A/V = 2/Z \qquad \text{for the cylinder} \tag{7b}$$

$$A/V = 1/Z \qquad \text{for the slab} \tag{7c}$$

Moreover , the solidified thickness at any given time can be obtained from the fraction solidified as follows,

$$z = Z (1 - f_s)^m \tag{8}$$

where m takes the values of 1/3 , 1/2 , and 1 , respectively, for the sphere, the cylinder and the slab. We note that all these relationships were derived for the situation in which the heat extraction takes place through all sides of the sample. However , the heat lost through the ends of the cylinder or through the edges of the slab has been neglected.

Equations (4)-(8) can be used to estimate cooling and freezing rates in a wide variety of RSP systems. The FORTRAN program RSPNN presented in Sec(5.1) below has been designed to perform these calculations.

b)   Lumped parameter models for continuous processes

Let H(x) be the local melt thickness (see Fig(2)). In this case we perform the overall heat balance on volume elements of size Δx along the downstream direction. These volume elements are assumed to be moving in a plug flow fashion. Proceeding as before, after integration , the following expressions for the temperature and the fraction solidified can be obtained,

$$T_{x+\Delta x} = (T_x - T_\infty) \exp(-h A \Delta x/V \rho C_p \bar{V}_x) + T_\infty \tag{9}$$

and

$$f_{s_{x+\Delta x}} = f_{s_x} + h A (T_f - T_\infty) \Delta x/V \rho L \bar{V}_x \tag{10}$$

51
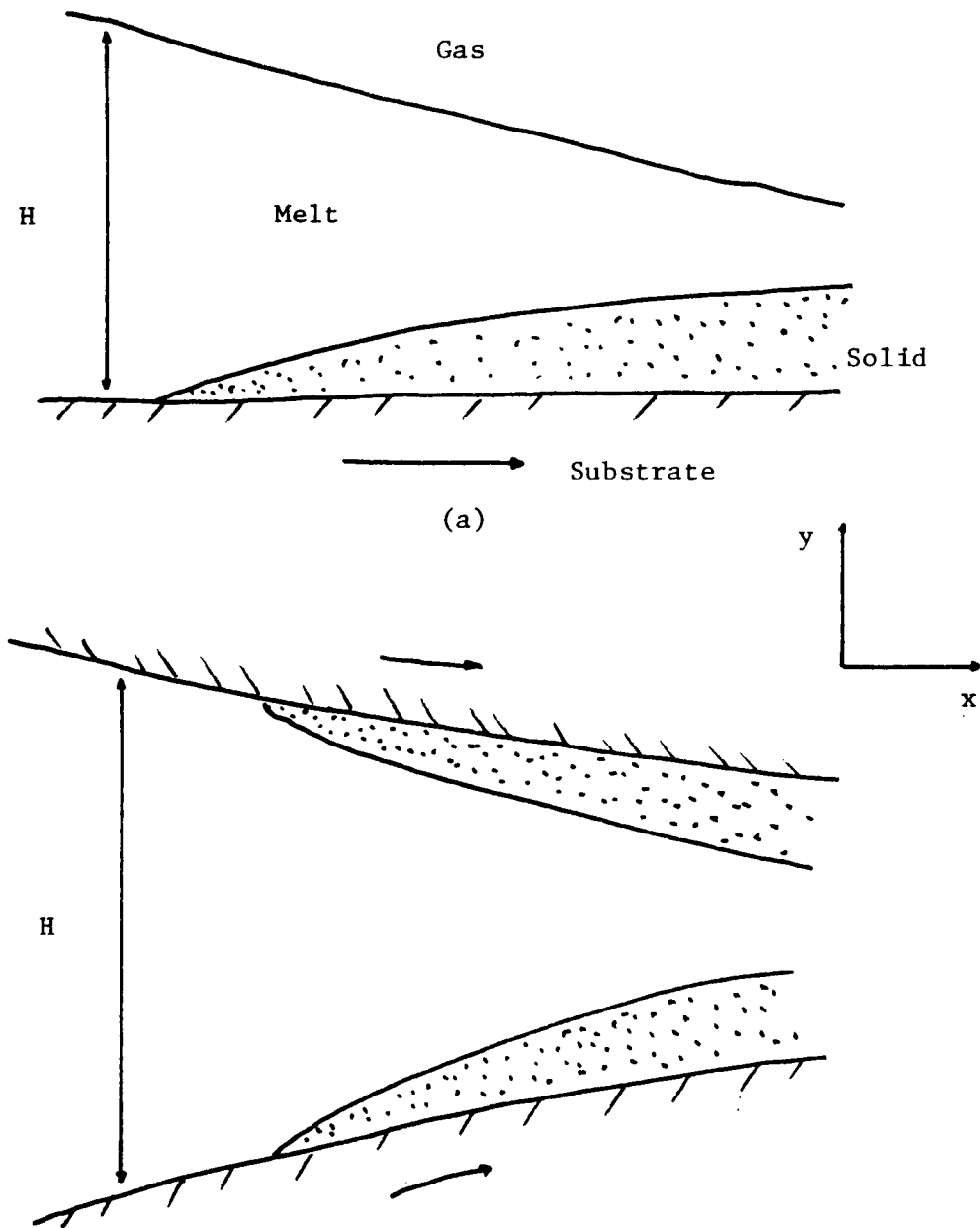
Fig(3.2.2).- Schematic representation of RSP systems used for heat transfer calculations according to the lumped parameter model. (a) Sheet cooled from one side, and (b) from two sides .

52

where the subindex x denotes the location along the downstream direction corresponding to a given T or a given f_s .

From geometrical considerations again , the quantity A/V is given by

$$A/V = 4/H \qquad \text{for the cylinder}$$

$$A/V = 2/H \qquad \text{for the sheet cooled from two sides}$$

and

$$A/V = 1/H \qquad \text{for the sheet cooled from one side.}$$

Moreover, the relationship between the actual solidified thickness and the local fraction solidified is ,

$$y_s = (H/2)(1 - (1 - f_s)^{1/2}) \qquad \text{for the cylinder}$$

$$y_s = (H/2) f_s \qquad \text{for the sheet cooled from two sides}$$

and

$$y_s = H f_s \qquad \text{for the sheet cooled from one side.}$$

Equations (9) and (10) must be applied repeatedly, marching forward along the downstream direction to obtain cooling and freezing profiles.

The single most important adjustable parameter in the above equations (as well as in those to be presented in Sec(3.3) below), is the heat transfer coefficient. The value of this coefficient directly determines the cooling and freezing rates of the rapidly

solidified sample. Since these rates are directly related to the structure of the material, the availability of realistic values of h is a question of great importance. The use of heat transfer coefficients to describe the complex heat transfer phenomena which take place at interfaces between phases is justified as long as there are no more rigurous means of describing such processes. For the convenience of the reader who wishes to perform heat transfer calculations similar to the ones reported in this thesis, and also for comparative purposes, we have compiled in Table (1) a list of suggested values of the heat transfer coefficients for a wide variety of casting/solidification processes. The sources have also been included.

In the past, thermal and microstructural measurements have been employed for the estimation of h . We now suggest the use of the coefficients in Table (1) to calculate thermal responses and the resulting microstructures .

3.3.-   Mathematical Models for RSP Systems.Non-Newtonian Cooling.

In some cases , the assumption of Newtonian cooling conditions can be grossly inadequate. It may be that the temperature gradients across the splat just cannot be neglected. This is particularly true for those RSP systems whose performance strongly depends on the existence of large temperature gradients across the splat.

Table (3.2.$\underline{1}$).-   Heat Transfer Coefficients Typical of Casting-Solidification Processing Operations.

System	Sample Size (μm)	h (cal/cm^{2}s^{o}C)	Source
Rotating Dish Atomization of IN-100 (P&W)	20 – 500	0.2 – 700	Glickstein et al(1978)
Gun-Ski jump Splat of Al on Ni	0.1 – 5	2.7 – 6.8	Predecki et al(1965)
Piston & Anvil Splat of Al on Fe	76	0.4 – 5	Harbour et al(1969)
Die Casting Al on Steel	1600	1.9	Mehrabian (1982)
Metal Splat on Metal Substrate	not given	2.4 – 24	" "
Atomization of Al (Radiation Cooling)	100	0.0013	Jones(1982)
Atomization of Al (Convection Cooling)	100	0.24 – 2.4	" "
Gun on Flat Substrate Al Splat	1 – 140	2	" "
Gun on Flat Substrate Fe Splat	1 – 100	1 – 1000	Ruhl(1967)

Table (3.2.1).- (contd.)

System	Sample Size (μm)	h (cal/cm^2 s^{o}C)	Source
Gun on Flat Substrate			
Al-Cu Splat on Glass	25 - 100	0.956	Scott(1974)
Piston & Anvil			
Al-Si Splat	25 - 50	24 - 215	Williams & Jones(1975)
Gun on Flat Substrate			
Al Splat	100	0.95	Jones(1971)
Gun Method Fe-Ni			
Glass Splat	0.1 - 0.3	24 - 240	Davies(1978)
Twin Roll Fe-Ni			
Glass Splat	40	2.4 - 24	" "
Chill Block MS			
Fe-Ni Glass Splat	20	2.4	" "
Chill Block MS			
Al-Si & Nimonic Splats	20 - 50	1.67	Vincent et al(1980)
Conventional Cast			
Al & Pb on Fe	20000	0.027	Sully(1976)
Continuous Cast			
Steel on Water Cooled Cu	50 000	0.03	Hills(1965)

Table (3.2.<u>1</u>).- (contd.)

System	Sample Size (μm)	h (cal/cm^2 s^{o}C)	Source
Free Flight MS Metglass on Brine	100	0.04	Kavesh(1976)
Planar Flow MS Fe-B Glass	20 - 40	12 - 50	Huang & Fiedler(1981)
Atomization of Undercooled Al	50	0.0678	Gill et al(1984)
Melt Extraction Fe-Ni Wires	25 - 1000	0.1	Robertson et al(1978)
Direct Chill Horizontal Continuous Casting Al, Pb, Sn, and Zn	20 000	0.024 - 0.86	Weckman & Niessen (1984)
Atomization	10	2.4	Cohen et al in Mehrabian et al(1980)
Melt Spinning	25	2.4	" "
Self-Quenching	10	very large	" "
Rod Casting, Al	50 000	0.05	Davies & Westby(1974)

The avoidance of the Newtonian cooling assumption can lead to additional, important results which cannot be obtained from the simpler models. Moreover, there is the hope that the fewer approximations that are introduced into the model the closer to reality its predictions will be.

The opposite extreme to Newtonian cooling is to assume that the splat is in perfect thermal contact with the chill. This condition is known as ideal cooling. From the well known solutions to heat conduction problems under ideal cooling conditions (e.g. Carslaw and Jaeger(1959)) and from Schwarz's solution to the solidification problem (Sec(3A.2)), Jones derived approximate expressions for cooling and freezing rates under ideal cooling conditions. These are (see Jones(1982)):

$$dT/dt \quad = \quad B/x^2 \tag{1}$$

and

$$R \quad = \quad dx/dt \quad = \quad B'/x \tag{2}$$

where x is the distance in the slab from the chill and B and B' are functions of the relevant temperature intervals and of the material properties.

It is perhaps not surprising that neither the assumption of Newtonian cooling nor the one of ideal cooling represented by Eqns(1) and (2) seem to be able to accurately represent observed behavior. This means that even though the thermal contact at the

58

splat-chill interface is far from perfect, the temperature gradients across the splat cannot be neglected. This, most frequently found cooling regime, is conveniently called intermediate cooling.

In the sequel we present the details of the formulation and the solution of a model of a typical RSP system working in the intermediate cooling regime. In the description we will concentrate on the PFMS system since the bulk of our calculations were performed for that configuration. However, summary comments on the modeling of other RSP systems are also presented. We hope our methods to be sufficiently general as to allow their application to any other RSP system. Thus, after a detailed description of the model of the PFMS system and of the results obtained from it, we discuss some points about the Twin Roll RS system, the Piston and Anvil system, the Melt Fragmentation processes and the systems based on Surface Heating and on Spray Deposition.

3.3.1.- A Model of the Planar Flow Melt Spinning Process.

The Melt Spinning (MS) process is one of the most commonly used methods of RST . The principle of the technique is very simple. A sample is melted inside a crucible and then a sudden pressure surge ia applied to produce a thin liquid jet from a nozzle at the bottom of the crucible. This jet is in turn directed towards the surface of a rapidly moving wheel. On impingement,

the liquid jet transforms into a small puddle. Finally, a thin solid
ribbon is dragged from underneath the puddle by the moving wheel.

Two main variants of the MS process exist, namely the Chill
Block and the Planar Flow systems. The most significant difference
between the two techniques is the detailed nature of the puddle
formed at the point of impingement of the molten jet on the
wheel. The arrangement used in the PF process restrains the puddle
and promotes its stability. In Fig(1) we show schematic
representations of the melt puddles formed, respectively , in the
CBMS and in the PFMS process. It can be readily seen that in
the latter the nozzle is brought into close proximity with the
wheel.

In the following pages we present our mathematical model of the
PFMS process. We start by describing its formulation, then we
discuss the solution methodology employed and conclude with a
description of the results and some recommendations.

a)   Formulation of the Model.

Because of its potential applications, the MS process has
received a great deal of attention from the RS community. Most
of the studies to date, however , have been concerned with the
CB process whereas the interesting PF process has been left
somewhat aside. Interestingly enough, the peculiar arrangement
used in this latter system produces a fluid flow configuration
very similar to those observed in Lubrication Technology

Nozzle

Gas

Puddle

Ribbon

Moving Substrate
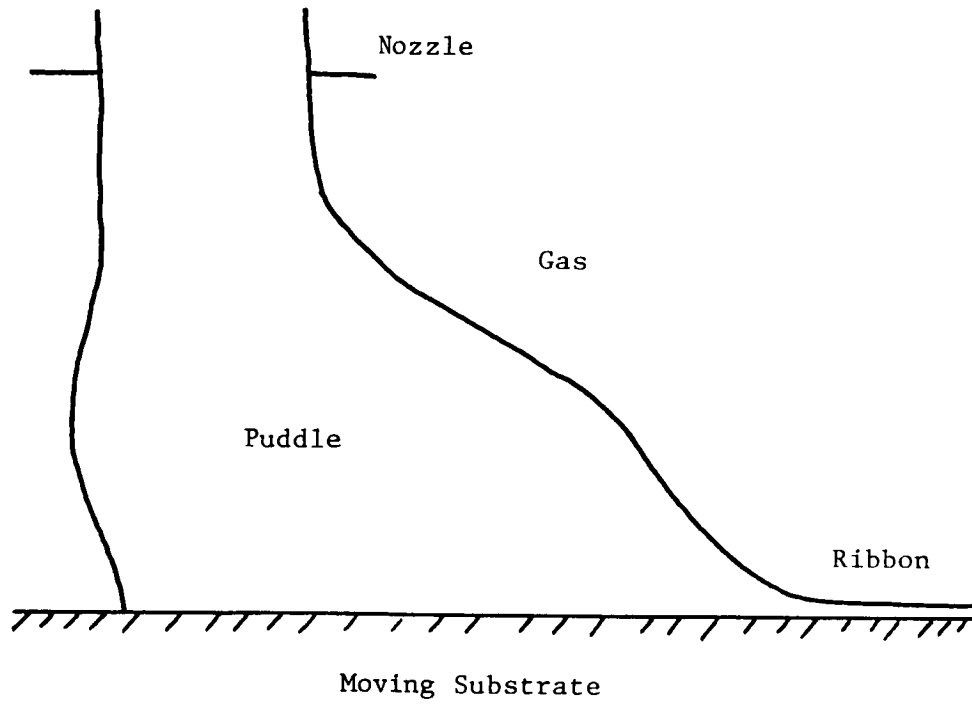
(a)
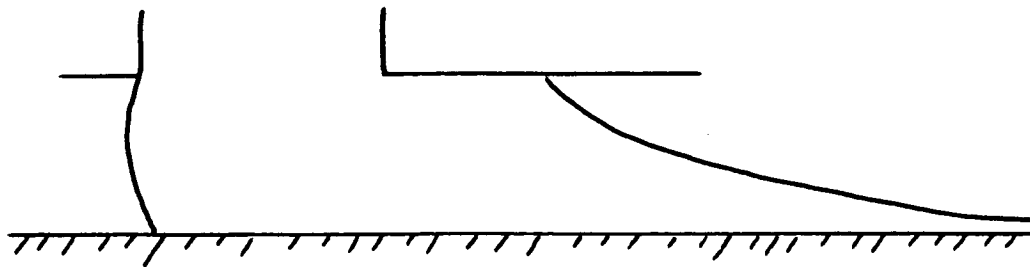
Fig(3.3.1.1).- Schematic comparison of melt puddle shapes for the (a) CBMS and (b) the PFMS systems.

systems. Since the two MS processes are closely related, we will

start this section by reviewing previous modeling work in this area.

Kavesh(1978) performed one of the first quantitative studies of

the effects of changes in the process parameters on the properties

of the products of CBMS . Using basic concepts from boundary

layer theory he constructed representations of the fluid flow

and the heat transfer phenomena taking place in the puddle.

Based on the well known smallness of the Prandtl number values

for metallic melts, he concluded that the mechanism responsible

for the final ribbon thickness emerging from the puddle was the

rate of heat transport out of the melt and into the chill. Kavesh

also presented closed form expressions relating the geometry of

the melt spun ribbons to important process parameters such as the

melt flow rate and the wheel velocity. These relationships have

been extensively used as a basis for many subsequent empirical

studies of the process (e.g. Charter et al(1980)).

Anthony and Cline(1978) also employed ideas from boundary layer

theory in the vorticity-stream function formulation. They obtained

closed form expressions demonstrating that the layer inside the

puddle in which most of the temperature change takes place was

many times larger than the shear layer due to wall induced

vorticity.

den Decker and Drevers(1980) used again boundary layer theory,

this time combined with the equations of phase change kinetics by

nucleation and growth and incorporating the temperature dependence

of the melt viscosity. They were able to compute both the final

ribbon thickness and the crystal to glass ratio in the resulting

ribbons as a function of the process parameters. In their conclu-

sions, they agreed with the results of previous researchers in

that the computed thermal boundary layers were much thicker than

the corresponding momentum boundary layers.

Katgerman(1980) modeled the flow in the puddle using the x-

component of the momentum balance equation in a coordinate

system fixed to the solidification interface. He also used

approximate closed form expressions to represent the freezing

and computed the thicknesses of the momentum and thermal boundary

layers for several cooling conditions at the splat-wheel inter-

face. He also concluded that the transfer of thermal energy

played a predominant role in the determination of the final ribbon

thickness.

Vincent et al(1982) reviewed work on the modeling of MS and,

using also concepts from boundary layer theory, concluded that

momentum transport was the dominant mechanism controlling the

final ribbon thickness. A similar conclusion was reached by

Takeshita and Shingu(1983) who incorporated the temperature

dependence of the melt viscosity in their calculations of flow

and heat transfer using the equations of boundary layer theory.

Three main points emerge as a result of the preceding review

of the literature. First , although all investigators have used

basically the same equations in one form or another, there is

no agreement as to the true mechanism controlling the final ribbon thickness. Momentum transport, heat transfer, and mixed mechanisms have all been proposed. Secondly , no distinction has been drawn between the CB and the PF processes , and the bulk of the simulations have been done for the first of these. We believe that the two processes , although very similar at first sight, possess however some features which warrant separate treatments. Finally we note that most of the previous models of the MS process have dealt with metallic glasses thus avoiding the problems associated with the release of the latent heat during solidification.

Miyazawa and Szekely(1981,1979) have used a different approach to model other, somewhat related RSP systems. They have chosen to represent the flow phenomena taking place inside the splat during RS by a modified form of the Navier-Stokes equations in which the inertia forces are considered negligible compared with the viscous and pressure forces. The same approach has long been used by mechanical engineers to represent systems in which moving solid surfaces are separated by thin fluid layers and the resulting equations constitute the basis of the so called theory of lubrication. The use of lubrication theory to represent fluid flow in RSP systems was considered appropriate since small sample sizes in at least one spatial direction are one of the important features of these systems. In this sense they are analogous to the systems encountered in ball bearings.

Encouraged by the results reported by Miyazawa and Szekely

for the piston and anvil and for the twin roll devices we decided
to proceed further and investigate the use of lubrication theory
for the representation of the flow behavior in the puddle of a
PFMS system producing crystalline ribbons.

The governing equations for fluid flow and heat transfer-
solidification subject to the assumption of negligible inertia
forces are (see Sec(3A.1)-(3A.3));

The equation of continuity

$$\text{div } \underline{V} \quad = \quad 0 \tag{1},$$

the equation of motion

$$\text{div}(\mu \text{ grad } \underline{V}) \quad = \quad \text{grad } P \tag{2},$$

the differential energy balance

$$\underline{V} \cdot \text{grad } E \quad = \quad \text{div}(K \text{ grad } T) \tag{3},$$

and the enthalpy-temperature relationship

$$E \quad = \quad \begin{cases} E_f + (T - T_L) \rho C_p & , \quad T > T_L \\ E_f((T - T_S)/(T_L - T_S)) & , \quad T_S \leq T \leq T_L \\ (T - T_S) \rho C_p & , \quad T < T_S \end{cases} \tag{4}.$$

Equations (1)-(3) may be simplified still further for the case of the schematic PFMS system shown in Fig(2) . So , by introducing the following simplifying assumptions,namely ; (i) planar flow conditions, (ii) negligible y-momentum compared with the x-momentum, (iii) velocity derivatives along the downstream coordinate negligible compared to derivatives across the puddle thickness, (iv)convection in the y-direction negligible compared to convection in the x-direction and viceversa for conduction, and (v)physical properties constant independent of temperature , Eqns(1)-(3) become,

$$Q/w = \int_0^H V_x \, dy = (Q_s + Q_1)/w \qquad (1a)$$

$$\mu \, d^2V_x/dy^2 = dP/dx \qquad (2a)$$

$$V_x \, dE/dx = K \, d^2T/dy^2 \qquad (3a)$$

Equations (1a)-(3a) and (4) must now be solved subject to appropriate boundary conditions. The ones we have chosen , again based on the schematic of Fig(2) are; (i) partial slip or no-slip at the splat-wheel interface, (ii) melt flow rate constant and given, (iii) heat transfer at the splat-wheel interface specified by a heat transfer coefficient, (iv) heat flow through the top surface of puddle negligible compared to the heat flow
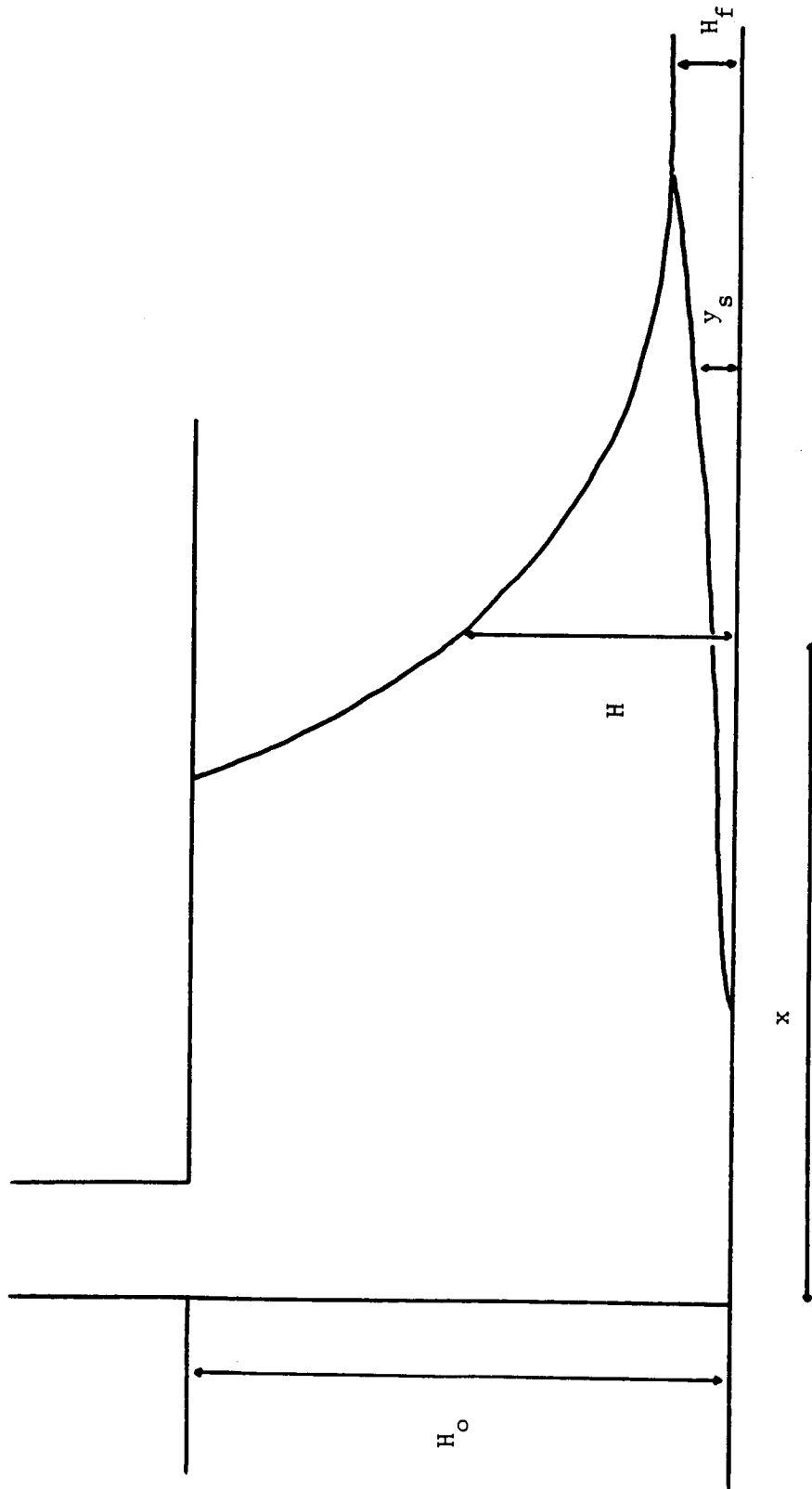
Fig(3.3.1.2).- Schematic representation of the PFMS system used in this study . See also Plate (3.3.1.1).
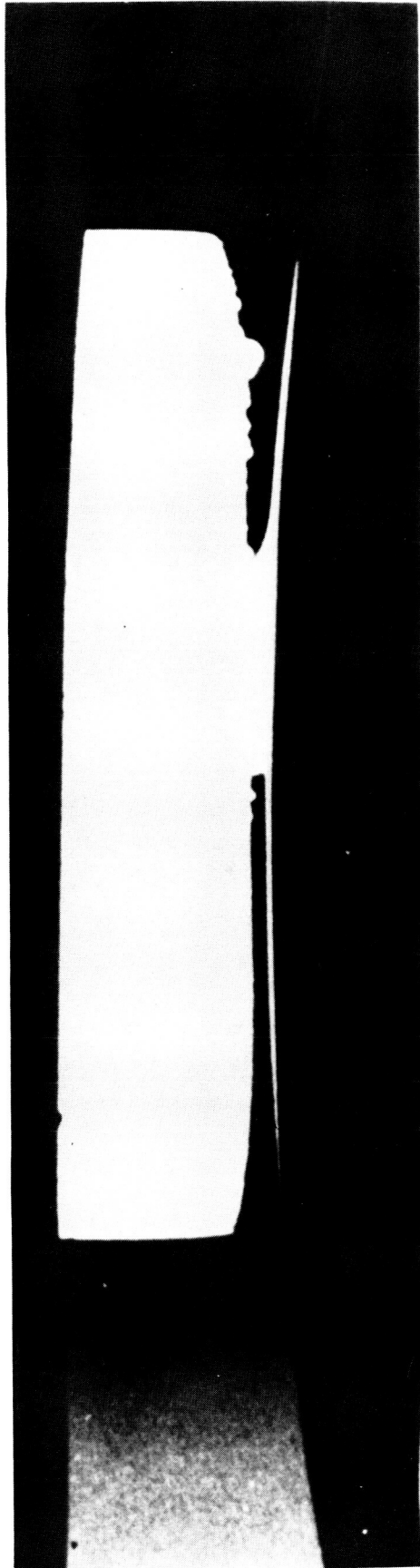
3.3.1.1.- Still frame from a high speed movie of the melt puddle during PFMS of Ni-base superalloy ribbons. The nozzle is at the top and the wheel at the bottom, moving from left to right. Courtesy of General Electric and NASA.

68

through the wheel, and (v) at the melt-gas interface downstream, the shear stress is so small that can be neglected but the normal stress is determined by the capillary pressure given by Laplace's equation.

We now briefly comment on the appropriateness of both the assumptions and the boundary conditions. Assumptions (i)-(iii) are considered adequate since the geometry of the system involves one characteristic spatial dimension which is much smaller than the other two. Assumption (iv) is plausible in view of the characteristic ability of molten metals to transmit heat more readily than momentum (small Prandtl number). Assumption (v) is also justified since we are interested in events happening inside the puddle and temperature extremes there are never greater thantwo or three hundred degrees.

Boundary condition (i) is used mainly to remove the stress singularity that it is known to result from the use of the no-slip condition at the line of contact melt-gas-wheel upstream. Condition (ii) is appropriate since the melt flow rate is ultimately specified by the imposed pressure in the crucible. Condition (iii) is adopted mainly as a means of making up for our ignorance about the details of the complicated events taking place at the splat-wheel interface. However, the best available values of h have been used. Boundary condition (iv) is justified as can be readily checked by comparing the heat losses due to radiation from the top with the heat lost by contact with

the wheel. Finally, condition (v) has been adopted to be able

to predict the exact location of the downstream meniscus and it

is based on the ideas of capillary hydrodynamics as described,

for example, by Levich(1962).

The complicating effects introduced by the consideration of

capillary phenomena warrant further comment. As can be seen in

Fig(2), the top surface of the puddle detaches itself from the

nozzle at some location along the downstream direction. After

this, the top surface of the puddle becomes free in the sense

that it is no more restrained by the solid nozzle lip. Moreover,

this free boundary adopts a shape determined both by the capillary

effect of the surface tension and by the solidification phenomena

taking place underneath the puddle. We must note that, since the

melt flow rate is constant, the amount of material passing through

any given section at constant x is the same regardless of the

particular location selected.

The solution of the complete free surface problem is a complex

matter. The addition of solidification effects would make the

problem intractable if it were not for the introduction of suitable

simplifying assumptions. Following Levich, we consider lubrication

theory still valid after the detachment point and assume that the

pressure acting across the puddle is given by Laplace's equation.

After some manipulation (Sec(3A.3)), the following expression for

the shape of the free surface is obtained ,

$$d^3 H_1/dx^3 \quad = \quad (3\mu/\sigma H_1^3)((Q_1/w) - V_{r_x} H_1) \qquad (5)$$

We have now completed the mathematical statement of the problem. What we have to do is to solve Eqns(1a)-(3a),(4) and (5) simultaneously subject to the boundary conditions mentioned above expressed in mathematical form. In the following section we describe our method of solution of this problem.

b) Solution Procedure.

We now describe the main features of the numerical algorithm we have used to solve the equations representing our model of the PFMS system. First, we note that for a given thickness of the solidified layer underneath the puddle, Eqns(1a) and (2a) may be readily integrated to produce closed form expressions for V_x and for P as function of the process parameters and of the material properties. However, in the region where the free surface forms after detachment from the nozzle, the thickness of the puddle is unknown in advance and must be calculated by solving Eqn(5) before we can proceed to integrate Eqns(1a) and (2a) to get V_x and P .

Once V_x is known, its average across the puddle thickness can be calculated and then Eqns(3a) and (4) can be solved to give the cooling and freezing rates at every point in the puddle. Since no closed form analytical solutions exist for this solidification problem, we resort to numerical methods. The simplest explicit finite difference scheme has been selected to perform this calculation. The scheme can be proved to be stable and consistent

as long as the step lengths satisfy the stability condition,

$$\alpha \ \Delta x \ / \ \overline{V}_x (\ \Delta y)^2 \ = \ 1/2 \qquad\qquad (6)$$

Equation (5) must also be solved numerically. We have found that the transformation of Eqn(5) into an equivalent set of three ordinary differential equations of first order which are then solved using a simple Euler forward scheme to advance the solution in the downstream direction, produces an algorithm which is both stable and consistent.

In summary, the complete set of steps we have used to solve the equations representing our model of the PFMS process is as follows:

(i) Before the detachment point, Eqns(1a) and (2a) are solved to obtain V_x and P . After detachment, however, Eqn(5) is solved first, advancing one step in the downstream direction to find the location of the free surface and then Eqns(1a) and (2a) are solved for V_x and P . In both cases , $\overline{V}_x$ is also computed.

(ii) Equations (3a) and (4) are then solved to find T(x,y) and the location of the solidification interfase y_s .

(iii) The puddle is swept in the downstream direction following the procedure indicated in (i) and (ii) until the free surface encounters the solidification interface. This is considered to be the end of the puddle. The point of intersection defines the final ribbon thickness.

We have constructed a FORTRAN computer program to perform the calculations indicated above. A typical run in the IBM 360 computer of the IPS at MIT using 31 grid points in the y-direction and about 5000 in the x- direction, required approximately 60 s of CPU time. The main criterion for the acceptance of the results was the satisfaction of overall mass conservation and thus only the results of runs for which this was true down to less than 0.1% were accepted. The program contains many comments which should make it easier to understand and it may readily be adapted into other computers having FORTRAN compilers. In the next section we describe and discuss the results that can be obtained with our program. The program listing itself, by the way, is included in Sec(5.4) below.

c)   Description of Results and Discussion.

We now present a summary description of the results that can be obtained with our model. The input data for the calculations have, for the most part, been kindly provided by G.E.-NASA. Additional data have been taken from the literature and, when values were lacking, the best available estimates were used. The material under study was a Ni-base superalloy and the whole set of input data is shown in Table(1) below.

Table (3.3.1.1).-   Input Data for the Calculations of the PFMS System.

Nozzle Breadth	0.064	cm
Crucible-Wheel Gap	0.030	cm
Slot Width	0.635	cm
Wheel Radius	12.7	cm
Wheel Velocity	1200	rpm
Ejection Pressure	$1.38 * 10^5$	$g/cm\ s^2$
Melt Flow Rate	3.86	cm^3/s
Pouring Temperature	1440	^{o}C
Puddle Length	0.29	cm
Ribbon Thickness	0.0038	cm
Melt Density	8.5	g/cm^3
Melt Viscosity	0.046	g/cm s
Melt Surface Tension	1778	g/s^2
Melt Specific Heat	0.15	$cal/g\ ^{o}C$
Melt Thermal Conductivity	0.0717	$cal/cm\ s\ ^{o}C$
Solidification Range	1315 - 1335	^{o}C
Latent Heat of Fusion	71.7	cal/g
Heat Transfer Coefficient	1 - 2	$cal/cm^2\ s\ ^{o}C$
Dynamic Contact Angle	160	^{o}
Initial Meniscus Curvature	6.89	cm^{-1}

Figure (3) shows the computed temperature field corresponding to what we have called the typical data set (see Table (1)). It should be noted that in Fig(3),as well as in Figs(2) and (4),the vertical scale has been enlarged considerably for clarity of representation. In reality, for the horizontal dimension shown, the vertical scale is about 1/10 to 1/20 of the size shown in these figures. This shoul give an idea of the size scales involved in the problem. Moreover, this should make clear that the isotherms in reality lie almost parallel to the surface of the substrate, and that most of the temperature change takes place inside a relatively thin layer close to the bottom surface of the puddle.

Other noticeable features in Fig(3) are as follows. First, as can be expected from the assumption of imperfect thermal contact at the splat-wheel interface, freezing does not start immediately on impingement at the point where the gas , the melt, and the wheel meet forming a line of contact. Moreover, when instead of a heat transfer coefficient we use a closed form expression representing ideal thermal contact (i.e. $h \rightarrow \infty$), solidification always started at the contact line. The resulting ribbon thicknesses , however, proved to be in all cases physically unrealistic since the solidified layer grew apparently too fast. Consistently throughout this work, the physically more satisfactory results were obtained when the assumption of non-ideal thermal contact at the splat-wheel interface was used.
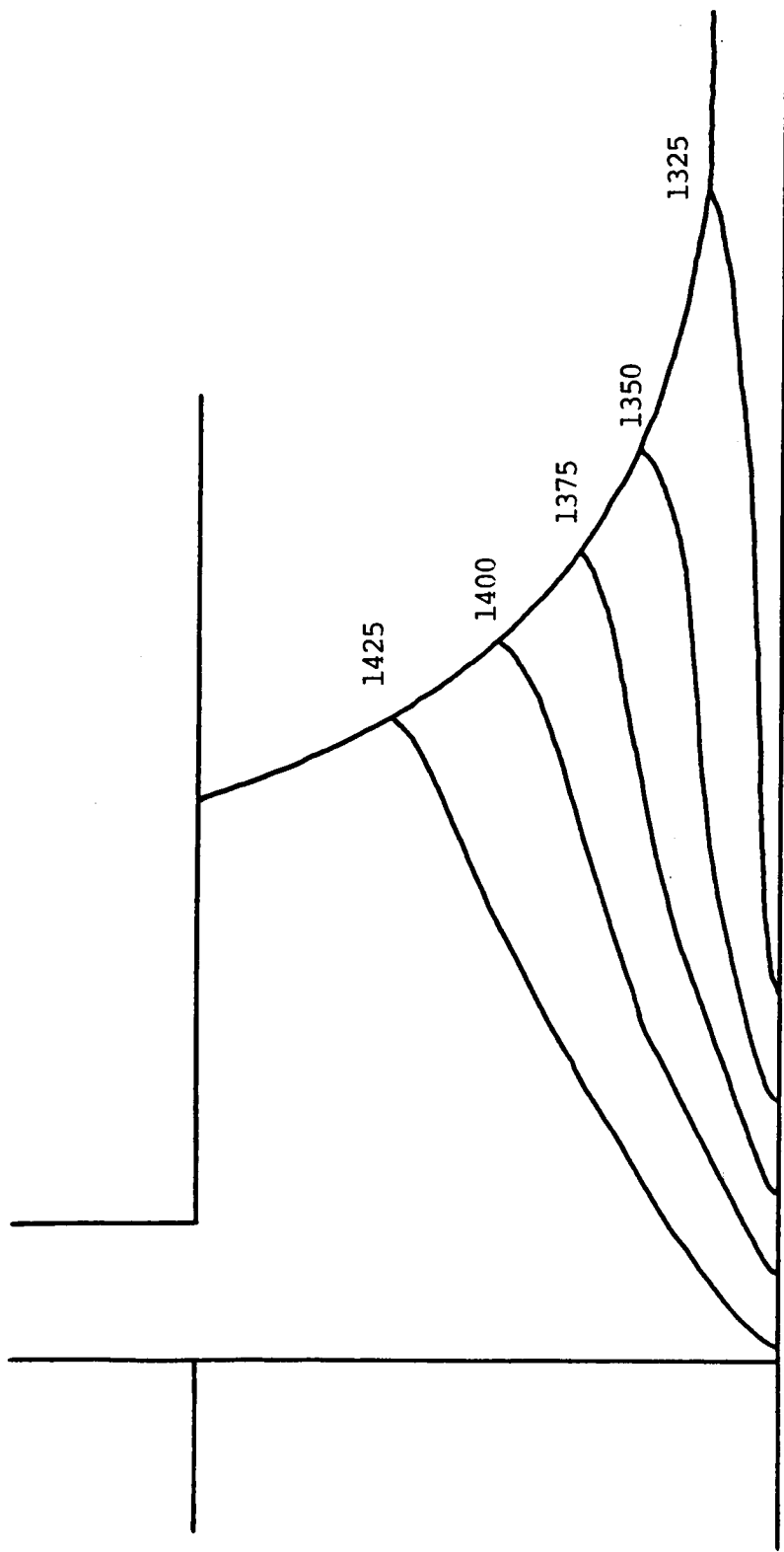
Fig(3.3.1.3).- Computed isotherm map inside the melt puddle. The solidifucation interface and the computed meniscus are also shown.

Also seen in Fig(3) is the inflexion point appearing on the isotherms as they approach the free surface. This change in curvature , corresponding to an increased cooling rate, coincides with the formation of the free surface after detachment. Apparently, the continuously diminishing puddle thickness observed after detachment has an influence on the thermal behavior in the form of increasing cooling and freezing rates. This observation leads to predictions about the variation of microstructure across the ribbon thickness which are in reasonably good agreement with measurements as described in more detail below.

Figure (4) illustrates the computed streamline pattern corresponding to the same typical run. We recall that when the values of the stream function on every pair of neighbouring streamlines differ by the same amount from one pair to the other, it is possible to perceive the variations in the magnitude and the direction of the velocity over the domain at a glance since the same mass is flowing between any pair of such lines. The existence of two characteristically different flow domains inside the puddle is readily noted. The closely spaced streamlines close to the moving wheel indicate the existence of large splat velocities there. The circulating streamlines lying on top, on the other hand,show that there is a large region of slowly recirculating flow centered approximately in the middle of the puddle at about the point of detachment.
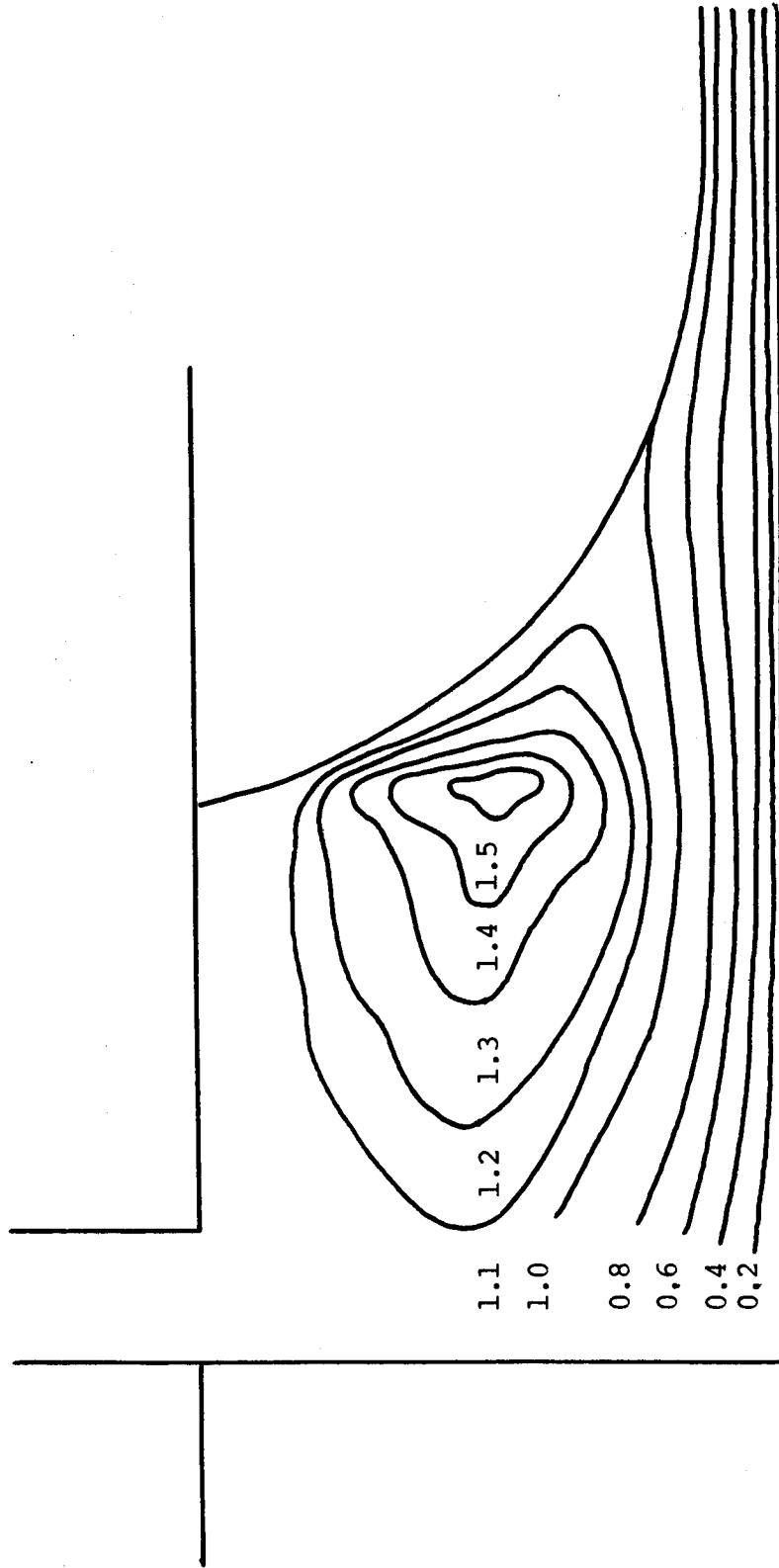
Fig(3.3.1.4).- Computed streamline map inside the melt puddle. See Plate(3.3.1.2).
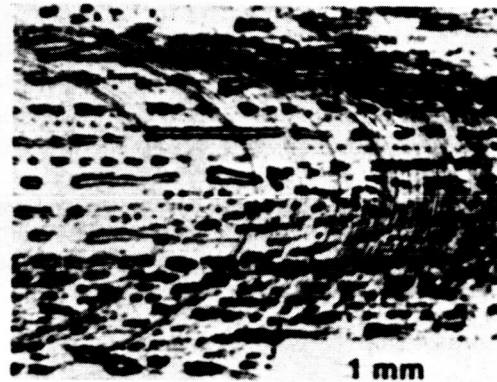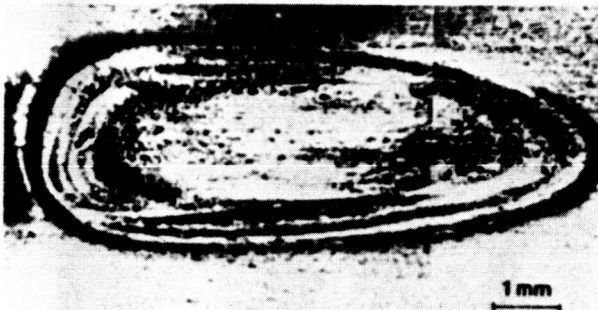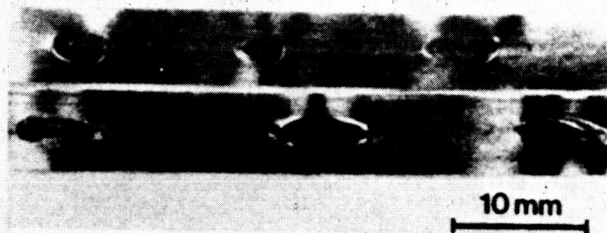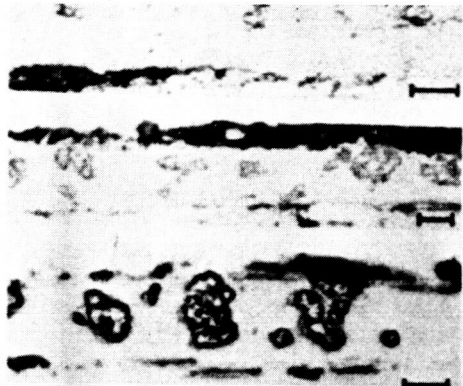
3.3.1.2.- Photographs of the longitudinal cross section, (a), and the top surface, (b)-(d), of planar flow melt spun ribbons obtained by introducing refractory powder together with the melt. The powder agglomerated and formed lumps inside the puddle. These lumps came out from the puddle at regular intervals of time. From Zielinski, P.G. and D.G. Ast(1983).

79

These regions of , respectively, recirculating and forward moving flow are separated by the streamline marked Υ = 1.0. This streamline , in turn, intersects the free surface at some location downstream forming what is called a stagnation point characterized by the velocity having the value of zero. It can also be seen in this figure that, inmediately after detachment, the layer of fluid lying above the partially solidified ribbon is dragged forward by the latter. However because of the melt fluidity, the liquid layer continues to thin down until the final ribbon thickness is reached. A final point worth noticing is the intense motion generated near the top surface of the puddle upon detachment resulting from the disappearance of the constraining effect of the nozzle wall.

The characteristic fluid flow field computed by our model certainly represents an alternative picture of the system when compared with the results of all previous mathematical studies of the flow in the melt puddle. Although the upward curvature of the streamlines near the wheel had been predicted before, and explained by the increasingly larger portion of the total flow rate carried by the partially solidified ribbon underneath moving downstream,no one had found a region of recirculating flow. Despite the difficulties involved in resolving this point we note that there seems to be some empirical evidence which strongly suggests the existence of such recirculatory flow in the puddle. Mention can be made,for example, of the experiments

performed by Zielinski and Ast(1983) where finelly divided powder

was introduced together with the melt. They suggest that the

regularly spaced lumps observed on the top surfaces of ribbons

produced by the PFMS process resulted from the agglomeration

of individual powder particles during the intense recirculating

motion taking place inside the puddle. In this sense, our results

provide the first quantitative evidence for the existence of

recirculatory motion inside the puddle of the PFMS system.

The photographs showing Zielinski and Ast's results have been

included here in Plate (3.3.1.2).

We note , finally , that the main features of the flow

phenomena taking place inside the PFMS puddle have also been

observed in other , somewhat related flow systems, namely in

the study of lubrication with cavitation (Savage(1977)) and in

the analysis of coating flows (Kistler and Scriven(1984)).

Figure (5) is a plot of the average cross-sectional cooling

rate calculated according to the formula

$$\bar{\dot{T}} = (1/H) \int_0^H V_x \ (dT/dx) \ dy \qquad (7)$$

against the downstream coordinate. One can readily see that the

cooling rate approaches 10^5 $^oC/s$ inside the puddle before the

start of solidification. However, the cooling rate peaks and then

decreases, first gradually and faster later as freezing sets in
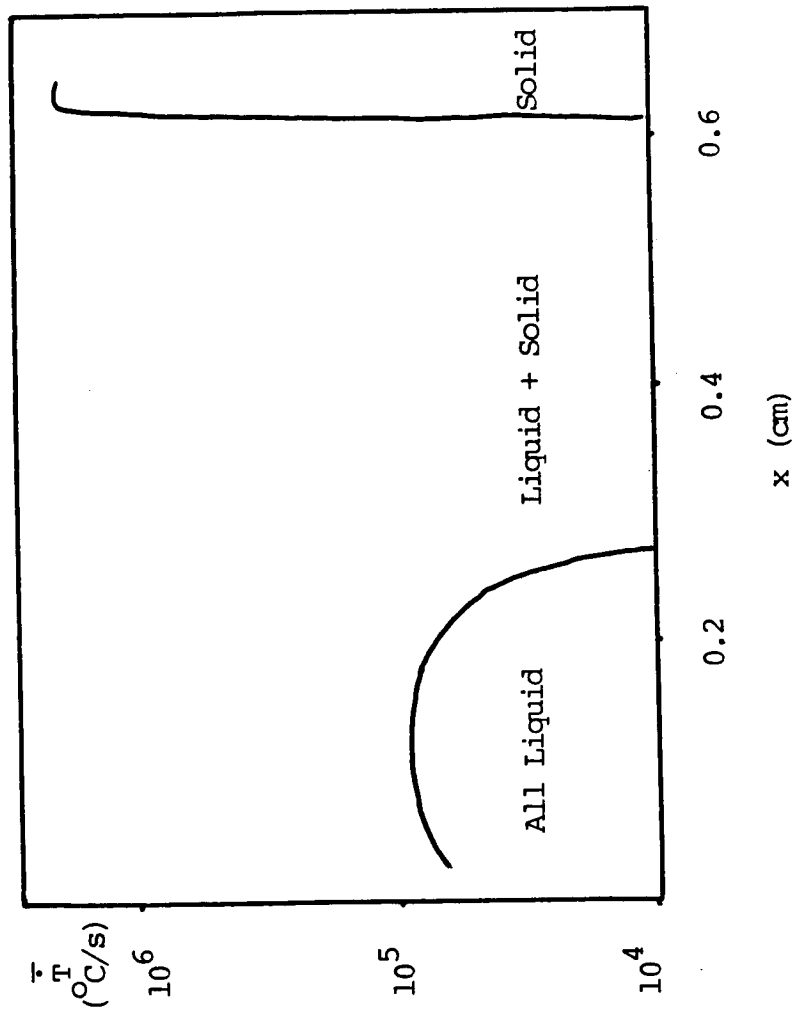
Fig (3.3.1.5).- Computed average cross-sectional cooling rate according to Eqn(7).

and the latent heat of fusion is released. Moreover , once the solidification is complete,and in agreement with the results of calculations for the Twin Roll system, the cooling rate rises again, this time reachinga value above 10^6 ^{o}C/s, mainly because of the smallness of the section being cooled. Most likely, since the splat is not firmly attached to the wheel, once the ribbon leaves the puddle the heat transfer coefficient should decrease and these high cooling rates may only be rarely observed.

It may be worth mentioning that a plot similar to Fig (5) can be constructed using the much simpler lumped parameter models described in Sec(3.2). So one may justifiedly ask why is it necessary to use the more complicated models which take into account the temperature gradients across the splat in order to represent mathematically the PFMS process ? .This can be answered by recalling the main purpose of our work which is the establishment of the relationships between the process parameters and the structure-properties of the resulting product. It should be understood that a model which neglects the existence of temperature differences across the splat will be unable to predict any microstructure variations across such thickness.

To point at the significance of the temperature differences existing across the thickness of the splat, in Fig(6) we present the computed temperatures on the top and bottom surfaces of the puddle/splat formed in the PFMS process, as a function of the downstream coordinate. As expected, one can readily see the
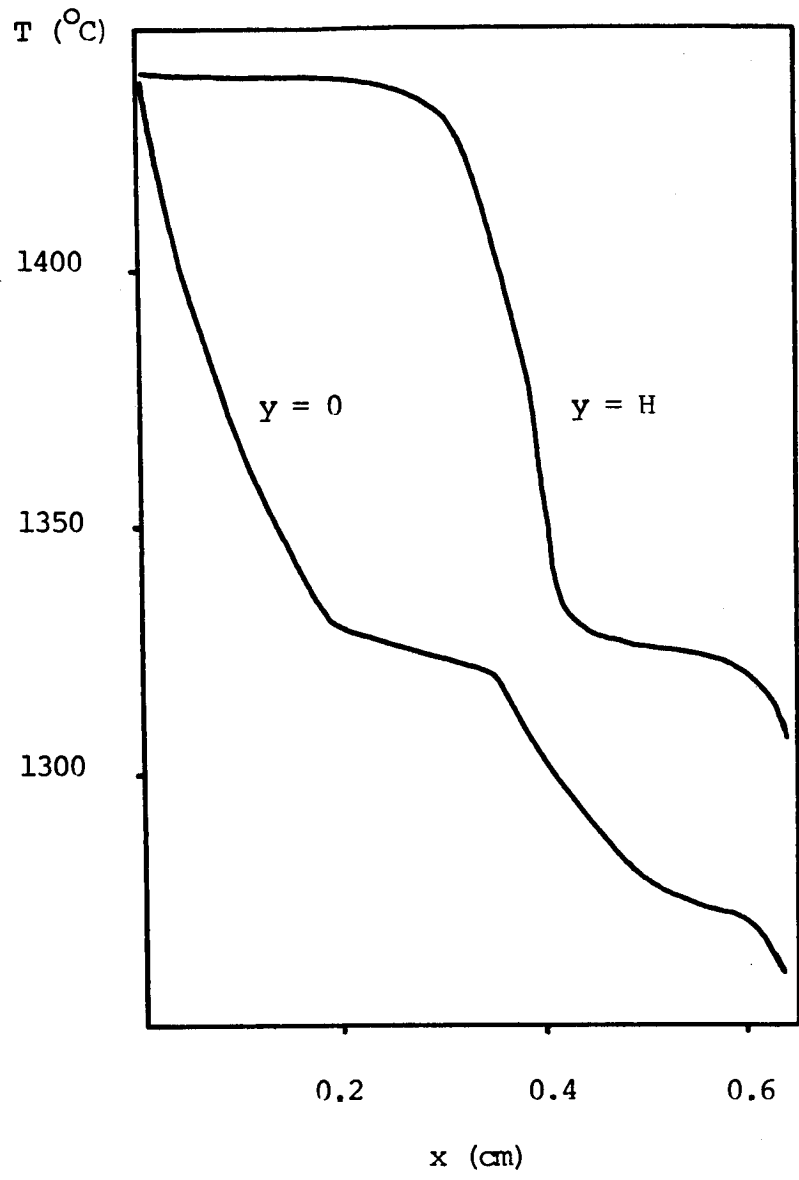
Fig (3.3.1.6).- Calculated temperatures along the top and bottom surfaces of the melt puddle as a function of the downstream coordinate.

Where (dT/dy) is the temperature gradient in the (approximately)
normal direction to the solidification interface, (dy_s/dx) is
the rate of thickening of the solidified layer along the down-
stream coordinate and V_x is the x- component of velocity at
the interface. From Eqn(8) , $\dot{T}_e$ can be calculated as a function
of the downstream location. To compare our calculations with
available experimental data we have used the fraction solidified
(relative to the final ribbon thickness) instead of the x
coordinate. The result of this calculation is shown in Fig(7).
The very large values of the cooling rate prevalent during the
first 1/10 fraction solidified are readily apparent. Also
clearly seen is the very sharp decrease from the large initial
values. A somewhat unexpected feature is the hump appearing
arounf f_s = 0.3 . This hump coincides with – and it may be the
result of – the detachment of the top surface of the puddle from
the nozzle. Finally, as the end of solidification is approached,
the effective cooling rate goes under 10^5 ^{o}C/s .

Considerable variations in the size of microstructural features
have long been observed in melt spun ribbons . For the alloys of
this study, measurements have been made to quantify this feature.
A photomicrograph of a longitudinal section of a ribbon has been
included here in Plate (3.3.1.3). We then decided to use the
result of our thermal calculations to attempt a prediction of
these microstructural variations. We started by looking for a
suitable dendrite arm spacing–cooling rate correlation. We were

C-2

very rapid decrease of the temperature of the bottom surface of the puddle following impingement. Somewhat unexpected, however, is the much slower decrease of the temperature of the top surface. Moreover, when the cooling rate on the bottom surface slows down as a consequence of the onset of solidification, the rate on the top surface increases markedly. This increase in cooling rate coincides and it may be related to the detachment from the nozzle. Finally, similarly to what happens to points along the bottom surface, the cooling rate slows down as the free surface approaches the solid-liquid interface. It can be seen that the cooling rate during solidification is somewhat smaller for the top surface than for the bottom surface of the ribbon. This is to be expected from the relative location of the chill with respect to these two surfaces. Finally, mention should be made also of the considerable temperature gradients existing in the puddle. We can expect these appreciable temperature differences (reaching even thousands of $^{\circ}C/cm$)to have a measurable effect on the nature of the resulting microstructure.

To further investigate this point we decided to compute the "effective" cooling rate experienced by points just ahead of the solidification interface. The effective cooling rate was computed from the following formula,

$$\dot{T}_e = (dT/dy)(dy_s/dx) V_x \qquad (8)$$
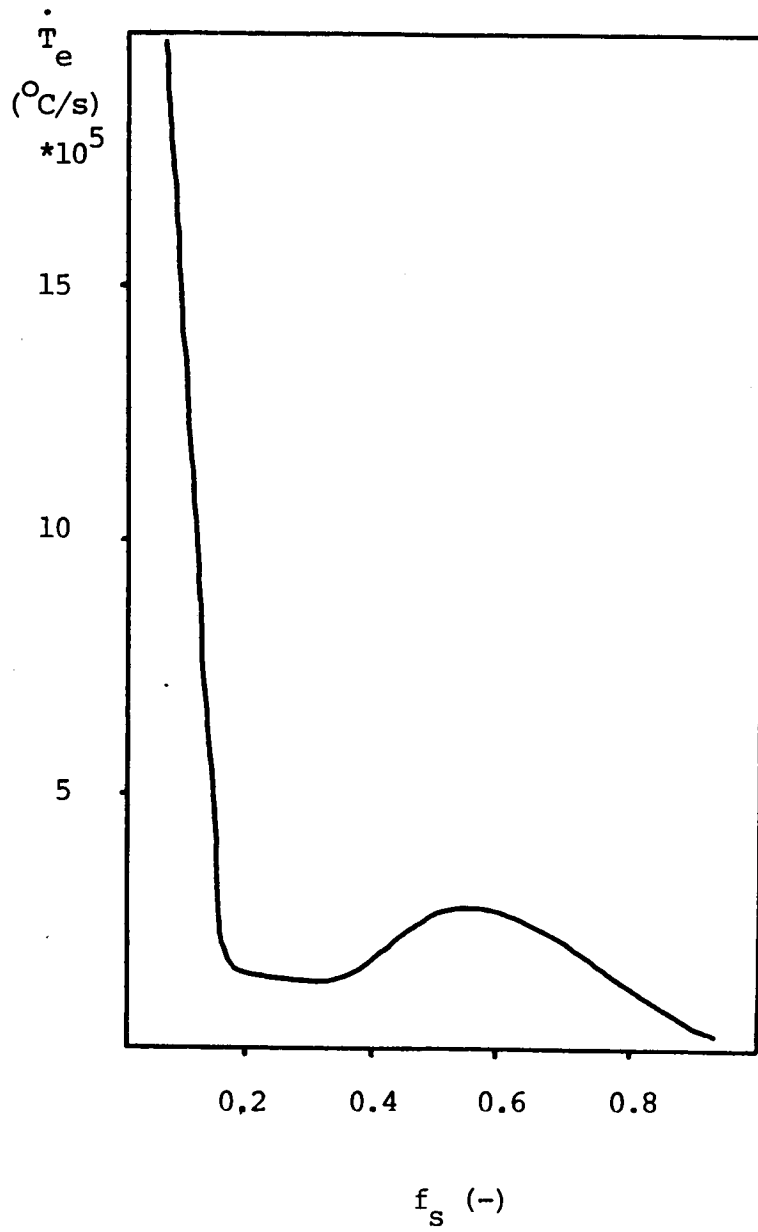
Fig (3.3.1.7).-   Calculated effective cooling rate just ahead
of the solidification interface as a function of the fraction
solidified .

not able to find the exact correlation valid for the alloys of our study so we decided to use a relationship proposed for the superalloy Inconel 718; this is (see Sec(2A.1)),

$$\lambda_s = 34 \ (\ \dot{T}_e \ )^{-0.34} \tag{9}$$

The result of combining Fig(7) with Eqn(9) is shown in Fig(8). In the same figure also appear the results of actual metallographic measurements performed by Ms Segal(1983) at MIT. The plot just shows secondary dendrite arm/cell spacings as a function of the fractional distance from the wheel surface (referred to the final ribbon thickness). The dashed line describing our results overestimates the spacing for the first third of the ribbon but corrects itself afterwards and remains in good agreement with the observed values during the last 2/3 of solidification. At this point we can only speculate on the reasons for the observed discrepancy during the initial stages of solidification. Several possible explanations can be offered. Among these we may mention: (i) The difficulty of accurately computing the value of the effective cooling rate at the beginning of solidification. The size of our computational grid being the ultimate limitation. This could produce a smaller rate of decrease of the effective cooling rate during the initial stages of freezing thus making the computed dendrite size curve closer to the measured values, (ii) the existence of phenomena unaccounted for by our model, as may be the case of undercooling in the melt layer next to the
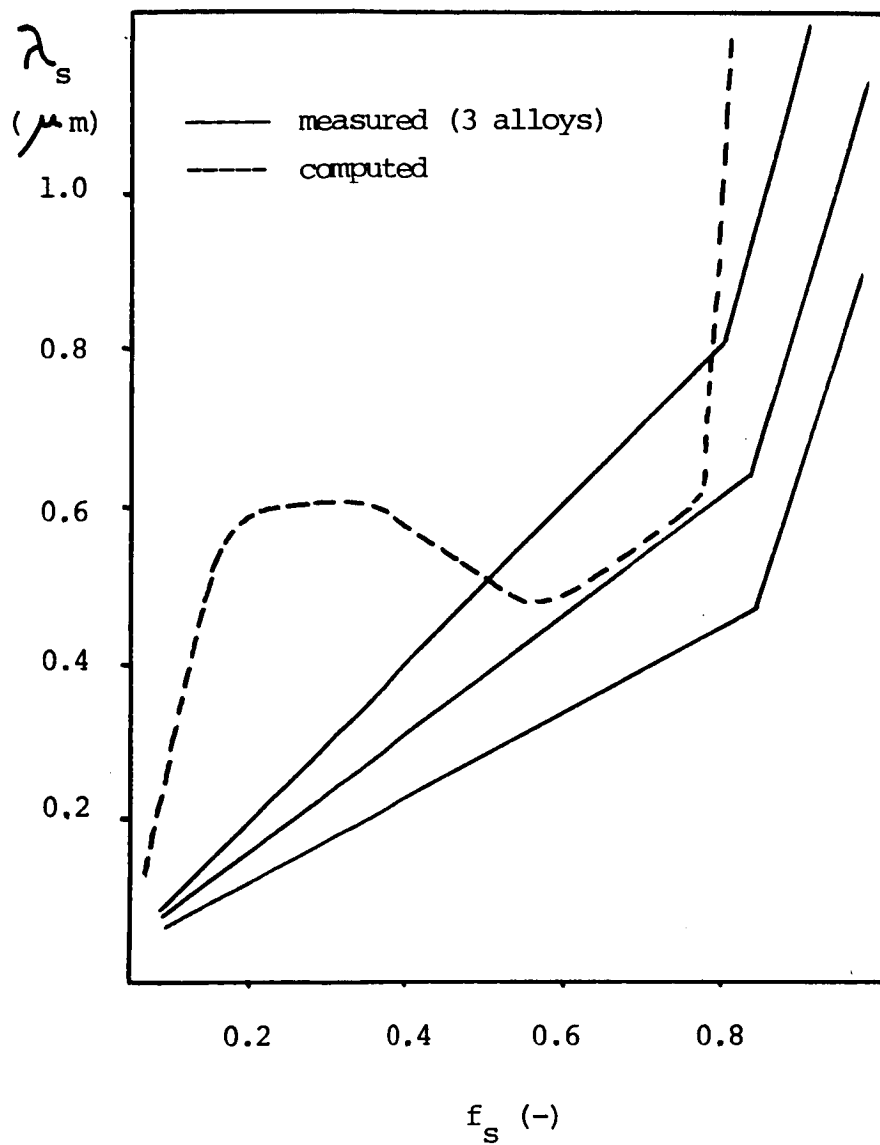
Fig (3.3.1.8).- Comparison between predictions and measurements of cell spacings as a function of the fraction solidified. See also Plate (3.3.1.3).
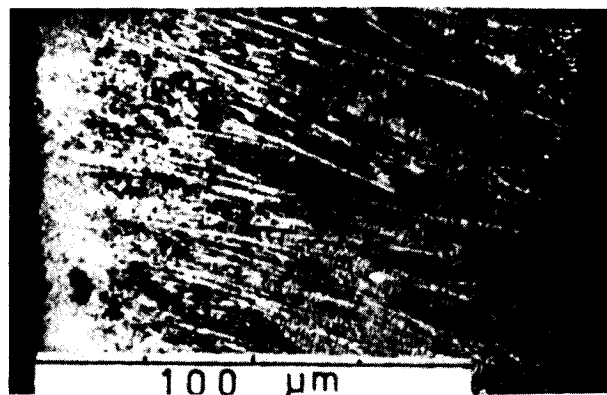
3.3.1.3.- Longitudinal section of melt spun ribbon of Inconel 718. The microstructure is similar to the one found in conventional castings, with the cell (dendrite) size increasing from bottom (wheel side) to top (free surface). From Warrington, D.H. et al., in Masumoto, T. and K. Suzuki (eds), (1982).

chill; the microstructure resulting from the solidification of such an undercooled layer can be expected to differ considerably from the ones characteristic of smaller cooling rates, (iii) it can also be the case that we just simply used the wrong dendrite size-cooling rate correlation. However, despite the apparent disagreement it is indeed remarkable that our model is capable of predicting microstructural sizes and cross sectional variations of microstructure of the correct order of magnitude, despite all the assumptions and uncertainties involved in our calculations.

One important feature of our model is the coupling of the solidification phenomena occurring next to the wheel surface to the capillary processes taking place on the free surface. Thus, one of the products of our calculations is always the precise location of the melt-gas interface in the downstream side. In Fig (9) we show a plot of the location of such meniscus as a function of the roll velocity. One can readily note that the three computed free surface shapes are all very similar and indeed almost identical throughout the first half of the puddle. We note that the same detachment point was used in these calculations. However, as the free surface approaches the solidification interface, the effect of freezing on the shape of the meniscus becomes more significant. Since the total flow rate is constant, for any given downstream location, the sum of the partial flow rates carried by , respectively, the solid ribbon and the liquid film on top of it, must be equal to the total flow rate. So,
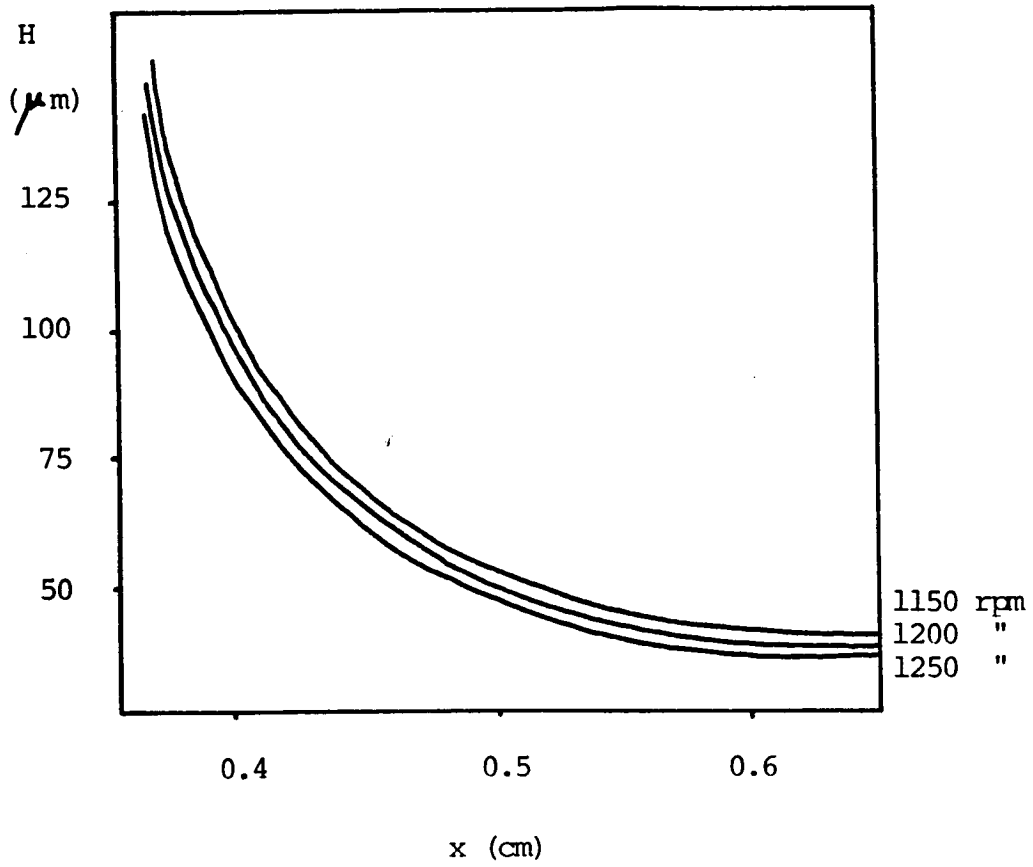
Fig (3.3.1.9).- Computed meniscus shapes with the wheel velocity as a parameter.

although the solidification rate is not altered significantly for changes in the wheel velocity within the range considered here, the total mass flow rate is an independent process parameter controlled mainly through the ejection pressure. Thus , for any given down-stream location, the partially solidified ribbon carries with it a larger fraction of the total flow rate when the roll velocity is large. This , in turn, has the effect of pulling the free surface down producing a thinner liquid film.

The behavior described above contrasts with the one observed in the somewhat analogous system obtained when a solid object is withdrawn from a liquid bath. In this case a thin layer of fluid adheres to the surface of the object. The thickness of this film decreases with increasing distance from the exit point from the bath until it reaches a limiting value under steady state con-ditions. The final liquid film thickness is calculated to be proportional to some fractional positive power of the withdrawal speed. However, when withdrawing solids from liquid baths,the supply of liquid is practically unlimited and the solid body is able to carry as much fluid as it can. On the other hand, during melt spinning, the melt flow rate is given by the ejection pressure and the final ribbon thickness represents a compromise between the imposed flow rate and the chilling effect of the wheel.

An important feature of the PFMS system is the widespread use of slot shaped nozzles. These rectangular nozzles allow for

the production of ribbons or sheets with a width essentially equal
to the width of the slot. For comparison, in the CBMS process,
circular nozzles have been used most of the time. The cylindrical
jet produced during CBMS , on impingement, spreads laterally
on the moving wheel producing ribbon with a width which is several
times larger than the diameter of the initial jet. Since the
resulting spreading phenomenon is difficult to control, variations
in width along the ribbon length are commonly observed. On the
other hand, during PFMS , the ribbon width is determined by the
width of the nozzle and since both the melt flow rate and the
exit velocity of the ribbon (= V_{r_x}) are fixed, an overall
mass balance leads to

$$H_f \quad = \quad Q/(w \, V_{r_x}) \qquad\qquad (10)$$

The behavior represented by Eqn(10), remarkable because of its
simplicity, is in sharp contrast with the more complicated
relationship involving the same quantities found to be valid in
the case of CBMS (see e.g. Kavesh). Needless to say, the more
complicated relationship in the case of CBMS arises because
of the additional factors involved with the lateral spreading of
the molten jet on impingement on the wheel, a phenomenon which
is characteristically absent during PFMS with slot shaped
nozzles.From Eqn(10) we see that we should expect the final
ribbon thickness to be inversely proportional to the wheel

velocity. We decided to run our program several times maintaining

everything constant except the wheel velocity (and, of course, the

melt flow rate). The result of such an experiment is shown in

Fig(10). As expected,the results of our calculations fall very

well along a straight line of negative slope. So, our results

certainly satisfy the overall mass conservation requirement. This,

however, is to be expected since the overall mass balance was used

throughout as a criterion for the correctness of the results.

It is indeed unfortunate that very few experimental data of this

kind, produced under carefully controlled conditions, are

available. The only experimental data we got , for the system

of this study, are included in Fig(10). However, caution must be

used when comparing measurements and calculations in this plot

since all the experimental data points were obtained under

entirely different process conditions, in particular , under

different melt flow rates. Nevertheless, it is encouraging to see

that our model predicts expected trends accurately.

Furthermore, we should note that, once the wheel velocity and

the melt flow rate are specified, the computed line shown in

Fig(10) is related to one and only one value of the heat transfer

coefficient at the splat-wheel interface. We could then expect

empirical curves analogous to the theoretical one shown, be used,

in conjunction with a model like ours, for the determination of

h .
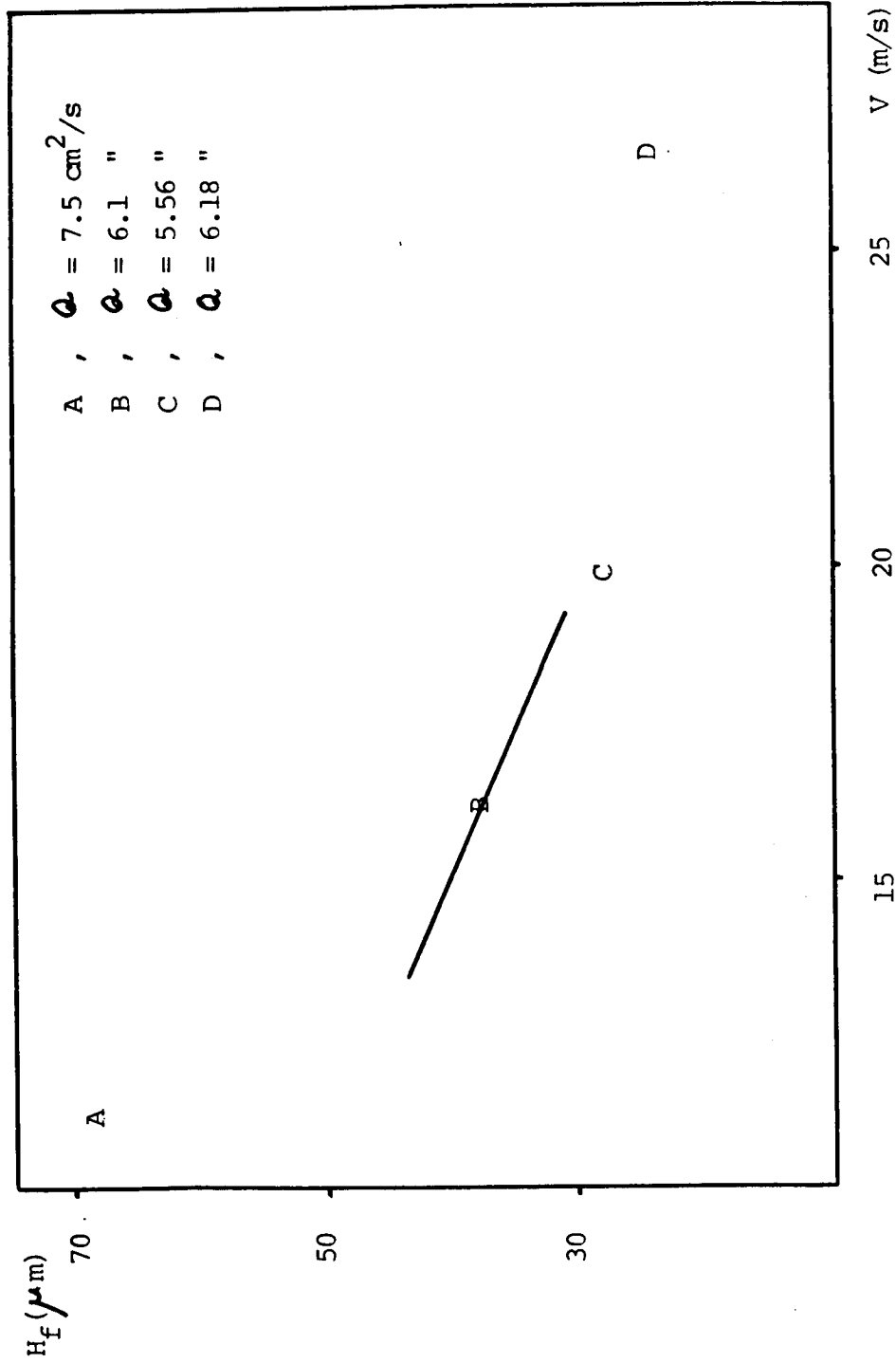
Fig (3.3.1.10).- Comparison between predictions and measurements of
the final ribbon thickness vs wheel velocity relationship.

From Eqn(10) we should also expect the final ribbon thickness to be directly proportional to the melt flow rate. We decided to perform several runs of our program in which the only parametric variation was the flow rate. Perhaps not surprisingly, we found that the overall mass balance could not be satisfied unless the length of the puddle was adjusted accordingly. This change in the size of the puddle with the flow rate is not unique to our calculations but has also been consistently found in the laboratory (see e.g. Huang and Fiedler(1981)). The results of our calculations of the influence of the melt flow rate on the final ribbon thickness and on the puddle length are shown in Fig (11). The results suggest that thicker ribbons may be produced simply by increasing the melt flow rate. This conclusion may be deceiving since larger flow rates produce bigger puddles which in turn are increasingly unstable because of surface tension effects. Moreover, as described before, thicker tapes would be subjected to larger temperature differences across their thicknesses unless something is done to attenuate the chilling effect of the wheel. The resulting thermal history will invariably lead to more significant variations of the microstructure of the strip across its thickness. Furthermore, it is clear that larger flow rates, because of the attending increased energy content, will require the substrate to be able to absorb more heat to be able to induce rapid solidification on the splat. The expert's consensus seems to be that melt spinning wheels are operating at
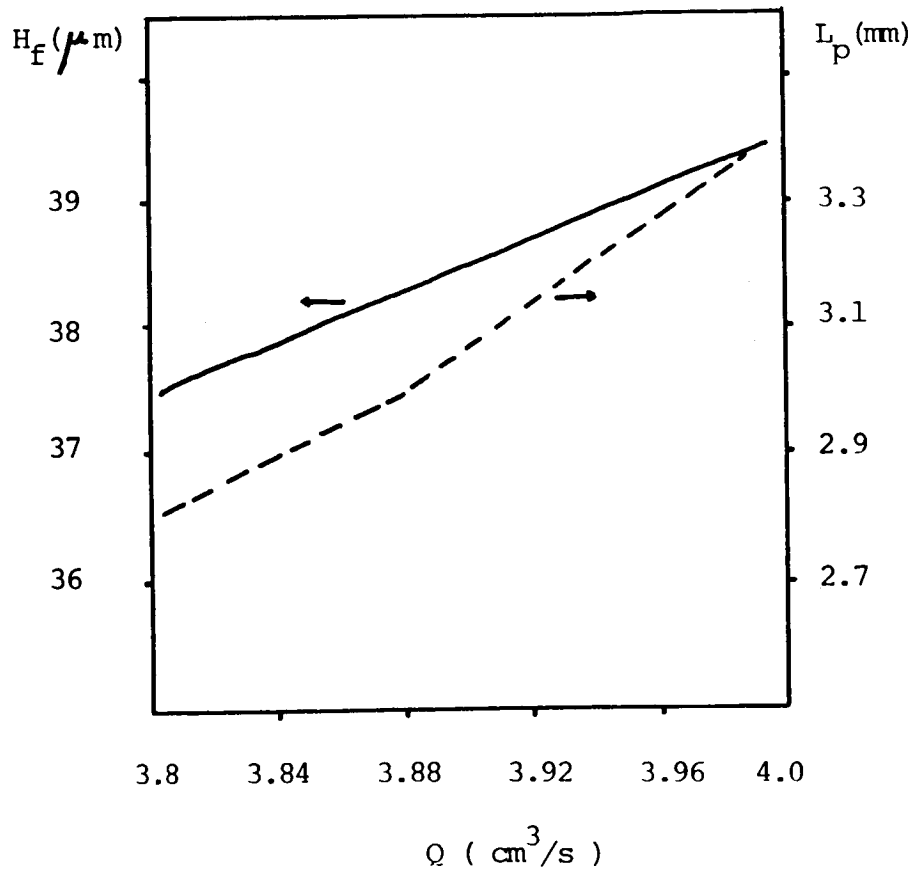
Fig (3.3.1.11).- Predicted effects of the melt flow rate on

the final ribbon thickness, H_f and on the size of the puddle,

L_p .

98

or very close to their maximum heat extraction capacities.

The heat extraction ability of the melt spinning wheel may be well described, in the context of this work, by the corresponding value of the heat transfer coefficient at the splat-wheel interface under given operating conditions. It must be clear that the value of such coefficient does not only depend on the physical properties of the wheel and the splat but it is intimately related to the actual values of the various process parameters. To further investigate this point we performed some calculations changing the value of h and adjusting the melt flow rate accordingly in such a way that the overall mass balance was always satisfied. As expected, the heat transfer coefficient appeared to have a strong influence on the final ribbon thickness achieved. The actual result of this calculation is shown in Fig(12). The point mentioned before can be seen here more clearly. Much more efficient heat absorbing substrates are required in order to produce melt spun ribbons using large melt flow rates. This constraint is so strong that in reality it is practically impossible to induce high cooling rates (of the order of , say 10^5 ^{o}C/s) in ribbons thicker than, say one hundred microns.

The superheat imposed on the melt prior to spinning is one easily controlled parameter. Figure (13) shows the computed final ribbon thickness as a function of the superheat of the melt. As expected on simple physical grounds, the final thickness decreases as the superheat is increased. This effect is particularly intense at high superheats. However, this results must be interpreted with
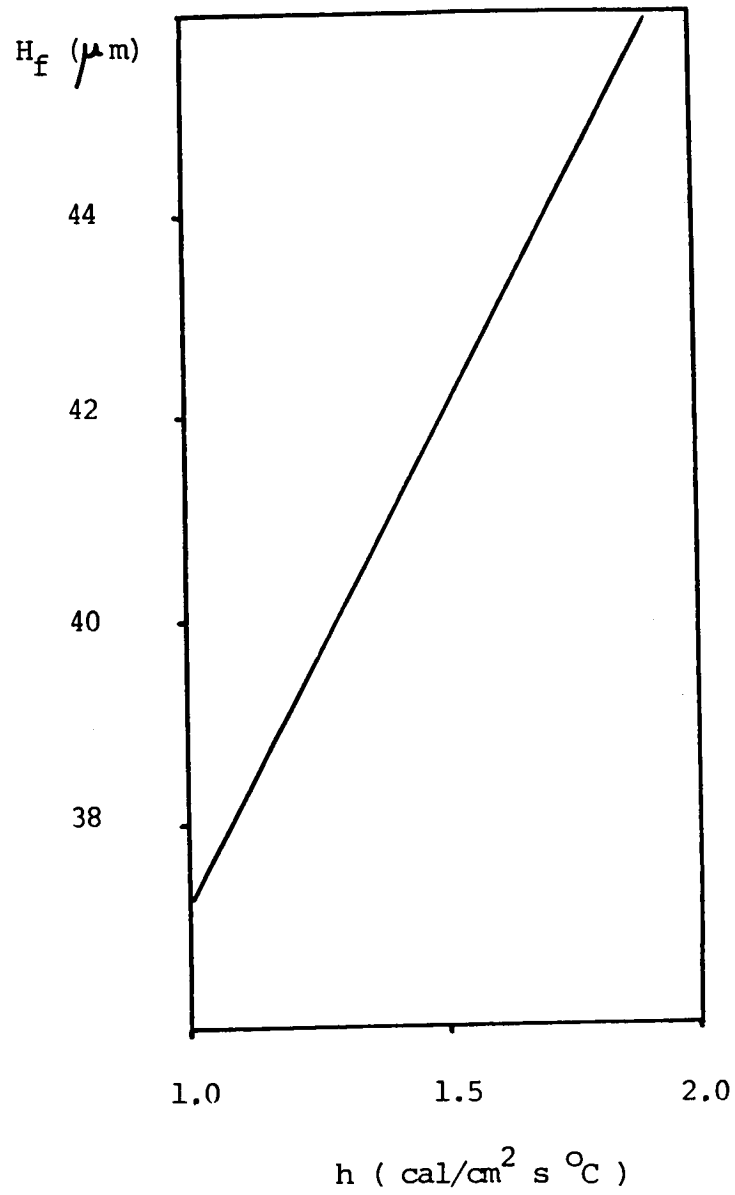
Fig (3.3.1.12).- Predicted effect of the heat transfer
coefficient at the splat-wheel interface on the final ribbon
thickness.

H_f (μm)

40

38

36

34

32

60   80   100   120   140

$T_p - T_L$ ($^{\circ}$C)
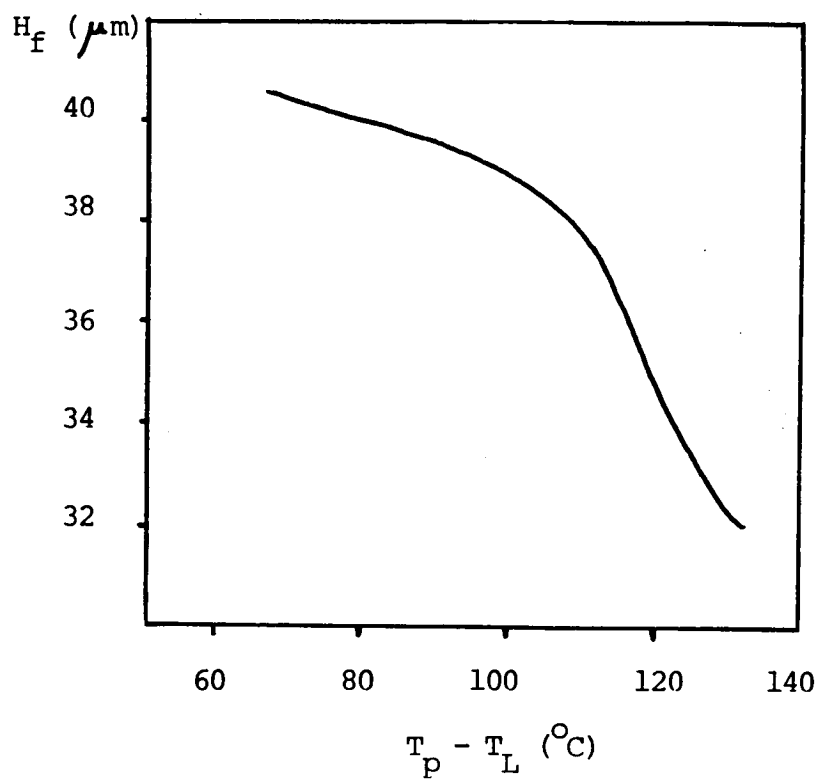
Fig (3.3.1.13).- Predicted effect of the melt superheat prior to spinning on the final ribbon thickness .

caution since the property changes produced by the higher pouring temperatures can modify the wetting behavior of the melt and lead to the apparently contradictory findings of some researchers (see e.g. Scott(1974)).

d)   Conclusions

1)   We have constructed and programmed a mathematical model of the PFMS process which is capable of predicting the dynamic behavior of the system, particularly regarding the relationship between process parameters and ribbon microstructure. Comparison of the computed results with the limited empirical data available, together with the extensive checks contained in our program, point towards the correctness of our approach.

2)   From our simulations we conclude that the most important process parameters of the PFMS technique are:

(i) The melt flow rate,

(ii) the wheel velocity,

(iii) the heat transfer coefficient,

(iv) the geometry of the system, and

(v) the physical properties of the materials involved.

Interestingly enough, a similar set of relevant process parameters was arrived at empirically by the NASA group (Jech et al(1984)).

Only a restricted set of values of these process parameters allows for the steady production of uniform ribbons. The restric-

tion to particular sets of values of the process variables, although significant, seems less stringent than the one observed in the case of the Twin Roll system. There seems to be an advantage in using the single roll device for RSP in view of its increased flexibility of operation and of the possibility for continuous processing. It would seem that the inevitable deterioration of both wheel and nozzle due to thermomechamical stresses and chemical effects is one of the main obstacles to the continuous production of strip.

3)   We have demonstrated how the basic principles of lubrication theory, capillary hydrodynamics and solidification heat transfer can be combined to produce a meaningful picture of a typical RSP system. The insight gained from this approach suggests the possibility of useful information to be obtained by extending our methods to other RSP systems.

4)   We believe that a computer program such as the one described here may well constitute the core of an on-line control mechanism for the automation of the PFMS process. Ideally, however, the program should be fine-tuned by comparing its predictions with the results of a carefully designed and controlled set of experiments in which not only the ribbon is characterized in terms of its microstructure and properties but all the relevant process parameters are also measured or controlled as accurately as possible.

5)   The FORTRAN listing of the program used to perform the calculations described in this section is included in Sec(5.4).

3.3.2.- Some Comments on the Modeling of Other RSP Systems.

In the next few pages we present a bird's eye view of some important aspects of the mathematical modeling of some selected RSP systems. Examples from all groups presented in Table(3.1.1) will be discussed. However, in all cases the discussion will be brief and limited to a few important points. We start with the Twin Roll and the Piston and Anvil RS processes since they are both good examples of splatting methods and are also somewhat related to the PFMS system described in the previous section. We then move on to the Melt Fragmentation techniques and summary comments are included about the various atomization processes. Finally, mention will be made of the modeling of RS Laser Processing and of Spray Forming techniques.

a)   Modeling the Twin Roll RS Process.

The most comprehensive model of the TRRS process to date has been presented by Miyazawa and Szekely(1981). Starting from the momentum balance equations in the lubrication approximation, they solved the differential energy balance equation with due account taken of the latent heat of solidification. Besides the thermal calculations, closed form expressions were obtained for the velocity field of the material in the roll gap. The phenomenon of solid deformation was accounted for by considering the solidified strip to be a creeping solid changing shape according to the

Norton-Bailey law of secondary creep.

For the solution of the thermal problem, an implicit front-tracking method was used after a coordinate transformation of the original equations. The pressure profile in the roll gap was obtained by integrating the expression for the pressure gradient along the casting direction using a Runge-Kutta method. We have repeated the pressure calculations performed by Miyazawa and Szekely but this time including the material parameters describing the strain rate in the solidified ribbon as given by Frost and Ashby(1982). Very large peak values of the pressure were encountered for the conditions used (Fig(1)). The listing of the program used to perform this calculation is included in Sec(5.5).

Among the most important conclusions of that study are the following:

(i)   Only a very narrow range of values of the process parameters allows for the steady operation of the process. Experimental precautions are required in order to obtain satisfactory performance. This has been verified in practice (Murty and Adler(1982)).

(ii)   The main parameters of the technique are; the roll gap, the roll velocity, the feed rate and the material properties. The final ribbon thickness decreases with increasing the roll speed and by decreasing the roll gap or the feed rate.

(iii) The roll separating force increases with decreasing the roll speed because of the increased reduction ratio. Moreover, slip between roll and splat accounts for the experimentally
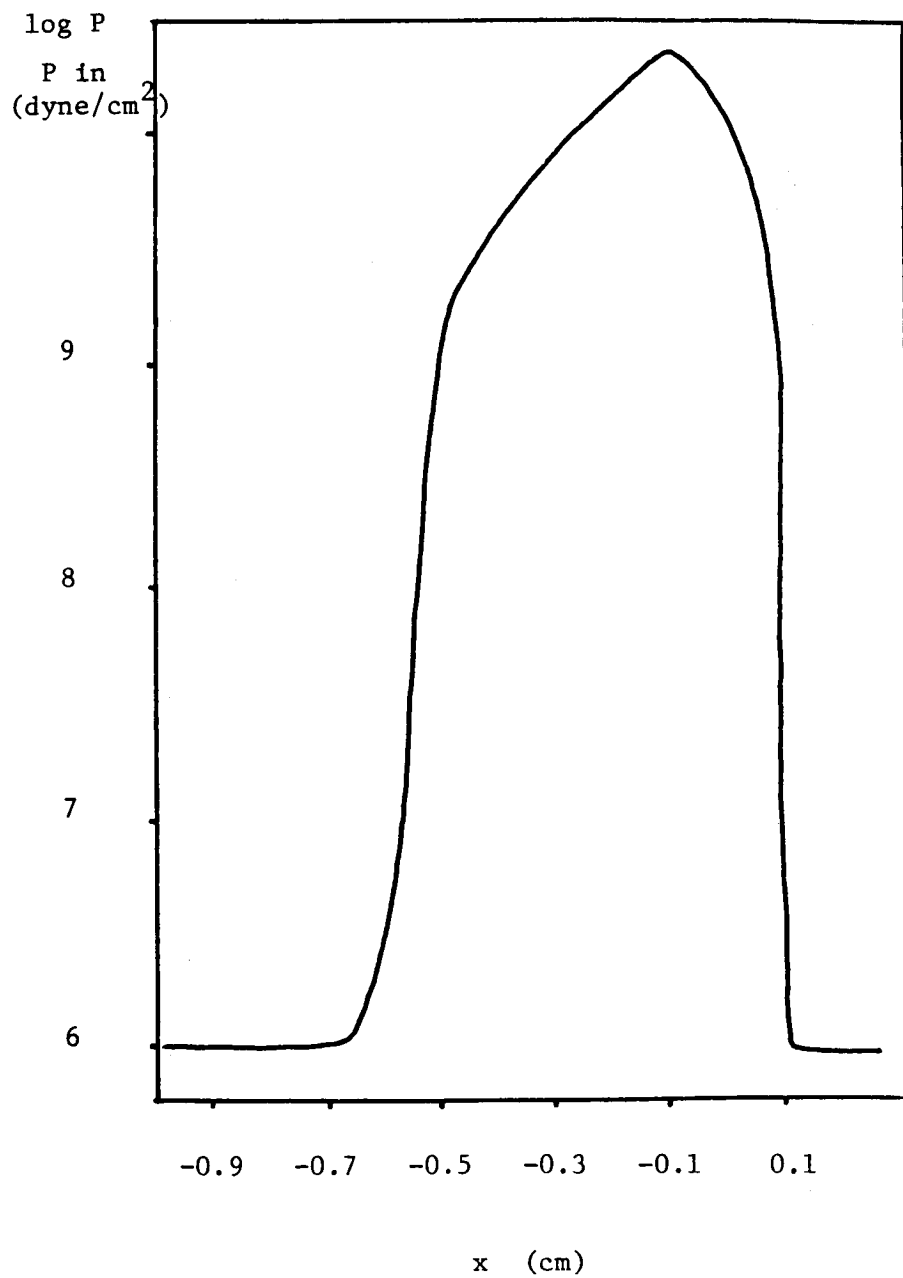
Fig (3.3.2.1).- The computed pressure distribution in the roll gap of the TRRS device for the data of Miyazawa and Szekely.

observed differences in velocity of wheel and ribbon.

Miyazawa et al(1983), have continued their study of the TRRS process. These papers should be consulted for further details.

b)   Modeling the Piston and Anvil System.

Bletry(1973) presented the first detailed calculations of temperatures and cooling rates for the piston and anvil system. The next important step was performed by Miyazawa and Szekely (1979) who incorporated the spreading and squeezing phenomena into the thermal calculations. They used the momentum equations in the squeeze flow approximation to obtain expressions for the velocity field. These were used , in turn, together with an explicit finite difference form of the differential energy balance equation, to calculate the cooling and freezing rates for the process. The most important process parameters of the technique were found to be; the piston speed, the sample size, and the pouring temperature. The main variables influenced by the values of these parameters are the final splat thickness and the attainable cooling rates.

c)   Modeling the Melt Fragmentation Techniques.

The two main groups are , as indicated in Table(3.1.1), the atomization processes and the impact disintegration processes.

Mathematical modeling techniques have been used only very little in the study of these processes. The explanation for this may be the highly complex nature of the phenomena which take place. We limit ourselves here to mentioning the main variables involved and the literature sources where more information can be found.

In centrifugal atomization, a spinning dish, cup or electrode produces fine particulates by first thinning of the melt and subsequent breaking up of the thinned layer. The main process parameters of this process have been found to be (see e.g. Hodkin et al(1973), Schmitt(1979) and Champagne and Angers(1984)); the dish diameter and speed, the melt density, surface tension,and viscosity, the feed rate and the pouring temperature. Using basic concepts from fluid mechanics,relationships have been derived giving, for example , the fluid film thickness at the rim of the rotating dish and the resulting mean droplet diameter. Interestingly enough, many similarities with the well known centrifugal atomization process widely used in chemical engineering technology, have been found. There is one additional complicating factor in this case, however, since the fluid not only has to be fragmented but the resulting particles must be cooled and solidified.

Gas and water atomization processes have long been used by the powder metallurgy industry. The introduction of ultrasonic gas atomization , with its resulting smaller particle size, has carried the fluid atomization processes into the realm of RST. The main

process parameters in this case have been recognized to be; the molten metal properties and flow geometry and the gas(water) jet flow rate and geometry. Fluid dynamic phenomena are strongly involved in the thinning and breaking up of the liquid metal jet during fluid atomization. The heat transfer processes of cooling and solidification which take place simultaneously add considerable complexity to the system. Tallmadge, for example, (1978) has performed extensive studies of metal atomization processes from a chemical engineering point of view, whereas Beddow(1978) and Lawley(1977) have presented comprehensive reviews of the subject. Grant(1983) also presents an overview of atomization processes but from the perspective of RST .
The calculation of the cooling and freezing rates of the undercooled metal droplets produced by metal atomization processes has been performed most recently by Gill et al(1984).

In the case of the vibrating electrode process (Ruthardt and Lierke(1981)) the melt is fragmented by the break up of the capillary waves induced on the thin melt layer by the vibrating electrode. In this case, the theory of capillary waves has been used to estimate the mean droplet size as a function of the melt surface tension, density, and viscosity and of the vibration frequency of the electrode.

Schmitt(1979) has described the basic physics of impact dis-integration processes. He found that the final particle size in

this system depended on ; the nozzle diameter, the impactor radius and size, the distance from the nozzle to the impact point, the impactor rotation velocity, and the material properties. Lynch (1982) has used the basic principle of impact disintegration processes to produce particulates from a continuous molten metal jet.

d) The Modeling of RS Laser and Electron Beam Processing and of Liquid Dynamic Compaction (Spray Forming).

The scanning of the surfaces of bulk materials with high intensity laser or electron beams can produce rapid melting and solidification of thin surface layers. In these processes the most important parameters are; the wavelength of the radiation, the incident power density, the interaction time , the detailed nature of the surface and the material properties.

Breinan and Kear(1983) have modeled RS laser processing by using the one dimensional heat conduction equation with a source term. In this way they were able to avoid the complicating factors introduced by the change of phase and the fluid motion inside the melt layer. They claim very good agreement between the results of their calculations and those obtained from a more sophisticated finite element analysis which took the latent heat into account. Moreover, they felt that the accuracy of their model was good enough for comparison with their own measurements.

Chan et al(1983) have presented a more comprehensive model of RS Laser Processing in which they take into account the fluid flow phenomena taking place in the molten layer. The heat transfer and fluid flow problems are solved simultaneously and predictions are made about cooling and freezing rates as well as of puddle morphology. Mawella(1984) constructed a thermal model for the Electron Beam Processing of solids based on the theory of surface sources of heat, popular in welding calculations . He claims good agreement between his calculations and the results of his own experiments.

Liquid Dynamic Compaction (also Spray Forming or Spray Deposition) is the name given to a group of RS processes in which relatively thick sections of rapidly solidified material are prepared by the continued showering of a substrate with a spray of molten metal droplets (which in turn may be produced by any of the various atomization processes). The structures and properties of the resulting products are functions of both the spray characteristics and the properties of the substrate. Singer and Evans(1983) have described the fundamentals of a statistical model for the representation of the spray. They have also suggested how to use the heat flow equations for the calculation of the specific conditions leading to the steady operation of the process. They have found the predictions of their model to be in good agreement with measurements performed in their own laboratory.

Apelian et al(1983), and El-Kaddah et al(1983) have performed

detailed heat transfer calculations for the closely related Plasma Deposition processes. They found that the events taking place in the plasma are as important or more that those happening once the molten particles impact the substrate. Their papers should be consulted for details.

In summary , although a large amount of work has been done on the mathematical modeling of RSP systems, there seem to be ample opportunities for additional research . Many systems have been studied only partially and nothing at all is known about a few others. Because of the relatively novel nature of RST , mathematical modeling can contribute to substitute costly trial and error procedures by more rational approaches to process development and control.

Chapter   4

CONCLUSIONS AND SUGGESTIONS FOR FURTHER WORK

Since most of the conclusions pertaining to the modeling of the PFMS   process were presented before (see Sec(3.3.1)), in this chapter we only add a few more points not explicitly mentioned there. On the other hand, we will include some conclusions of a more general nature about the potential of the mathematical approach to help in the understanding of the complex features of RSP systems. Specific suggestions are made regarding the directions in which mathematical modeling can be applied to the study of RST . In the sequel we simply present our points without following any particular order.

a)   One important limitation of the PFMS   process is the result of two conflicting requirements. On the one hand, to obtain RS effects a small sample size is needed in at least one spatial direction. On the other, the production of thicker strip requires larger melt puddles. Since surface forces are what holds the puddle together during the production of thin ribbons,as mentioned

in Sec(3.3.1) above, it is clear that the question of the stability

of the melt puddle is critical to the success of the process. It

may be seen that the production of relatively thick tapes is faced

with big problems. It might be helpful to artificially constrain

the puddle in some way instead of letting the surface forces

do the job alone. However, according to our results, the thicker

the produced tapes, the more significant the microstructure

variations across the splat thickness will be. It is an intrinsic

feature of the heat transfer-solidification processes taking

place in this system that causes the highest cooling rates to

be limited to that portion of the splat which is closer to the

moving chill.

b)   It is well known that the unavoidable roughness always

present on the wheel surface during PFMS is one important

reason for the considerable variations in surface quality and

microstructure of melt spun ribbons. The uneven wheel surface

produces localized regions of relatively good thermal contact,

which are separated by areas where the contact is poor (lift-off

areas). Ways must be devised to deal with this problem if one

wishes to optimize the process. One possible alternative frequently

suggested consists in homogenizing the cooling power of the wheel

surface by eliminating the areas of good thermal contact. One way

of doing this is by coating the surface of the wheel by a thin layer

of a heat insulating material, (e.g. glass). This layer should be

sufficiently thick to thermally homogenize the surface but thin

enough as to not to impair the heat extraction ability of the wheel.

c)   More attention should be paid to the spreading and wetting phenomena taking place during PFMS. In particular, the contact line formed in the rear of the puddle at the point of impingement should be looked at more closely. This contact line is the locus of many important processes involving fluid flow and heat transfer and the understanding of these may prove to be vital for the successful implementation of the technique. Both experimental and theoretical work is required in this area.

d)   The additional effects introduced by the presence of inertia forces (which were neglected in our calculations) should be more fully explored. Although because of the large surface tensions characteristic of metallic melts, this effects are likely to be small, more work is needed to verify this expectation.

e)   An effort should be made to perform carefully planned experiments aiming at the verification of the existing mathematical models of RSP systems. Work can proceed along the lines of the research performed on the CBMS system or following the pattern set by Miyazawa et al.. It is indeed unfortunate that so little information of this type is available for the PFMS process. In any case, the aim of experimental programs should be the establishment of the relationships linking the process parameters to the structure and properties of the resulting products.

f)   The entire area of melt fragmentation processes remains a
challenging ground for modeling work. The powder metallurgy
industry has motivated much of the existing work on metal atomi-
zation. However very little of this research has been of the
theoretical kind. Many aspects of the various melt fragmentation
techniques still remain obscure with empirical correlations being
the only quantitative means of studying the processes. There
are considerable opportunities for useful contributions from
mathematical modeling in this whole area. The abundance of complex
hydrodynamic phenomena coupled to heat transfer-solidification
processes always present in these systems should attract the
attention of the mathematically oriented engineer as well as that
of the fluid dynamicist or applied mathematician. Work in this
area could start from the important contributions by Hinze(1955),
Dombrowski and Johns(1963), and , particularly, the one by
Bradley(1973). A good summary of the theory of fluid jets and
their stability can also be found in Anno(1977).

g)   A somewhat related set of problems is found in the area of
liquid dynamic compaction (spray forming). Here, the detailed
structure and properties of the deposited product depend on the
fluid dynamics of the swarm of droplets of varying sizes, on the
interaction of such droplets with the underlying substrate and on
the heat transfer phenomena taking place both during flight and
after impingement of the droplets on the deposit.

Needless to say, obtaining deposits with low porosity and desirable properties should be achieved more easily by using a rational approach in which the use of empirical trial and error is minimized.

h)   The use of high intensity energy beams to alter the surface the bulk samples by rapid heating and cooling is now well established at an industrial level. Heat treating, welding, surface melting and freezing and surface alloying have all been demonstrated. However, despite the successes, there are still areas where knowledge is scanty.

In all surface heating systems one invariably finds thin layers of material subjected to very large temperature gradients. In particular, during RS laser or electron beam processing, thin molten layers form on the surface of the object which solidify once the heat source is removed. The behavior of these thin layers of fluid is governed by the same basic principles of continuum mechanics. Because of the small scale, capillary phenomena play an important role in these systems. We believe that increased understanding of the detailed behavior of these systems can be obtained from a more extensive application of the equations of fluid dynamics and heat transfer with change of phase. Even more knowledge can be gained if these thermal calculations are coupled with crystal growth kinetics for the prediction of the microstructure of the surface layers resulting from processing.

i) The intrinsic limitation of RSP to small sample sizes invary-
ably results in systems with a disproportionately large surface
area to volume ratio. This makes imperative a more detailed study
of the interfacial phenomena taking place at interphase interfaces.
The peculiar behavior of lines of contact, which are almost always
present in RSP systems certainly deserves more careful consid-
eration. Very often, these contact lines are the locus of complex
heat transfer and fluid flow phenomena which take place at the
same time.

Both the chemical and the physical aspects of the various
interfaces should be watched more carefully. Important outcomes
of this work could be , for example, the microscopic interpre-
tation of heat transfer coefficients at splat-chill interfaces
on the basis of the structural features of such interfaces and
of the capillary phenomena taking place there, or an understanding
of the complex capillary flows which take place in shallow molten
pools and which, in many cases, determine the final shape of the
heat affected zone.

Convenient starting points for the quantitative study of
interface phenomena in RSP systems are the works by Dussan(
1979), Timsit(1982) and Hocking(1983), on spreading and wetting
processes and the paper by Levich and Krylov(1969) on fluid flow
phenomena in which surface phenomena play an important part.

j) The success of numerical methods for the prediction of

cooling and solidification rates in conventional casting systems
(e.g. Brody and Apelian(1982) and Dantzig and Berry(1984)), should
be an incentive for a more widespread use of mathematical modeling
in RS research. In particular, it would seem that considerable
benefit can be obtained with a modest amount of effort from the
application of the now well established method of weak solutions
to the calculation of solidification processes during RS .

k) The complicated fluid flow phenomena taking place in most
RST configurations certainly warrant further study for their
own sake. Needless to say, such phenomena are also important
from a practical point of view since, ultimately, cooling and
freezing rates are strongly influenced by the convective fluid
motion taking place . It may well be that simplifications
introduced for the sake of mathematical simplicity are such that
important physical processes actually taking place are being
disregarded. For this reason,more complete solutions of the fluid
flow problem are needed. This study can be helped a great deal
if some of the commercially available computer programs for fluid
flow and heat transfer calculations are used. One good package
which has produced much of the results in our group at MIT is the
one prepared by Patankar and Spalding. In Sec(4A.1) we review
the basic features of the Patankar-Spalding algorithm hoping that
it finds more use within the RS community. Furthermore , in
Sec(5.7) we present the FORTRAN listing of a program we

constructed, based on the P-S algorithm, for the calculation of heat transfer by conduction-convection in a system where the flow is given by lubrication theory. It should be noted that this program is only a very simplified version of the P-S algorithm and is included here more to indicate the main ideas involved in the commercially available version.

1)   Last but not least is the problem of compacting the products of RS . Since engineering components almost always will come in sizes much larger than those typical of rapidly solidified samples, some form of compaction is unavoidable. Although a few RS techniques avoid this problem (e.g. liquid dynamic compaction), most do not. Although compacting is a very complex process, it is also subject to the laws of continuum mechanics. We can foresee increased application of both finite difference and finite element methods for the solution of compaction problems .

Chapter 5

COMPUTER PROGRAMS

In this chapter we present the FORTRAN listings of some of the computer programs we have developed to perform our calculations of RSP systems, particularly those described in Sec(3.2)and (3.3). We have also included , for completeness, additional listings of other programs we have developed and found useful in gaining insight into the complex problems of RST. All the programs are fully commented for easier use.

In Sec(5.1) we present a program capable of performing the thermal calculations for a wide range of RS configurations based on the assumption of Newtonian cooling conditions (Sec(3.2)). A great deal of useful information can be obtained from this program regarding cooling and freezing rates for specific systems. In Secs(5.2) and (5.3) computer programs for the calculation of temperature profiles and freezing rates in semiinfinite media under various boundary conditions, are given. The codes are simply programmed versions of the equations presented in Sec(3A.2).

In Sec(5.4) we present the program for the calculations of the PFMS system described in Sec(3.3.1). This program is the most important one in the set since it produced the bulk of the results reported in this thesis. The program can be made to run in an iterative fashion by modifying a selected process parameter at a time, incrementally, until the overall mass balance is satisfied. However, we have found this process to be very expensive and not always convergent. Instead, we have found more convenient to do the iterations by performing several runs of the program and effecting in between reasonable changes in the required process parameter until our mass balance was satisfied. This way of running the program certainly was more economic. In any case it is relatively straightforward to make the program to perform the iterations automatically.

Section(5.5) presents the program used to perform the rolling force calculations described in Sec(3.3.2). The program could also be used to perform calculations in related systems such as for the rolling of thin sheets. Section(5.6) presents a very simple program for the solution of systems of linear algebraic equations with tridiagonal matrices. This code can be used as the basis of an algorithm for the solution of transport phenomena problems in discrete form.

Finally, in Sec(5.7) we include a sample program we have constructed to perform calculations of temperatures in two-dimensional domains when heat is being transferred both by

conduction and by convection. In this program the fluid flow field
is not calculated numerically but through closed form expressions
obtained from lubrication theory. It is included here just to
give an idea of the nature of one of the most widely used,
commercially available computer programs for heat transfer and
fluid flow calculations.

5.1.- Program RSPNN . Heat Transfer during RSP under Newtonian Cooling.

```
C--------THIS PROGRAM COMPUTES TEMPERATURE,COOLING RATE,SOLIFIED FRAC-    RSP00010
C-----TION AND FREEZING RATE AS A FUNCTION OF TIME FOR VARIOUS RAPID      RSP00020
C-----SOLIDIFICATION PROCESSING CONFIGURATIONS.FOR SIMPLICITY, COOLING    RSP00030
C-----IS ASSUMED TO OCCUR ACCORDING TO NEWTON'S LAW. THE INPUT DATA       RSP00040
C-----ARE AS FOLLOWS:  TP=POURING TEMPERATURE , TO=TEMPERATURE OF THE     RSP00050
C-----QUENCHING MEDIUM , H = HEAT TRANSFER COEFFICIENT (CAL/CM.CM.S.C),   RSP00060
C-----RHO= MELT DENSITY (G/CC) , CP=MELT SPECIFIC HEAT (CAL/G.C) ,        RSP00070
C-----TF=MELTING POINT (C) , HF=HEAT OF FUSION (CAL/G) , 2R=SMALLEST      RSP00080
C-----DIMENSION OF THE SPLAT EXCEPT FOR THE CASE OF THE SLAB COOLED       RSP00090
C-----THROUGH ONE SIDE ONLY WHERE  R = THICKNESS OF THE SPLAT (CM),       RSP00100
C----- AOV = RATIO OF HEAT TRANSFER AREA TO SPECIMEN VOLUME (1/CM),       RSP00110
C-----TIME= TIME (S), T=TEMPERATURE (C), CR=COOLING RATE (C/S) , FS=      RSP00120
C-----FRACTION SOLIDIFIED (-) , FR=FREEZING RATE (1/S) , RR=SOLIDIFIED    RSP00130
C-----DISTANCE (CM) ; GROWTH RATE (CM/S) ;  GP=GEOMETRIC PARAMETER (-).   RSP00140
C-----THE PARAMETERS FOR THE GAS ARE AS FOLLOWS: RHOG= GAS DENSITY ,      RSP00150
C-----TCG=THERMAL CONDUCTIVITY OF GAS , CPG=SPECIFIC HEAT OF GAS ,        RSP00160
C-----EMUG=VISCOSITY OF GAS , VG=RELATIVE VELOCITY OF GAS.                RSP00170
      TP=840.                                                            RSP00180
      TO=0.                                                             RSP00190
      RHO=2.7                                                           RSP00200
      CP=0.206                                                          RSP00210
      TF=660.                                                           RSP00220
      HF=95.                                                            RSP00230
      TCG=0.000042                                                      RSP00240
      RHOG=0.00163                                                      RSP00250
      CPG=0.124                                                         RSP00260
      EMUG=0.000225                                                     RSP00270
      VG=10000.0                                                        RSP00280
      COEFF=100.0                                                       RSP00290
      EN=0.375                                                          RSP00300
      RSTAR=0.0025                                                      RSP00310
      DR=0.0005                                                         RSP00320
      RINI=RSTAR + DR                                                   RSP00330
      WRITE(6,50) RHO,CP,TF,HF                                          RSP00340
      WRITE(6,50) TP,TO                                                 RSP00350
      WRITE(6,50) RHOG,CPG,TCG,EMUG                                     RSP00360
      WRITE(6,50) VG,DR,RINI                                            RSP00370
      WRITE(6,50) COEFF,EN                                              RSP00380
      WRITE(6,500)                                                      RSP00390
                       R=RSTAR                                          RSP00400
                       DO 7 J=1,21                                      RSP00410
                       R= R + DR                                        RSP00420
                 RE=2.*R*RHOG*VG/EMUG                                   RSP00430
                 PR=CPG*EMUG/TCG                                        RSP00440
      H=TCG*(2. + 0.6*(RE**.5)*(PR**.333))/(2.*R)                       RSP00450
      AOV=3./R                                                          RSP00460
      GP=1./3.                                                          RSP00470
C-----AOV=3./R (SPHERE); 2./R (CYLINDER);  1./R (SLAB)                   RSP00480
C-----GP=1./3. (SPHERE) ; 1./2. (CYLINDER) ; 1. (SLAB)                   RSP00490
      DTIME=0.0005                                                      RSP00500
      WRITE(6,50) RE,PR                                                 RSP00510
      WRITE(6,50) H                                                     RSP00520
      WRITE(6,50) R,AOV,GP                                              RSP00530
        TIME=0.0                                                        RSP00540
        DO 1 I=1,1000                                                   RSP00550
```

124

```
            TIME=TIME + DTIME                                       RSP00560
            TAO=(RHO*CP)/(AOV*H)                                    RSP00570
                T= (TP-TO)*EXP(-TIME/TAO) + TO                      RSP00580
                CR= - (TP-TO)*EXP(-TIME/TAO)/TAO                    RSP00590
C           WRITE(6,100) TIME,T,CR                                  RSP00600
            IF(T.LE.TF) GO TO 2                                     RSP00610
    1       CONTINUE                                                RSP00620
    2       CONTINUE                                                RSP00630
            DAS=COEFF*((ABS(CR))**(-EN))                            RSP00640
            WRITE(6,100) TIME,T,CR                                  RSP00650
            WRITE(6,100) DAS                                        RSP00660
            TSS=TIME                                                RSP00670
            WRITE(6,300) TSS                                        RSP00680
            FSO=0.0                                                 RSP00690
            DO 3 I=1,1000                                           RSP00700
            TIME=TIME + DTIME                                       RSP00710
            C1=(1./(RHO*HF))*AOV                                    RSP00720
            C2=H*(TF-TO)                                            RSP00730
                FS=C1*C2*(TIME-TSS)                                 RSP00740
                FR=C1*C2                                            RSP00750
            IF(FS.GE.0.99999) FS=0.99999                            RSP00760
            RR= R*(1. - (1.-FS)**GP)                                RSP00770
            GR= (GP*R)*(1./(1.-FS)***(1.-GP))*FR                    RSP00780
C           WRITE(6,200) TIME,FS,FR,RR,GR                           RSP00790
            IF(FSO.LE.0.5.AND.FS.GT.0.5) WRITE(6,200) TIME,FS       RSP00800
            IF(FS.GE.0.99999) GO TO 4                               RSP00810
            FSO=FS                                                  RSP00820
    3       CONTINUE                                                RSP00830
    4       CONTINUE                                                RSP00840
            TES=TIME                                                RSP00850
            WRITE(6,300) TES                                        RSP00860
            DO 5 I=1,1000                                           RSP00870
            TIME=TIME+DTIME                                         RSP00880
            TAO=(RHO*CP)/(AOV*H)                                    RSP00890
                T=(TF-TO)*EXP(-(TIME-TES)/TAO) + TO                 RSP00900
                CR=-(TF-TO)*EXP(-(TIME-TES)/TAO)/TAO                RSP00910
C           WRITE(6,100) TIME,T,CR                                  RSP00920
            IF(T.LE.200.) GO TO 6                                   RSP00930
    5       CONTINUE                                                RSP00940
    6       CONTINUE                                                RSP00950
            WRITE(6,100) TIME,T,CR                                  RSP00960
            WRITE(6,500)                                            RSP00970
    7       CONTINUE                                                RSP00980
   50       FORMAT(5X,4F16.8)                                       RSP00990
  100       FORMAT(10X,3F20.9)                                      RSP01000
  200       FORMAT(2X,5F14.7)                                       RSP01010
  300       FORMAT(25X,F15.8)                                       RSP01020
  500       FORMAT(/)                                               RSP01030
            STOP                                                    RSP01040
            END                                                     RSP01050
```

5.2.- Program NEUMANN . Neumann's Solution to the Stefan Problem.

```
C---r-----THIS PROGRAM COMPUTES TEMPERATURES, COOLING AND FREEZING       NEU00010
C-------RATES FOR THE CLASSICAL ONE-DIMENSIONAL STEFAN PROBLEM            NEU00020
C-------ACCORDING TO NEUMANN'S SOLUTION FOR THE SEMI-INFINTE MEDIUM.      NEU00030
C-------SEE CARSLAW AND JAEGER (1959), CH. 11 .                           NEU00040
C---------THE INPUT AND OUTPUT VARIABLES ARE AS FOLLOWS: TCL = THERMAL    NEU00050
C-------CONDUCTIVITY OF LIQUID , TCS = THERMAL CONDUCTIVITY OF SOLID ,    NEU00060
C-------TDIFL = THERMAL DIFFUSIVITY OF LIQUID , TDIFS = THERMAL           NEU00070
C-------DIFFUSIVITY OF SOLID , SPHTL = SPECIFIC HEAT OF LIQUID , SPHTS    NEU00080
C------- = SPECIFIC HEAT OF SOLID , TINI = INITIAL TEMPERATURE OF THE     NEU00090
C-------MELT , TWALL = WALL TEMPERATURE , TF = MELTING POINT , HEATF =    NEU00100
C-------LATENT HEAT OF FUSION , X = DISTANCE , T = TIME , XS =            NEU00110
C-------SOLIDIFIED THICKNESS , TEMP = TEMPERATURE .  QUANTITIES           NEU00120
C-------IN CGS UNITS . TEMPERATURES IN CELSIUS . ENERGY IN CALORIES.      NEU00130
C---------THE DATA SHOWN CORRESPOND TO ALUMINUM SOLIDIFYING AGAINST       NEU00140
C-------A COPPER CHILL .                                                  NEU00150
        TCL=.5                                                           NEU00160
        TCS=.5                                                           NEU00170
        TDIFL=.925                                                       NEU00180
        TDIFS=.925                                                       NEU00190
        SPHTL=.2                                                         NEU00200
        SPHTS=.2                                                         NEU00210
        TINI=760.                                                        NEU00220
        TWALL=25.                                                        NEU00230
        TF=660.                                                          NEU00240
        HEATF=95.                                                        NEU00250
        DALAMB=0.001                                                     NEU00260
        ALAMB=0.                                                         NEU00270
        DO 1 I=1,1000                                                    NEU00280
        ALAMB=ALAMB + DALAMB                                             NEU00290
        FLHS= EXP(-ALAMB*ALAMB)/ERF(ALAMB)                               NEU00300
        COEF1= TCL*SQRT(TDIFS)/(TCS*SQRT(TDIFL))                         NEU00310
        COEF2= (TINI - TF)/(TF - TWALL)                                  NEU00320
        COEF3= EXP(-TDIFS*ALAMB*ALAMB/TDIFL)                             NEU00330
        COEF4= 1. - ERF(ALAMB*SQRT(TDIFS/TDIFL))                         NEU00340
        SLHS= - COEF1*COEF2*COEF3/COEF4                                  NEU00350
        RHS=ALAMB*HEATF*SQRT(3.1416)/(SPHTS*(TF-TWALL))                  NEU00360
        DIF= FLHS + SLHS - RHS                                           NEU00370
        IF(DIF.LE.0.001) GO TO 2                                         NEU00380
    1   CONTINUE                                                         NEU00390
    2   CONTINUE                                                         NEU00400
        ALAMB=ALAMB                                                      NEU00410
        WRITE(6,3) ALAMB                                                 NEU00420
    3   FORMAT(18X,F15.8)                                                NEU00430
        T=0.                                                             NEU00440
        DO 5 J=1,10                                                      NEU00450
        DT=0.001                                                         NEU00460
        T=T + DT                                                         NEU00470
        X=0.                                                             NEU00480
        XS=2.*ALAMB*SQRT(TDIFS*T)                                        NEU00490
        WRITE(6,6) XS,T                                                  NEU00500
        DO 4 K=1,6                                                       NEU00510
        DX=.05                                                           NEU00520
        TS=((TF - TWALL)/ERF(ALAMB))*ERF(X/(2.*SQRT(TDIFS*T))) + TWALL   NEU00530
        TL= TINI - (TINI-TF)*(1.-ERF(X/(2.*SQRT(TDIFL*T))))/(1.-         NEU00540
    1 ERF(ALAMB*SQRT(TDIFS/TDIFL)))                                      NEU00550
        IF(TS.GE.TF) GO TO 22                                            NEU00560
   11   CONTINUE                                                         NEU00570
        TEMP=TS                                                          NEU00580
        GO TO 33                                                         NEU00590
   22   CONTINUE                                                         NEU00600
        TEMP=TL                                                          NEU00610
   33   CONTINUE                                                         NEU00620
        WRITE(6,6) X,TEMP                                                NEU00630
        X=X+DX                                                           NEU00640
    4   CONTINUE                                                         NEU00650
    5   CONTINUE                                                         NEU00660
        WRITE(6,7) DT,DX,J                                               NEU00670
    6   FORMAT(5X,F15.5,5X,F20.8)                                        NEU00680
    7   FORMAT(/10X,2F15.8,5X,I3/)                                       NEU00690
        STOP                                                             NEU00700
        END                                                              NEU00710
```

126

5.3.– Program SCHWARZ . Schwarz's Solution of the Stefan Problem.

```
C---------THIS PROGRAM COMPUTES TEMPERATURES, COOLING AND FREEZING      SCH00010
C-------RATES FOR THE CLASSICAL ONE-DIMENSIONAL STEFAN PROBLEM          SCH00020
C-------ACCORDING TO SCHWARZ'S SOLUTION FOR A SEMI-INFINTE MEDIUM.      SCH00030
C-------SEE CARSLAW AND JAEGER (1959) , CH. 11 .                        SCH00040
C---------THE VARIABLES HERE ARE THE SAME AS IN PROGRAM NEUMANN         SCH00050
C-------(SEC.5.2) EXCEPT THAT THE THERMAL CONDUCTIVITY AND DIFFUSIVITY  SCH00060
C-------OF THE MOLD, RESPECTIVELY TCMOLD AND TDIFM , ARE ALSO INCLUDED. SCH00070
C-------MOREOVER,  V  HERE DENOTES THE VELOCITY OF THE SOLIDIFICATION   SCH00080
C-------INTERFACE . THE UNITS ARE THE SAME AS IN NEUMANN .              SCH00090
         TCMOLD=.94                                                     SCH00100
         TCL=.29                                                        SCH00110
         TCS=.53                                                        SCH00120
         TDIFM=1.1                                                      SCH00130
         RHOS=2.8                                                       SCH00140
         RHOL=2.8                                                       SCH00150
         CPS=.23                                                        SCH00160
         CPL=.26                                                        SCH00170
         TDIFL=TCL/(RHOL*CPL)                                           SCH00180
         TDIFS=TCS/(RHOS*CPS)                                           SCH00190
         SPHTL=CPL                                                      SCH00200
         SPHTS=CPS                                                      SCH00210
         TINI=700.                                                      SCH00220
         TWALL=25.                                                      SCH00230
         TF=660.                                                        SCH00240
         HEATF=95.                                                      SCH00250
         DALAMB=0.001                                                   SCH00260
         ALAMB=0.                                                       SCH00270
         DO 1 I=1,1000                                                  SCH00280
         ALAMB=ALAMB + DALAMB                                           SCH00290
         COE1=TCMOLD*SQRT(TDIFS)*EXP(-ALAMB*ALAMB)                      SCH00300
         COE2=TCS*SQRT(TDIFM) + TCMOLD*SQRT(TDIFS)*ERF(ALAMB)           SCH00310
         FLHS= COE1/COE2                                                SCH00320
         COEF1= TCL*SQRT(TDIFS)/(TCS*SQRT(TDIFL))                       SCH00330
         COEF2= (TINI - TF)/(TF - TWALL)                                SCH00340
         COEF3= EXP(-TDIFS*ALAMB*ALAMB/TDIFL)                           SCH00350
         COEF4= 1. - ERF(ALAMB*SQRT(TDIFS/TDIFL))                       SCH00360
         SLHS= - COEF1*COEF2*COEF3/COEF4                                SCH00370
         RHS=ALAMB*HEATF*SQRT(3.1416)/(SPHTS*(TF-TWALL))                SCH00380
         DIF= FLHS + SLHS - RHS                                         SCH00390
         IF(DIF.LE.0.001) GO TO 2                                       SCH00400
1        CONTINUE                                                       SCH00410
2        CONTINUE                                                       SCH00420
         ALAMB=ALAMB                                                    SCH00430
         WRITE(6,3) DIF,ALAMB                                           SCH00440
3        FORMAT(18X,2F15.8)                                             SCH00450
         T=0.                                                           SCH00460
         DO 5 J=1,10                                                    SCH00470
         DT=0.01                                                        SCH00480
         T=T + DT                                                       SCH00490
         X=0.                                                           SCH00500
         XS=2.*ALAMB*SQRT(TDIFS*T)                                      SCH00510
         V= ALAMB*SQRT(TDIFS/T)*TDIFS                                   SCH00520
         WRITE(6,7) XS,V,T                                              SCH00530
         DO 4 K=1,10                                                    SCH00540
         DX=0.05                                                        SCH00550
```

127

```
      AM1= TCS*SQRT(TDIFM)*(TF-TWALL)                                  SCH00560
      AM2= TCS*SQRT(TDIFM) + TCMOLD*SQRT(TDIFS)*ERF(ALAMB)             SCH00570
      AMOLD= AM1/AM2                                                   SCH00580
      TMOLD= AMOLD*(1.+ERF(X/(2.*SQRT(TDIFM*T)))) + TWALL             SCH00590
      AS1= (TF-TWALL)/AM2                                              SCH00600
      AS2= TCS*SQRT(TDIFM)                                             SCH00610
      AS3= TCMOLD*SQRT(TDIFS)                                          SCH00620
      TS= TWALL + AS1*(AS2 + AS3*ERF(X/(2.*SQRT(TDIFS*T))))           SCH00630
      AL1=(TINI-TF)/(1.-ERF(ALAMB*SQRT(TDIFS/TDIFL)))                SCH00640
      TL= TINI - AL1*(1.-ERF(X/(2.*SQRT(TDIFL*T))))                  SCH00650
      IF(X.LE.O.) GO TO 33                                            SCH00660
      IF(TS.GE.TF) GO TO 22                                           SCH00670
11    CONTINUE                                                        SCH00680
      TEMP=TS                                                         SCH00690
      GO TO 44                                                        SCH00700
22    CONTINUE                                                        SCH00710
      TEMP=TL                                                         SCH00720
      GO TO 44                                                        SCH00730
33    CONTINUE                                                        SCH00740
      TEMP=TMOLD                                                      SCH00750
44    CONTINUE                                                        SCH00760
      WRITE(6,6) X,TEMP                                               SCH00770
      X=X+DX                                                          SCH00780
4     CONTINUE                                                        SCH00790
      AL2=EXP(-ALAMB*ALAMB*TDIFS/TDIFL)                              SCH00800
      AL3=4.*ALAMB*ALAMB*ALAMB*TDIFS*SQRT(TDIFS/TDIFL)/SQRT(3.141592) SCH00810
      AL=-AL1*AL2*AL3                                                 SCH00820
      CR=AL/(XS*XS)                                                   SCH00830
      WRITE(6,8) CR                                                   SCH00840
5     CONTINUE                                                        SCH00850
6     FORMAT(5X,F15.5,5X,F20.8)                                      SCH00860
7     FORMAT(1X,3F20.9)                                              SCH00870
8     FORMAT(13X,F25.9)                                              SCH00880
      STOP                                                            SCH00890
      END                                                             SCH00900
```

5.4.– Program PFMS . Calculation of Heat Transfer and Fluid

Flow in the Planar Flow Melt Spinning Process.

```
C---THIS PROGRAM COMPUTES SOLIDIFIED THICKNESS FOR THE CASE OF SINGLE   CCS00010
C---ROLL STRIP CASTING OF METALS. THE ALGORITHM IS BASED ON THE ENTHALPYCCS00020
C---METHOD AND THE PARTICULAR SCHEME USED HAS BEEN AN EXPLICIT ONE.     CCS00030
C---ENTHALPIES (AND THUS TEMPERATURES) ARE COMPUTED EXPLICITLY FOR A    CCS00040
C---ROW OF GRID POINTS AT A GIVEN DOWNSTREAM LOCATION BY USING THE VALUECCS00050
C---OF ENTHALPY AND TEMPERATURE OF THE GRID POINTS ALONG THE INMEDIATLY CCS00060
C---PRECEEDING UPSTREAM LOCATION.                                       CCS00070
C---HERE WE ASSUME "PLUG FLOW" TYPE MOTION OF THE METAL BEING CAST.     CCS00080
C---HOWEVER, VELOCITY PROFILES ARE COMPUTED AT EVERY DOWNSTREAM LO-     CCS00090
C---CATION TAKING INTO ACCOUNT THE PRESENCE OF A SOLIDIFIED SHELL.      CCS00100
C---DURING THE LAST STAGES OF SOLIDIFICATION, FLUID FLOW AND HEAT       CCS00110
C---TRANSFER INTERACT MUCH STRONGER SINCE THE FREE MELT-GAS SURFACE     CCS00120
C---IS COMPUTED FROM THE SOLIDIFIED THICKNESS AND THIS, IN TURN .       CCS00130
C---DEPENDS ON THE PRECISE LOCATION OF THE FREE BOUNDARY.              CCS00140
        REAL UO(32),UN(32),HO(32),HN(32),CTU(32),TEMP(32),TEMPO(32)    CCS00150
        REAL TINI(32),CR(32),VX(32),VXO(32),STREAM(32)                 CCS00160
C---THE VARIABLES IN THE ARRAYS ARE: UO =OLD PSEUDO TEMPERATURE (SEE    CCS00170
C---BELOW); UN = NEW PSEUDO TEMPERATURE; HO = OLD ENTHALPY ; HN = NEW   CCS00180
C---ENTHALPY; CTU = C TIMES U (SEE BELOW); TEMP = ACTUAL TEMPERATURE;   CCS00190
C---TEMPO = OLD TEMPERATURE; TINI = INITIAL TEMPERATURE ; CR = COOLING  CCS00200
C---RATE ; VX = X-COMPONENT OF VELOCITY ; VXO = OLD VELOCITY ; STREAM   CCS00210
C--- = STREAM FUNCTION (DIMENTIONLESS).                                 CCS00220
        TFUS=1325.0                                                    CCS00230
        HFUS=71.7                                                     CCS00240
        TC=0.0717                                                     CCS00250
        CP=0.1434                                                     CCS00260
        RHO=8.5                                                       CCS00270
        EMU=0.046                                                     CCS00280
        SIGMA=1778.0                                                  CCS00290
        TCR=0.16                                                      CCS00300
C       TCR=0.93                                                      CCS00310
        RHOR=7.86                                                     CCS00320
C       RHOR=8.94                                                     CCS00330
        CPR=0.15                                                      CCS00340
C       CPR=0.0914                                                    CCS00350
        TDR= TCR/(RHOR*CPR)                                           CCS00360
        WRITE(6,110) TFUS,HFUS,TC,CP                                  CCS00370
        WRITE(6,110) RHO,EMU,SIGMA                                    CCS00380
        WRITE(6,110) TCR,RHOR,CPR,TDR                                 CCS00390
C--- QUANTITIES WILL BE GIVEN IN   CGS   UNITS.                        CCS00400
C---ENERGIES WILL BE GIVEN IN   CALORIES  AND  TEMPERATURES IN CELSIUS. CCS00410
C---THE PHYSICAL PROPERTY DATA ARE AS FOLLOWS: TFUS = MELTING POINT OF  CCS00420
C---THE SUBSTANCE BEING CAST (NOTE: IN THE CASE OF AN ALLOY, INSTEAD OF CCS00430
C---TFUS A LIQUIDUS AND A SOLIDUS HAVE TO BE SPECIFIED); HFUS = LATENT  CCS00440
C---HEAT OF FUSION ; TC = THERMAL CONDUCTIVITY ; CP = SPECIFIC HEAT ;   CCS00450
C--- RHO = DENSITY ; EMU = VISCOSITY ; SIGMA = SURFACE TENSION ; TCR =  CCS00460
C--- THERMAL CONDUCTIVITY OF ROLL ; RHOR = DENSITY OF ROLL ; CPR = SPE- CCS00470
C---CIFIC HEAT OF ROLL ; TDR = THERMAL DIFFUSIVITY OF ROLL .           CCS00480
        PI=3.14159                                                    CCS00490
        TWALL=25.0                                                    CCS00500
        TBULK=1440.0                                                  CCS00510
        BN=0.064                                                      CCS00520
        HIN=0.0300                                                    CCS00530
        W=0.635                                                       CCS00540
        OMEGA=1200.0                                                  CCS00550
```

```
      RR=12.7                                                CCS00560
      Q=3.86                                                 CCS00570
      PL=0.29                                                CCS00580
      THETA=20.0                                             CCS00590
      VRXR= OMEGA*2.0*PI*RR/60.0                             CCS00600
      QPUW= Q/W                                              CCS00610
      COEFI= 3.0*EMU/SIGMA                                   CCS00620
      TW= TWALL*TCR                                          CCS00630
      TF= TFUS*TC                                            CCS00640
      TB= TBULK*TC                                           CCS00650
      HF= HFUS*RHO                                           CCS00660
      XI=-0.60                                               CCS00670
      XB= XI + BN                                            CCS00680
      XD= XI + PL                                            CCS00690
      XF=0.0                                                 CCS00700
      XINI= XI - XI                                          CCS00710
      XBRE= XB - XI                                          CCS00720
      XDET= XD - XI                                          CCS00730
      XFIN= XF - XI                                          CCS00740
      FO= HF*Q/(W*(1.5*PL))                                  CCS00750
      TGR= FO/TCR                                            CCS00760
      H10= HIN                                               CCS00770
      H20= - TAN(THETA*2.0*PI/360.0)                         CCS00780
      H30= 1.0/(PL/2.)                                       CCS00790
      SLIPE=0.25                                             CCS00800
      HTCO=1.035                                             CCS00810
      YFS=0.0                                                CCS00820
      PO=0.0                                                 CCS00830
      PF=101300000.0                                         CCS00840
      ALFA=0.0                                               CCS00850
      BETA=0.333                                             CCS00860
      GAMA=1.002                                             CCS00870
      WRITE(6,110) TWALL,TBULK                               CCS00880
      WRITE(6,110) BN,HIN,W                                  CCS00890
      WRITE(6,110) OMEGA,RR,Q                                CCS00900
      WRITE(6,110) PL,THETA                                  CCS00910
      WRITE(6,110) VRXR,QPUW,COEFI                           CCS00920
      WRITE(6,110) XI,XB,XD,XF                               CCS00930
      WRITE(6,110) XINI,XBRE,XDET,XFIN                       CCS00940
      WRITE(6,110) FO,TGR                                    CCS00950
      WRITE(6,110) H10,H20,H30                               CCS00960
      WRITE(6,110) SLIPE,HTCO                                CCS00970
      WRITE(6,110) BETA,GAMA                                 CCS00980
C---THE PROCESS PARAMETERS ARE : TWALL =  TEMPERATURE OF THE ROLL (SEE  CCS00990
C---BELOW) ; TBULK = POURING TEMPERATURE ; BN = NOZZLE BREADTH ; HIN =  CCS01000
C---WHEEL-NOZZLE GAP ; W = NOZZLE (STRIP) WIDTH ; OMEGA = ANGULAR VELO-  CCS01010
C---CITY OF ROLL (RPM); RR = ROLL RADIUS ; Q = MELT FLOW RATE ; PL =    CCS01020
C---PUDDLE LENGTH ; THETA = CONTACT ANGLE MELT-NOZZLE (DOWNSTREAM) ;    CCS01030
C---VRXR = SURFACE VELOCITY OF ROLL ; XINI,XBRE,XDET AND XFIN ARE,RESPECCCS01040
C---TIVELY THE LOCATIONS OF : THE UPSTREAM EDGE OF PUDDLE , THE END OF   CCS01050
C---NOZZLE BREADTH , THE DETACHMENT POINT AND THE (APPROXIMATE) END-     CCS01060
C---POINT OF SOLIDIFICATION ; H10,H20 AND H30 ARE USED TO INITIATE THE   CCS01070
C---NUMERICAL SOLUTION FOR THE FREE SURFACE ; SLIPE = SLIP EXPONENT (    CCS01080
C---SEE BELOW --LBL. 16) ; HTCO = HEAT TRANSFER COEFFICIENT (SEE BELOW   CCS01090
C---,-LBL. 33) ; BETA = FRACTION TO DEFINE THE LOCATION OF SOLID-LIQUID  CCS01100
```

```
C---INTERFACE (SEE AFTER LBL. 37) ; GAMA = COEFFICIENT TO DECIDE IF A       CCSO1110
C---GIVEN GRID POINT HAS SOLIDIFIED (SEE AFTER LBL. 37 BELOW).               CCSO1120
C                                                                           CCSO1130
        N= 31                                                               CCSO1140
        NMAX=N                                                              CCSO1150
        NMIN1= N-1                                                          CCSO1160
        NT= 8000                                                            CCSO1170
C                                                                           CCSO1180
C---THE GRID PARAMETERS ARE: N =  NUMBER OF POINTS ALONG THE   Y  (VER-      CCSO1190
C---TICAL, PERPENDICULAR TO THE WHEEL) DIRECTION , NT =  NUMBER OF           CCSO1200
C---POINTS ALONG THE   X  (DOWNSTREAM) DIRECTION .                          CCSO1210
C---THE FOLLOWING LOOP INITIALIZES BOTH TEMPERATURE AND ENTHALPY.           CCSO1220
        DO 10 I= 1,N                                                        CCSO1230
        UO(I)= TB                                                           CCSO1240
        HO(I)= ((RHO*CP)/TC)*(UO(I)-TF) + HF                                CCSO1250
        UN(I)= TB                                                           CCSO1260
        TINI(I)= UO(I)/TC                                                   CCSO1270
   10   CONTINUE                                                            CCSO1280
        WRITE(6,100) (TINI(I),I= 1,N)                                       CCSO1290
        TIME= 0.                                                           CCSO1300
        X= XI                                                               CCSO1310
        DISTX= 0.0                                                          CCSO1320
                        KOUNT1=0                                            CCSO1330
                        KOUNT2=0                                            CCSO1340
C---THE FOLLOWING LOOP ADVANCES THE CALCULATION ALONG THE DOWNSTREAM        CCSO1350
C---DIRECTION, JUMPING FROM A LINE OF GRID POINTS AT CONSTANT X TO THE       CCSO1360
C---NEXT. THIS IS THE MAIN "OUTER LOOP" OF THE CALCULATION .                CCSO1370
C---NOTE; TIME,KOUNT1 AND KOUNT2 ARE ONLY COUNTERS.                         CCSO1380
                DO 50 K=1,NT                                                CCSO1390
                KOUNT1=KOUNT1+1                                            CCSO1400
                KOUNT2=KOUNT2+1                                            CCSO1410
C---"OLD" TEMPERATURE IS CALCULATED.                                        CCSO1420
                DO 12 J=1,NMAX                                              CCSO1430
                TEMPO(J)=UO(J)/TC                                           CCSO1440
   12           CONTINUE                                                    CCSO1450
C---IN THE FOLLOWING THE GRID SPACING IS COMPUTED, SINCE THE METHOD IS       CCSO1460
C---AN EXPLICIT ONE , DX AND  DY  ARE RELATED BY THE STABILITY CONDI-        CCSO1470
C---TION. THIS PART OF THE PROGRAM (UP TO LBL. 15) COMPUTES THE LOCA-        CCSO1480
C---TION OF THE UPPER BOUNDARY. THEN , UP TO LBL 16, THE GEOMETRICAL         CCSO1490
C---PARAMETERS OF THE GRID ARE SET.                                         CCSO1500
C---THE GAS-MELT INTERFACE HAS TO BE SPECIFIED (DISTX.GT.XDET) EITHER        CCSO1510
C---BY SOME (ASSUMED) SHAPE OR BY NUMERICALLY SOLVING THE CAPILLARY          CCSO1520
C---EQUATIONS (PREFERRED).                                                   CCSO1530
C---THE NEXT THREE CONDITIONS CONTROL WHERE THE MELT-GAS INTERFACE HAS       CCSO1540
C---TO BE CALCULATED DEPENDING ON THE PROGRESS OF SOLIDIFICATION AND         CCSO1550
C---ON IF DISTX IS .GT. XDET .                                               CCSO1560
                        H = HIN                                            CCSO1570
                        HMYFS = H - YFS                                    CCSO1580
                IF(HMYFS.LE.0.0001) GO TO 51                                CCSO1590
                IF(UN(NMAX).LE.GAMA*TF) H = HFIN                            CCSO1600
                IF(UN(NMAX).LE.GAMA*TF) GO TO 15                            CCSO1610
                IF(DISTX.LT.XDET) GO TO 15                                  CCSO1620
   14           CONTINUE                                                    CCSO1630
                HMYFSC=HMYFS*HMYFS*HMYFS                                    CCSO1640
                HMYFSS=HMYFS*HMYFS                                         CCSO1650
```

```
            FUNCT= COEFI*((QLPUW/HMYFSC) - (VRX/HMYFSS))          CCSO1660
            H3= H30 + FUNCT*DX                                    CCSO1670
            H2= H20 + H3*DX                                       CCSO1680
            H1= H10 + H2*DX                                       CCSO1690
            IF(H2.GE.0.0001) GO TO 51                             CCSO1700
            H10=H1                                                CCSO1710
            H20=H2                                                CCSO1720
            H30=H3                                                CCSO1730
            HMYFS = H1                                            CCSO1740
            H= HMYFS + YFS                                        CCSO1750
            IF(H.GT.HIN) H = HIN                                  CCSO1760
     15     CONTINUE                                              CCSO1770
                VELAV= Q/(W*HIN)                                  CCSO1780
                V=Q/(W*H)                                         CCSO1790
                DY=HIN/FLOAT(NMIN1)                               CCSO1800
                DX=(DY*DY)*VELAV/2.                               CCSO1810
                DT=DX/VELAV                                       CCSO1820
                C=DT/(DY*DY)                                      CCSO1830
                TIME=TIME+DT                                      CCSO1840
                DISTX=DISTX+DX                                    CCSO1850
                X=X + DX                                          CCSO1860
     16         CONTINUE                                          CCSO1870
C                                                                 CCSO1880
                        SLIPC= DISTX/XFIN                         CCSO1890
                        IF(DISTX.GE.XFIN) SLIPC=1.00              CCSO1900
                        VRX= VRXR*SLIPC**SLIPE                    CCSO1910
C                                                                 CCSO1920
C---THE NEXT 4 STATEMENTS SERVE TO ACCOUNT FOR THE PRESENCE OF    CCSO1930
C---THE FREE SURFACE AFTER DETACHMENT. GRID POINTS OUTSIDE THE    CCSO1940
C---MELT ARE NOT COMPUTED THERE.                                  CCSO1950
                DIF=(HIN + 0.5*DY - H)/DY                         CCSO1960
                KDIF=INT(DIF)                                     CCSO1970
                NMAXM1=(N-1) - KDIF                               CCSO1980
                NMAX= NMAXM1 + 1                                  CCSO1990
                NMAXM2= NMAXM1 - 1                                CCSO2000
                Y=0.0                                             CCSO2010
C---WITH THIS LOOP WE ADVANCE THE CALCULATION IN THE VERTICAL (Y) CCSO2020
C---DIRECTION. FROM THE EQN.  V*DH/DX = K D(DT/DY)/DY  WE CONSTRUCT CCSO2030
C---THE EXPLICIT F.D. EQN.:  HN= HO + C*(UO(J-1)-2UO(J)+UO(J+1)).  CCSO2040
C---THE RESULT OF THIS CALCULATION IS  HN(K) .                    CCSO2050
C---THIS IS THE MAIN "INNER" LOOP OF THE PROGRAM.                 CCSO2060
            DO 20 I=2,NMAXM1                                      CCSO2070
            IP1=I+1                                               CCSO2080
            IM1=I-1                                               CCSO2090
            CTU(I)=C*(UO(IM1)+UO(IP1)-2.*UO(I))                   CCSO2100
            HN(I)=HO(I)+CTU(I)                                    CCSO2110
     20     CONTINUE                                              CCSO2120
C---THE FOLLOWING STATEMENTS (UP TO 30) SIMPLY COMPUTE THE PSEUDOTEM- CCSO2130
C---PERATURES CORRESPONDING TO THE JUST CALCULATED VALUES OF  HN  BY CCSO2140
C---USING THE THERMODYNAMIC RELATIONSHIP BETWEEN  ENTHALPY AND TEMPE- CCSO2150
C---RATURE.                                                       CCSO2160
                DO 30 I=2,NMAXM1                                  CCSO2170
            IF(HN(I).GT.HF)GO TO 27                               CCSO2180
     23     CONTINUE                                              CCSO2190
            IF(HN(I).LE.HF.AND.HN(I).GE.0.)GO TO 26               CCSO2200
```

132

```
      24      CONTINUE                                                           CCSO2210
              UN(I)=TF + HN(I)*(TC/(RHO*CP))                                     CCSO2220
              GO TO 30                                                           CCSO2230
      26      CONTINUE                                                           CCSO2240
              UN(I)=TF                                                           CCSO2250
              GO TO 30                                                           CCSO2260
      27      CONTINUE                                                           CCSO2270
              UN(I)=TF + (HN(I)-HF)*(TC/(RHO*CP))                                CCSO2280
      30            CONTINUE                                                     CCSO2290
C---TO COMPUTE THE TEMPERATURE AT THE WHEEL-SPLAT INTERFACE IMPERFECT            CCSO2300
C---THERMAL CONTACT IS ASSUMED.THE TEMPERATURE AT THE SURFACE OF THE             CCSO2310
C---WHEEL CAN BE GIVEN BY THE FORMULA FOR PEAK TEMPERATURE IN A                  CCSO2320
C---THICK SOLID UNDER A MOVING HEAT SOURCE. TWO ALTERNATIVE B.C'S FOR            CCSO2330
C---THIS BOUNDARY ARE THAT  UW = TW  AND THAT UN(1) = UW (VARIABLE)              CCSO2340
C---,WHICH WOULD CORRESPOND TO IDEAL COOLING (I.E. HTCO VERY LARGE).             CCSO2350
C---MOREOVER, HTC  CAN BE MADE VARIABLE AS A FUNCTION OF VRX.                    CCSO2360
      33            CONTINUE                                                     CCSO2370
              DU=(2.*FO)*SQRT(TDR*(DISTX/VRXR)/PI)                               CCSO2380
              UWR= TW + DU                                                       CCSO2390
              TSR= UWR/TCR                                                       CCSO2400
C             UW=UWR                                                            CCSO2410
              UW= TW                                                             CCSO2420
              TSURF= UW/TCR                                                      CCSO2430
              CHTC=1.0                                                           CCSO2440
              IF(UN(1).GT.GAMA*TF) CHTC=VRX/VRXR                                 CCSO2450
              HTC=HTCO*CHTC                                                      CCSO2460
              UN(1) = ((TC/DY)*UN(2) + HTC*UW)/((TC/DY) + HTC)                   CCSO2470
C             UN(1) = UW*TC/TCR                                                 CCSO2480
C                                                                               CCSO2490
                  HN(1) = ((RHO*CP)/TC)*(UN(1) - TF)                            CCSO2500
          IF(UN(1).GE.TF) HN(1) = ((RHO*CP)/TC)*(UN(1) - TF)   +   HF           CCSO2510
C                                                                               CCSO2520
C---THE FOLLOWING STATEMENTS (UP TO 37) INTRODUCE THE BOUNDARY CONDITIONCCSO2530
C---ON THE NOZZLE (FREE SURFACE) SIDE OF THE GRID. NOTE THAT   BENEATH          CCSO2540
C--- THE NOZZLE BREADTH THE TEMPERATURE IS TAKEN AS THE POURING VALUE           CCSO2550
C---WHILE AFTER THE BREADTH AND ALONG THE FREE SURFACE A ZERO HEAT FLOW         CCSO2560
C---CONDITION IS USED.                                                          CCSO2570
              UN(NMAX)=UN(NMAXM1)                                               CCSO2580
              HN(NMAX)=HN(NMAXM1)                                               CCSO2590
                IF(DISTX.LE.XBRE) GO TO 36                                       CCSO2600
      35        GO TO 37                                                         CCSO2610
      36        CONTINUE                                                         CCSO2620
              UN(NMAX)=TB                                                        CCSO2630
              HN(NMAX)=((RHO*CP)/TC)*(TB-TF) + HF                                CCSO2640
      37        CONTINUE                                                         CCSO2650
C---THE FOLLOWING PORTION (FROM 37 UP TO 38) COMPUTES VELOCITY PROFILES CCSO2660
C---IN THE SPLAT UNDER THE ASSUMPTIONS OF LUBRICATION THEORY. ACCOUNT            CCSO2670
C---IS TAKEN OF THE THICKNESS SOLIDIFIED BY MEANS OF   ALFA .                    CCSO2680
                      YFS=0.0                                                    CCSO2690
                      IF(UN(1).LE.GAMA*TF) YFS=BETA*DY                           CCSO2700
                  DO 301 J=2,NMAXM1                                              CCSO2710
                  JM1=J-1                                                        CCSO2720
                  JP1=J+1                                                        CCSO2730
                  IF(UN(J).LE.GAMA*TF) YFS= (FLOAT(JM1)-BETA)*DY      CCSO2740
                  IF(UN(J).LE.TF/GAMA) YFS= (FLOAT(JM1)+0.5*BETA)*DYCCSO2750
```

133

```
                    UNPR= (UN(JP1) + UN(J))/2.                          CCSO2760
                    IF(UNPR.LE.GAMA*TF) YFS= (FLOAT(JM1)+BETA)*DY        CCSO2770
                    IF(UNPR.LE.TF/GAMA) YFS= (FLOAT(JM1)+1.5*BETA)*DY    CCSO2780
                    IF(UN(J).GT.GAMA*TF) GO TO 302                       CCSO2790
301                 CONTINUE                                            CCSO2800
302                 CONTINUE                                            CCSO2810
              IF(UN(NMAX).LE.GAMA*TF) YFS=(FLOAT(NMAXM1) - BETA)*DY     CCSO2820
                    ALFA= YFS/H                                         CCSO2830
                    IF(ALFA.GE.1.000) ALFA=0.9999                       CCSO2840
                    FOA= 1. - 3.*ALFA + 3.*ALFA*ALFA - ALFA*ALFA*ALFA   CCSO2850
                        IF(DISTX.GE.XDET) GO TO 305                     CCSO2860
303                     CONTINUE                                        CCSO2870
            PPO2E= 6.*( VRX*(H/2.)*(1.-ALFA) + VRXR*H*ALFA - QPUW )/    CCSO2880
          1 ((H*H*H)*FOA)                                              CCSO2890
            A2= PPO2E                                                  CCSO2900
            A1= VRX/(H*(ALFA-1.)) - PPO2E*H*(ALFA+1.)                  CCSO2910
            AO= PPO2E*H*H*ALFA - VRX/(ALFA-1.)                         CCSO2920
            QLPUW= - PPO2E*((H*H*H)/6.)*FOA + VRX*(H/2.)*(1.-ALFA)     . CCSO2930
            GO TO 307                                                  CCSO2940
305         CONTINUE                                                   CCSO2950
            PPO2E= (3./2.)*( VRX*H*(1.-ALFA) + VRXR*H*ALFA - QPUW )/    CCSO2960
          1 ((H*H*H)*FOA)                                              CCSO2970
            A2= PPO2E                                                  CCSO2980
            A1= - PPO2E*2.*H                                           CCSO2990
            AO= VRX - PPO2E*H*H*(ALFA*ALFA - 2.*ALFA)                  CCSO3000
            QLPUW= - PPO2E*(2./3.)*(H*H*H)*FOA + VRX*H*(1.-ALFA)       CCSO3010
307         CONTINUE                                                   CCSO3020
                              ATH= ALFA*H                              CCSO3030
                              ATHS= ALFA*H*ALFA*H                      CCSO3040
                              ATHC= ALFA*H*ALFA*H*ALFA*H              CCSO3050
                                PP= 2.*EMU*PPO2E                       CCSO3060
                                PN= PO + PP*DX                         CCSO3070
                      IF(PN.GE.PF.AND.PO.LT.PF) XPRESS=DISTX           CCSO3080
                                PO=PN                                  CCSO3090
                    Y=0.0                                              CCSO3100
                    DO 38 I=1,NMAX                                     CCSO3110
                    IF(ALFA*H.GT.0.0.AND.Y.LT.ALFA*H) GO TO 330        CCSO3120
310                 CONTINUE                                           CCSO3130
                    VX(I)= A2*(Y*Y) + A1*Y + AO                        CCSO3140
                    STREAM(I)=(VRXR*ALFA*H + (A2/3.)*( Y*Y*Y - ATHC ) + CCSO3150
          1         (A1/2.)*( Y*Y - ATHS ) + AO*( Y - ATH ))/QPUW      CCSO3160
                    GO TO 350                                          CCSO3170
330                 CONTINUE                                           CCSO3180
                    VX(I)=VRXR                                         CCSO3190
                    STREAM(I)= VRXR*Y/QPUW                             CCSO3200
350                 CONTINUE                                           CCSO3210
                    Y=Y+DY                                             CCSO3220
38                  CONTINUE                                           CCSO3230
            IF(UN(1).LE.TF.AND.UO(1).GT.TF) XSS=DISTX                  CCSO3240
            IF(VX(NMAX).GE.0.00.AND.VXO(NMAX).LT.0.00) XSTAG2=DISTX    CCSO3250
            IF(UN(NMAX).LE.GAMA*TF.AND.UO(NMAX).GT.GAMA*TF) HFIN = H   CCSO3260
            IF(UN(NMAX).LE.TF/GAMA.AND.UO(NMAX).GT.TF/GAMA) GO TO 51   CCSO3270
C---TO AVOID HAVING TO STORE THE WHOLE GRID, THE FOLLOWING LOOP RESETS CCSO3280
C---UO TO BE THE FRESHLY CALCULATED VALUE I.E.  UN . SAME WITH  HN .   CCSO3290
39          CONTINUE                                                  CCSO3300
```

134

```
          DO 40 I=1,NMAX                                              CCSO3310
          UO(I)=UN(I)                                                 CCSO3320
          HO(I)=HN(I)                                                 CCSO3330
          VXO(I)=VX(I)                                                CCSO3340
   40     CONTINUE                                                    CCSO3350
C---THE FOLLOWING LOOP RECOVERS THE ACTUAL TEMPERATURES AND ALSO      CCSO3360
C---COMPUTES THE VALUES OF THE COOLING RATE FOR EVERY GRID POINT.     CCSO3370
C---BESIDES, AVERAGE COOLING RATES ACROSS THE SPLAT FOR FIXED  X      CCSO3380
C---LOCATION ARE CALCULATED.                                          CCSO3390
          DO 41 I=1,NMAX                                              CCSO3400
          TEMP(I)=UN(I)/TC                                            CCSO3410
   41     CONTINUE                                                    CCSO3420
          SUM=0.0                                                     CCSO3430
          DO 42 I=1,NMAX                                              CCSO3440
          CR(I)=(TEMP(I)-TEMPO(I))*(VX(I)/DX)                         CCSO3450
          SUM= SUM + CR(I)                                            CCSO3460
   42     CONTINUE                                                    CCSO3470
          AVERCR= SUM/NMAX                                            CCSO3480
C---WITH THE FOLLOWING STATEMENTS IT IS POSSIBLE TO PRODUCE OUTPUT WITH CCSO3490
C---DIFFERENT FREQUENCIES IN THE DIFFERENT REGIONS OF THE DOMAIN.     CCSO3500
          IF(ALFA.GT.0.20) GO TO 48                                  CCSO3510
   44     IF(KOUNT1.NE.200) GO TO 50                                 CCSO3520
   46     GO TO 49                                                    CCSO3530
   48     IF(KOUNT2.NE.200) GO TO 50                                 CCSO3540
   49     CONTINUE                                                    CCSO3550
C444      GO TO 50                                                    CCSO3560
C---FINALLY RESULTS ARE WRITEN  .                                     CCSO3570
          WRITE(6,102) K,IP1,IM1,NMAX,NMAXM1                         CCSO3580
          WRITE(6,99) H,DY,DISTX,X,DX,TIME                           CCSO3590
C         WRITE(6,100) (HN(I),I=1,NMAX)                              CCSO3600
          WRITE(6,123) TSURF,TSR,YFS,ALFA                            CCSO3610
          WRITE(6,126) AVERCR                                        CCSO3620
          WRITE(6,126) PP,PN                                         CCSO3630
          WRITE(6,100) (TEMP(I),I=1,NMAX)                            CCSO3640
          WRITE(6,105) (CR(I),I=1,NMAX)                              CCSO3650
          WRITE(6,100) (VX(I),I=1,NMAX)                              CCSO3660
          WRITE(6,107) (STREAM(I),I=1,NMAX)                          CCSO3670
          KOUNT1=0                                                    CCSO3680
          KOUNT2=0                                                    CCSO3690
   50     CONTINUE                                                    CCSO3700
   51     CONTINUE                                                    CCSO3710
          QF= VRXR*W*H                                               CCSO3720
          ERRORQ= (Q - QF)/Q                                         CCSO3730
          WRITE(6,102) K,IP1,IM1,NMAX,NMAXM1                         CCSO3740
          WRITE(6,99) H,DY,DISTX,X,DX,TIME                           CCSO3750
          WRITE(6,124) TSURF,XSS,XSTAG2,XDET                         CCSO3760
          WRITE(6,125) YFS,ALFA,QF,ERRORQ                            CCSO3770
          WRITE(6,126) PP,PN,XPRESS,HFIN                             CCSO3780
          WRITE(6,100) (TEMP(I),I=1,NMAX)                            CCSO3790
          WRITE(6,105) (CR(I),I=1,NMAX)                              CCSO3800
          WRITE(6,100) (VX(I),I=1,NMAX)                              CCSO3810
          WRITE(6,107) (STREAM(I),I=1,NMAX)                          CCSO3820
   99     FORMAT(5X,6F10.6)                                          CCSO3830
  100     FORMAT(1X,4F15.5)                                          CCSO3840
  102     FORMAT(15X,5I10)                                           CCSO3850

  105     FORMAT(1X,4E15.5)                                          CCSO3860
  107     FORMAT(1X,4F15.8)                                          CCSO3870
  110     FORMAT(5X,4F16.6)                                          CCSO3880
  123     FORMAT(10X,4F15.5)                                         CCSO3890
  124     FORMAT(5X,5F13.5)                                          CCSO3900
  125     FORMAT(12X,4F15.5)                                         CCSO3910
  126     FORMAT(12X,4E15.5)                                         CCSO3920
  101     CONTINUE                                                    CCSO3930
          STOP                                                        CCSO3940
          END                                                         CCSO3950
```

5.5.- Program PRESSTRQ . Calculation of Rolling Forces in the

Gap of a Twin Roll RS Device .

```
C--------THIS PROGRAM COMPUTES THE PRESSURE DISTRIBUTION IN THE          PRE00010
C------TWIN-ROLL-QUENCHING MACHINE FOR SPLAT COOLING. THE PROGRAM        PRE00020
C------USES A SINGLE-STEP,FOURTH-ORDER RUNGE KUTTA METHOD AS             PRE00030
C------DESCRIBED IN  FERZIGER J. NUMERICAL METHODS FOR ENGINEERING,      PRE00040
C------WILEY,1981.P.                                                     PRE00050
C--------THE VARIABLES NEEDED FOR THE CALCULATION ARE; Q. THE            PRE00060
C------VOLUME FLOW RATE PER UNIT WIDTH, R, THE ROLL RADIUS;HO,           PRE00070
C------THE MINIMUM GAP BETWEEN THE ROLLS;OMEG. THE ANGULAR VELOCI-       PRE00080
C------TY OF THE ROLLS; X1 THE LIFT-OFF POINT;X4,THE POINT OF INITIAL    PRE00090
C------CONTACT WITH THE ROLLS;XN, THE SLIP COEFFICIENT;PL AND B          PRE00100
C------ARE THE RHEOLOGICAL PROPERTIES OF THE SPLAT.                      PRE00110
C--------PNEW IS THE REQUIRED PRESSURE AND DDX IS THE STEP SIZE USED     PRE00120
C------IN THE CALCULATIONS.DPDX IS THE PRESSURE GRADIENT AND X IS THE    PRE00130
C------SPACE AXIS IN THE ROLLING DIRECTION.                             PRE00140
C--------NOTE THAT THE CALCULATED DPDX VALUES ARE BASED ON THE           PRE00150
C------ASSUMPTIONS OF THE THEORY OF LUBRICATION.                        PRE00160
C                                                                        PRE00170
        DIMENSION H(3),SL(3),VRX(3),VRXP(3),A(3),C1(3),DPDX(3)           PRE00180
        Q=.97                                                            PRE00190
        R=5.0                                                            PRE00200
        HO=0.005                                                         PRE00210
        OMEG=160.00                                                      PRE00220
C---CALCULATION OF THE LIFT-OFF POINT                                    PRE00230
        COEO= Q*60./(3.1416*OMEG)                                        PRE00240
        COE1= HO + R                                                     PRE00250
        COE2= SQRT( COE1**2. - COEO )                                    PRE00260
        COE3= (COE1 + COE2)/2.                                           PRE00270
        X1= SQRT(ABS(R**2. - COE3**2.))                                  PRE00280
        X4=-0.9                                                          PRE00290
        H4= HO+R-SQRT(R*R-X4*X4)                                         PRE00300
        VIN=Q/(2.*H4)                                                    PRE00310
        XN=0.0                                                           PRE00320
        PL=5.0                                                           PRE00330
C------THE VALUE OF  B  DEPENDS ON THE TEMPERATURE                       PRE00340
        B=0.0000000126                                                   PRE00350
        FAC1=(PL+2.)*(2.*3.1416*OMEG/60.)                                PRE00360
        FAC2=B**PL                                                       PRE00370
        BETA=(FAC1/FAC2)**(1./PL)                                        PRE00380
        DDX= 0.0025                                                      PRE00390
        WRITE(6,567) B,PL,DDX,Q,OMEG,HO                                  PRE00400
567     FORMAT(5X,6E11.4//)                                             PRE00410
        EMU=1./B                                                         PRE00420
        POLD=1010000.0                                                   PRE00430
        PINI=POLD                                                        PRE00440
        PNEW=POLD                                                        PRE00450
        PP= 0.0                                                          PRE00460
        FORCE = 0.0                                                      PRE00470
        IND= 0                                                           PRE00480
         X=X1                                                            PRE00490
        WRITE(6,100) X1,PP,PNEW,IND                                      PRE00500
C------MAIN LOOP, DIRECTS THE STEP-BY-STEP ADVANCEMENT OF THE SOLUTION.  PRE00510
            DO 2 J=1,800                                                 PRE00520
            VIN=Q/(2.*H4)                                                PRE00530
            POLD=PNEW                                                    PRE00540
C------SECONDARY LOOP,COMPUTES THE REQUIRED DPDX VALUES AT THE INTER-    PRE00550
```

```
C------MEDIATE GRID POINTS CONTAINED WITHIN ONE MAIN X-STEP. THE       PRE00560
C------CALCULATED VALUES ARE STORED IN ARRAYS.                         PRE00570
                    DO 1 I =1,3                                         PRE00580
                    H(I)=HO+R-SQRT(R*R-X*X)                             PRE00590
                    SL(I)=ABS((X4-X)/(X4+X1))                           PRE00600
                    VRX(I)=2.*3.1416*OMEG*SQRT(R*R-X*X)/60.             PRE00610
                    VRXP(I)=(VRX(I)-VIN)*SL(I)**XN + VIN               PRE00620
          A(I)=(PL+2.)*(VRXP(I)*H(I)-Q/2.)/((PL+1.)*H(I)**(PL+2.))      PRE00630
          C1(I)=((PL+1.)**(1./PL))*EMU                                  PRE00640
          DPDX(I)=C1(I)*((ABS(A(I)))**((1./PL)-1.))*(A(I))             PRE00650
C                     WRITE(6,99) X                                     PRE00660
C                     WRITE(6,101) H(I),SL(I),VRX(I),VRXP(I),A(I),DPDX(I)   PRE00670
                    X=X-DDX/2.                                          PRE00680
   1                          CONTINUE                                  PRE00690
C------END OF INNER LOOP.                                               PRE00700
                    X=X+DDX/2.                                          PRE00710
C--------RUNGE-KUTTA FORMULA FOR THE CALCULATION OF THE PRESSURE.       PRE00720
C                                                                       PRE00730
                    PNEW=POLD - DDX*(DPDX(1)+4.*DPDX(2)+DPDX(3))/6.    PRE00740
C                                                                       PRE00750
                        PDN=(PNEW-PINI)/BETA                           PRE00760
          IF(X.LT.-X1+DDX.AND.X.GT.-X1-DDX) PMAX= PNEW                  PRE00770
                    SHEAR= H(2)*DPDX(2)                                 PRE00780
                    FRICOE= SHEAR/PNEW                                  PRE00790
                    FORCE= FORCE + PNEW*DDX                             PRE00800
                    IF(PNEW.LE.1010000.0.AND.J.GE.25) GO TO 102        PRE00810
                    WRITE(6,100) X,DPDX(2),PNEW,PDN,FRICOE,J            PRE00820
   99               FORMAT(/20X,E15.5/)                                 PRE00830
  100               FORMAT(1X,5E12.5,3X,I3)                             PRE00840
  101               FORMAT(1X,6E11.4)                                   PRE00850
   2            CONTINUE                                                PRE00860
C------END OF MAIN LOOP.                                                PRE00870
  102                     CONTINUE                                      PRE00880
                    TORQUE = FORCE*ABS(X1)                              PRE00890
                       FD= FORCE/(BETA*R)                               PRE00900
                    WRITE(6,99) PMAX,FORCE,TORQUE,FD                    PRE00910
                         STOP                                           PRE00920
                         END                                           PRE00930
```

5.6.- Program LUDECT. The Solution of Systems of Linear Algebraic Equations with Tridiagonal Matrices.

```
C---------THIS PROGRAM SOLVES THE SYSTEM OF LINEAR ALGEBRAIC EQUATIONS    LUD00010
C------- M X = BB  BY L-U DECOMPOSITION . HERE A(N) IS THE VECTOR         LUD00020
C------- FORMED BY THE DIAGONAL ELEMENTS OF  M , B(N) AND C(N) ARE,       LUD00030
C------- RESPECTIVELY THE VECTORS FORMED BY THE ELEMENTS ALONG THE        LUD00040
C------- LOWER AND UPPER DIAGONALS OF  M . EL(N) IS THE VECTOR FORMED      LUD00050
C------- BY THE ELEMENTS ON THE LOWER TRIANGULAR MATRIX AFTER L-U         LUD00060
C------- DECOMPOSITION . UP(N) IS THE VECTOR OF THE UPPER TRIANGULAR      LUD00070
C------- ELEMENTS .  X(N) IS THE SOLUTION VECTOR  AND  N  IS THE SIZE     LUD00080
C------- OF THE ORIGINAL SYSTEM .                                         LUD00090
C---------THE PROGRAM IS DESIGNED SPECIFICALLY TO DEAL WITH TRIDIAGONAL   LUD00100
C------- MATRICES AND THE SPECIFIC EXAMPLE HERE IS FOR THE CASE WHEN      LUD00110
C------- M  HAS  2'S ALONG THE MAIN DIAGONAL AND  - 1'S ALONG THE         LUD00120
C------- NEIGHBORING DIAGONALS .                                          LUD00130
C---------THE VECTOR ON THE RHS  BB(N) IN THIS CASE HAS ALL COMPONENTS    LUD00140
C------- EQUAL TO ZERO EXCEPT THE FIRST .                                 LUD00150
        REAL A(10),B(10),C(10),BB(10),EL(10),UP(10),D(10)                 LUD00160
        REAL Y(10),X(10)                                                  LUD00170
        N=10                                                              LUD00180
        DO 5 I=1,N                                                        LUD00190
        A(I)=2.                                                           LUD00200
        B(I)=-1.                                                          LUD00210
        C(I)=-1.                                                          LUD00220
        BB(I)=0.                                                          LUD00230
5       CONTINUE                                                          LUD00240
        BB(1)=1.                                                          LUD00250
                D(1)=A(1)                                                 LUD00260
                UP(1)=C(1)                                                LUD00270
                DO 10 I=2,N                                               LUD00280
                IM1=I-1                                                   LUD00290
                EL(I)= B(I)/D(IM1)                                        LUD00300
                D(I)= A(I) - EL(I)*UP(IM1)                                LUD00310
                UP(I)=C(I)                                                LUD00320
10              CONTINUE                                                  LUD00330
C                                                                         LUD00340
C                                                                         LUD00350
                Y(1)=BB(1)                                                LUD00360
                DO 20 I=2,N                                               LUD00370
                IM1=I-1                                                   LUD00380
                Y(I)= BB(I) - EL(I)*Y(IM1)                                LUD00390
20              CONTINUE                                                  LUD00400
                X(N)=Y(N)/D(N)                                            LUD00410
                DO 30 IK=2,N                                              LUD00420
                I=N+1-IK                                                  LUD00430
                IP1=I+1                                                   LUD00440
                X(I)= (1/D(I))*(Y(I) - UP(I)*X(IP1))                      LUD00450
30              CONTINUE                                                  LUD00460
        WRITE(6,50) (X(I),I=1,N)                                          LUD00470
50      FORMAT(5X,F15.8)                                                  LUD00480
                        STOP                                              LUD00490
                        END                                               LUD00500
```

5.7.- Program PS . The Calculation of Heat Flow Including Convection. Patankar-Spalding Method .

```
      COMMON/IND/R,HO,OMEG,Q,EMU,PL,TCL,TCS,RHO,CP              PS100010
      COMMON/ROLL/TROLL,HTC,TCR,ALFR                            PS100020
      COMMON/ZONE/X,X1,X2,X3,X4,DX,DT,XN,IVV                    PS100030
      COMMON/NODES/NX,NY,III                                    PS100040
      COMMON/COEF/ B1,B2,B3,B4,B5                               PS100050
      COMMON/VELO/VELX(12,6),VELY(12,6)                         PS100060
      COMMON/TEMP/TA(12,6),T(12,6),CR(12,6),RE(12,6)            PS100070
      DIMENSION TOLD(12,6)                                      PS100080
C                                                               PS100090
C--------THIS PROGRAM DIRECTS THE CALCULATION OF FLOW AND TEMPERATURE  PS100100
C------IN LUBRICATION TYPE FLUID FLOW CONFIGURATIONS.          PS100110
C--------TOLD IS THE INITIAL (GUESSED) TEMPERATURE FIELD.      PS100120
C                                                               PS100130
C---------BOTH , NEWTONIAN AND NON-NEWTONIAN POWER LAW FLUIDS CAN  PS100140
C-------BE CONSIDERED .                                         PS100150
      DATA TOLD/72*760.0/                                       PS100160
C     DATA TOLD/72*660.0/                                       PS100170
C                                                               PS100180
C----------FOLLOWING ARE THE GEOMETRICAL AND MATERIALS DATA REQUIRED  PS100190
C-----R=ROLL RADIUS(CM),HO=MINIMUM GAP(CM),OMEG=RPM OF ROLL    PS100200
C-----Q=VOLUMETRIC FLOW RATE PER UNIT WIDTH(CM2/S)             PS100210
C-----PLL=POWER LAW EXPONENT FOR LIQUID,PLS=POWER LAW EXPONENT FOR SOLIDPS100220
C-----EMUL=VISCOSITY OF THE LIQUID(G/CM S)                     PS100230
C-----B=FLUIDITY OF THE SOLID (UNITS DEPEND ON PLS)            PS100240
C-----TCL=THERMAL CONDUCTIVITY OF THE LIQUID(CAL/CM S K)       PS100250
C-----TCS=THERMAL CONDUCTIVITY OF THE SOLID(CAL/CM S K)        PS100260
C-----RHO=DENSITY(G/CM3),CP=SPECIFIC HEAT(CAL/G K)             PS100270
C-----TROLL=TEMPERATURE OF THE ROLL (K)                        PS100280
C-----HTC=HEAT TRANSFER COEFFICIENT TO THE ROLL (CAL/CM2 S K)  PS100290
C-----TCR=THERMAL CONDUCTIVITY OF THE ROLL (CAL/CM S K)        PS100300
C-----ALFR=THERMAL DIFFUSIVITY OF THE ROLL (CM2/S)             PS100310
C-----X1=LOCATION OF  NEUTRAL AND LIFT-OFF POINTS (CM)         PS100320
C-----X2=LOCATION OF THE END OF SOLIDIFICATION (CM)            PS100330
C-----X3=LOCATION OF THE BEGINING OF SOLIDIFICATION (CM)       PS100340
C-----X4=LOCATION OF THE ENTRANCE TO THE ROLL GAP (CM)         PS100350
C-----NX=NUMBER OF GRIDS ALONG X, NY=NUMBER OF GRIDS ALONG Y   PS100360
C-----DX=GRID SPACING ALONG X (CM),DY=GRID SPACING ALONG Y (CM) PS100370
C-----XN=EXPONENT TO DESCRIBE THE SLIP IN VELOCITY AT THE SPLAT/ROLL  PS100380
C-----DT=FICTICIOUS TIME STEP REQUIRED IN THE HEAT FLOW EQUATION (S)  PS100390
C                                                               PS100400
      R= 5.0                                                    PS100410
      HO= 0.005                                                 PS100420
      OMEG= 160.0                                               PS100430
      Q= 1.0                                                    PS100440
      PLS= 4.5                                                  PS100450
      B= 0.0000000126                                           PS100460
      PLL= 1.0                                                  PS100470
      EMUL= 0.01                                                PS100480
      TCL= 0.15                                                 PS100490
      TCS= 0.50                                                 PS100500
      RHO= 2.7                                                  PS100510
      CP= 0.25                                                  PS100520
      TROLL= 25.0                                               PS100530
      HTC= 1.0                                                  PS100540
      TCR= 0.1                                                  PS100550
```

```
      ALFR= 0.10                                             PS100560
C                                                            PS100570
C-----ASSUMED VALUES OF X1,X2,X3 AND X4                      PS100580
C                                                            PS100590
      COE0= Q*60./(3.1416*OMEG)                              PS100600
      COE1= H0+R                                             PS100610
      COE2= SQRT( COE1**2. - COE0 )                          PS100620
      COE3= (COE1 + COE2)/2.                                 PS100630
      X1= SQRT( ABS( R*R -COE3*COE3 ) )                      PS100640
C     X2= -0.57                                              PS100650
      X2= X1                                                 PS100660
      X3= X1                                                 PS100670
      X4= -0.90                                              PS100680
C                                                            PS100690
C-----GRID PARAMETERS                                        PS100700
C                                                            PS100710
      NX= 12                                                 PS100720
      NY=  6                                                 PS100730
C     DXL= 0.011                                             PS100740
       DXL= -(X4-X1)/FLOAT(NX-1)                             PS100750
C     DXL= -(X4-X3)/FLOAT(NX)                                PS100760
C     DXS= 0.0633333                                         PS100770
      DXS= -(X2-X1)/FLOAT(NX)                                PS100780
CC-----STEP SIZE FOR THE CALCULATION OF THE MAXIMUM LOAD ON THE ROLLS  PS100790
CC    DXS= -(X4+X1)/(FLOAT(NX))                              PS100800
      DT= 1.0                                                PS100810
C                                                            PS100820
C-----EXPONENTS OF THE SLIP COEFFICIENT.                     PS100830
C                                                            PS100840
      XNL= 0.5                                               PS100850
      XNS= 0.0                                               PS100860
C                                                            PS100870
C---------------HERE ANY OF X=X4 OR X=X2 MUST BE CHOSEN ACCORDING  PS100880
C---------------TO THE DESIRED CALCULATION.IF CALCULATIONS ARE DESI-  PS100890
C---------------RED IN THE LIQUID REGION CHOSE THEN X=X4.SELECT X=X2  PS100900
C---------------FOR COMPUTATIONS IN THE (FULLY) SOLID REGION.  PS100910
C                                                            PS100920
      X= X4                                                  PS100930
C     X= X2                                                  PS100940
C                                                            PS100950
C--------THE NEXT LOOP CREATES THE INITIAL TEMPERATURE FIELD TO BE  PS100960
C--------SENT TO THE ROUTINE THAT SOLVES THE HEAT FLOW PROBLEM.  PS100970
C                                                            PS100980
                  DO 1 I = 1,NX                              PS100990
                    DO 2 J = 1,NY                            PS101000
                    TA(I,J)= TOLD(I,J)                       PS101010
    2               CONTINUE                                 PS101020
    1             CONTINUE                                   PS101030
C                                                            PS101040
C------THE FOLLOWING CONDITION COLLECTS ADDITIONAL VALUES WHICH ARE  PS101050
C------FIXED AS SOON AS X HAS BEEN SELECTED.                 PS101060
C                                                            PS101070
      IF(X.GE.X2) GO TO 10                                   PS101080
    9 CONTINUE                                               PS101090
      DX= DXL                                                PS101100
```

140

```
          XN= XNL                                                  PS101110
          EMU= EMUL                                                PS101120
          PL= PLL                                                  PS101130
          TC= TCL                                                  PS101140
          GO TO 20                                                 PS101150.
   10     CONTINUE                                                 PS101160
          DX= DXS                                                  PS101170.
          XN= XNS                                                  PS101180
          EMU= (1./B)                                              PS101190
          PL= PLS                                                  PS101200
          TC= TCS                                                  PS101210
   20     CONTINUE                                                 PS101220
C                                                                  PS101230
          WRITE(6,99) R,HO,OMEG,Q,EMUL,PLL,B,PLS,TCL,TCS,RHO,CP    PS101240
          WRITE(6,99) TROLL,HTC,TCR,ALFR                           PS101250
          WRITE(6,99) X,X1,X2,X3,X4,DX,DT,XN                       PS101260
          WRITE(6,98) NX,NY                                        PS101270
C                                                                  PS101280
C-----THE ROUTINES FOR THE CALCULATION OF VELOCITY AND TEMPERATURE PS101290
C-----FIELDS ARE CALLED NOW. DEPENDING ON THE REGION OF CALCULATION PS101300
C-----SELECT EITHER X=X4+DX OR X=X2+DX .                           PS101310
C                                                                  PS101320
      X= X4                                                        PS101330
C                                                                  PS101340
      CALL VELOZ                                                   PS101350
C                                                                  PS101360
C     GO TO 100                                                    PS101370
   91     CONTINUE                                                 PS101380
C                                                                  PS101390
      X= X4+DX                                                     PS101400
C                                                                  PS101410
      DO 92 I=1,NX                                                 PS101420
         DO 92 J=1,NY                                              PS101430
          T(I,J)=TA(I,J)                                           PS101440
   92     CONTINUE                                                 PS101450
                         DO 93 III=1,800                           PS101460
      CALL TDMA                                                    PS101470
                         RESMAX=0.0                                PS101480
                       DO 94 IV=1,NX                               PS101490
                          DO 95 JV=1,NY                            PS101500
                       IF(RESMAX.LT.RE(IV,JV)) RESMAX=RE(IV,JV)    PS101510
                       RE(IV,JV)=0.0                               PS101520
   95                    CONTINUE                                  PS101530
   94                    CONTINUE                                  PS101540
                       IF(RESMAX.LT.0.0001) GO TO 97              PS101550
   93                      CONTINUE                                PS101560
   97                  CONTINUE                                    PS101570
          WRITE(6,99) ((T(I,J),J=1,NY),I=1,NX)                     PS101580
          WRITE(6,66) RESMAX,III                                  PS101590
   66     FORMAT(//,25X,E12.5,3X,I3)                              PS101600
C                                                                  PS101610
C         WRITE(6,99) R,HO,OMEG,Q,EMUL,PLL,B,PLS,TCL,TCS,RHO,CP    PS101620
   98     FORMAT(/20X,2I10///)                                     PS101630
   99     FORMAT(1X,6E12.5)                                        PS101640
  100     CONTINUE                                                 PS101650
      STOP                                                         PS101660
      END                                                          PS101670
```

141

```
      SUBROUTINE VELOZ                                            PS200010
C----------THIS ROUTINE COMPUTES THE VELOCITY FIELD .             PS200020
C                                                                 PS200030
      COMMON/IND/R,HO,OMEG,Q,EMU,PL,TCL,TCS,RHO,CP                PS200040
      COMMON/ZONE/X,X1,X2,X3,X4,DX,DT,XN,IVV                      PS200050
      COMMON/NODES/NX,NY                                          PS200060
      COMMON/VELO/VELX(12,6),VELY(12,6),Z(12,6),ST(12,6)         PS200070
      COMMON/COEF/B1,B2,B3,B4,B5                                  PS200080
      DIMENSION VELOX(24,12),VELOY(24,12),ZINT(24,12),STRE(24,12) PS200090
      DIMENSION P(26)                                             PS200100
C                                                                 PS200110
C----------CALCULATION OF THE VELOCITY FIELD                      PS200120
C-----THE VALUES OF THE FUNCTIONS THAT ONLY DEPEND ON X ARE COMPUTED PS200130
C-----FIRST, WITH THE MAIN DO LOOP.THE VELOCITIES ARE CALCULATED SUB- PS200140
C-----SEQUENTLY FOR FIXED X AND VARYING Y.                        PS200150
C-----MAIN DO LOOP.                                               PS200160
C                                                                 PS200170
      PBRY= 1010000.0                                             PS200180
      DX= DX/2.                                                   PS200190
      NNX= NX*2 - 1                                               PS200200
      DO 1 I=1,NNX                                                PS200210
      HI= H(R,HO,X)                                               PS200220
      B1= VRXP(OMEG,R,X,Q,HO,X2,X4,XN,X1)                         PS200230
      B2= A(R,X,OMEG,HO,PL,Q,X2,X4,XN,X1)                         PS200240
      B3= COEFI(R,X,OMEG,HO,PL,Q,X2,X4,XN,X1)                     PS200250
      B4= - DADX(R,X,Q,OMEG,HO,PL,X2,X4,XN,X1)/(PL+2.)            PS200260
      B5= VRYP(OMEG,R,X,Q,HO,X2,X4,XN,X1)                         PS200270
      SS= 2.*EMU*B2*HI                                            PS200280
      DPDX= (((PL+1.)**(1./PL))*EMU)*((ABS(B2))**((1./PL)-1.))*B2 PS200290
      P(I) = PBRY + DPDX*DX                                       PS200300
C     WRITE(6,3) B1,B2,B3,B4,B5,SS,DPDX                           PS200310
  3   FORMAT(1X,7E11.4)                                           PS200320
C     WRITE(6,33) X,DPDX,P(I),HI                                  PS200330
 33   FORMAT(5X,4E15.7)                                           PS200340
 34   FORMAT(2X,5E12.5)                                           PS200350
C                                                                 PS200360
C-----SECONDARY DO LOOP.THE VELOCITIES ARE COMPUTED FOR THE NY NODES PS200370
C-----LYING ALONG THE I-TH X-STEP.                                PS200380
C                                                                 PS200390
      Y=0.0                                                       PS200400
      NNY= NY*2 -1                                                PS200410
      DO 10 J=1,NNY                                               PS200420
      HI=H(R,HO,X)                                                PS200430
      DY=HI/(2.*(FLOAT(NY-1)))                                    PS200440
C---------------CALCULATION OF VELOCITY COMPONENTS                PS200450
      VX= B1 + B2*(Y**(PL+1.0) - HI**(PL+1.0))                    PS200460
      VY= B3*Y + B4*Y**(PL+2.)                                    PS200470
C---------------CALCULATION OF INTENSITY OF THE RATE OF DEFORMATION PS200480
      ZZ=(ABS(B2*(PL+1.)*Y**PL))**2.                              PS200490
C---------------CALCULATION OF THE STREAM FUNCTION                PS200500
      PSI= ((B1 - B2*HI**(PL+1.0))*(HI-Y)  +                      PS200510
     1      (B2*(HI**(PL+2.) - Y**(PL+2.)))/(PL+2.))*2.0/Q        PS200520
            IF(PSI.LE.0.0001) PSI=0.0                             PS200530
C           WRITE(6,34) B1,VX,VY,ZZ,PSI                           PS200540
C-----THE CALCULATED VALUES ARE STORED IN ARRAYS                  PS200550
```

```
                          VELOX(I,J)=VX                              PS200560
                          VELOY(I,J)=VY                              PS200570
                          ZINT(I,J)=ZZ                              PS200580
                          STRE(I,J)=PSI                             PS200590
C                                                                   PS200600
                     Y = Y +DY                                      PS200610
   10                 CONTINUE                                      PS200620
C----- END OF INNER LOOP                                            PS200630
          X=X+DX                                                    PS200640
    1     CONTINUE                                                  PS200650
C                                                                   PS200660
C-----OUTER LOOP CONCLUDED                                          PS200670
C                                                                   PS200680
          DO 150 I=2,NNX,2                                          PS200690
             DO 150 J=1,NNY,2                                       PS200700
             K=I/2                                                  PS200710
             L=(J+1)/2                                              PS200720
             VELX(K,L)=VELOX(I,J)                                   PS200730
  150     CONTINUE                                                  PS200740
C                                                                   PS200750
          DO 160 I=3,NNX,2                                          PS200760
             DO 160 J=2,NNY,2                                       PS200770
             K=(I+1)/2                                              PS200780
             L=J/2                                                  PS200790
             VELY(K,L)= VELOY(I,J)                                  PS200800
  160     CONTINUE                                                  PS200810
C     GO TO 180                                                     PS200820
  174 CONTINUE                                                      PS200830
C-----WRITING OF THE RESULTS                                        PS200840
C                                                                   PS200850
C.        WRITE(6,177)                                              PS200860
  177     FORMAT(/25X,10HVELOCITY-X)                                PS200870
          WRITE(6,176) ((VELX(I,J),J=1,NY),I=1,NX-1)                PS200880
  175     CONTINUE                                                  PS200890
C     GO TO 180                                                     PS200900
  1755    CONTINUE                                                  PS200910
C         WRITE(6,178)                                              PS200920
  178     FORMAT(/25X,10HVELOCITY-Y)                                PS200930
          WRITE(6,1766) ((VELY(I,J),J=1,NY-1),I=2,NX-1)             PS200940
          GO TO 180                                                 PS200950
  1788    CONTINUE                                                  PS200960
C         WRITE(6,179)                                              PS200970
  179     FORMAT(/15X,32HINTENSITY OF RATE OF DEFORMATION)          PS200980
          WRITE(6,176) ((Z(I,J),J=1,NNY),I=1,NNX)                   PS200990
C         WRITE(6,181)                                              PS201000
  181     FORMAT(/25X,15HSTREAM FUNCTION)                           PS201010
          WRITE(6,176) ((ST(I,J),J=1,NNY),I=1,NNX)                  PS201020
  180     CONTINUE                                                  PS201030
  176     FORMAT(1X,6E12.5)                                         PS201040
  1766 FORMAT(1X,5E12.5)                                            PS201050
C180     CONTINUE                                                   PS201060
          RETURN                                                    PS201070
       END                                                          PS201080
```

```
C---------THE FOLLOWING FUNCTIONS ARE REQUIRED FOR THE COMPUTATION          PS300010
C-------OF THE FLOW .                                                       PS300020
C                                                                           PS300030
      FUNCTION H(R,HO,X)                                                    PS300040
C     H=HO+R-SQRT(R*R-X*X)                                                  PS300050
      H=HO(1. + 0.05*(X/X4))                                               PS300060
      RETURN                                                                PS300070
      END                                                                   PS300080
C                                                                           PS300090
C-----X-COMPONENT OF THE TANGENTIAL VELOCITY OF THE ROLLS(CM/S)             PS300100
C                                                                           PS300110
      FUNCTION VRX(OMEG,R,X)                                                PS300120
      VRX=2.*3.1416*OMEG*SQRT(R+R-X*X)/60.                                 PS300130
      RETURN                                                                PS300140
      END                                                                   PS300150
C                                                                           PS300160
C-----Y-COMPONENT OF THE TANGENTIAL VELOCITY OF THE ROLLS(CM/S)             PS300170
C                                                                           PS300180
      FUNCTION VRY(OMEG,R,X)                                                PS300190
      VRY= 2.*3.1416*OMEG*X/60.0                                           PS300200
      RETURN                                                                PS300210
      END                                                                   PS300220
C                                                                           PS300230
C-----DERIVATIVE OF H (DIMENSIONLESS)                                       PS300240
C                                                                           PS300250
      FUNCTION DHDX(R,X)                                                    PS300260
      DHDX=X/SQRT(R*R-X*X)                                                 PS300270
      RETURN                                                                PS300280
      END                                                                   PS300290
C                                                                           PS300300
C-----DERIVATIVE OF VRX (1/S)                                               PS300310
C                                                                           PS300320
      FUNCTION DVRXDX(OMEG,R,X)                                             PS300330
      C1=2.*3.1416*OMEG/60.                                                PS300340
      DVRXDX=-C1*(X/SQRT(R*R-X*X))                                         PS300350
      RETURN                                                                PS300360
      END                                                                   PS300370
C                                                                           PS300380
C-----FLOW COEFFICIENT (UNITS DEPEND ON THE MATERIAL)                       PS300390
C                                                                           PS300400
      FUNCTION A(R,X,OMEG,HO,PL,Q,X2,X4,XN,X1)                             PS300410
      VR=VRXP(OMEG,R,X,Q,HO,X2,X4,XN,X1)                                   PS300420
      HI= H(R,HO,X)                                                        PS300430
      C1=(PL+2.)*(VR*HI-Q/2.)/(PL+1.)                                      PS300440
      C2=HI**(PL+2.)                                                       PS300450
      A= C1/C2                                                              PS300460
      RETURN                                                                PS300470
      END                                                                   PS300480
C                                                                           PS300490
C-----DERIVATIVE OF THE FLOW COEFFICIENT (VARIABLE UNITS)                   PS300500
C                                                                           PS300510
      FUNCTION DADX(R,X,Q,OMEG,HO,PL,X2,X4,XN,X1)                          PS300520
      VR=VRXP(OMEG,R,X,Q,HO,X2,X4,XN,X1)                                   PS300530
      VRP=DVRXPP(OMEG,R,X,Q,HO,X2,X4,XN,X1)                                PS300540
      HI= H(R,HO,X)                                                        PS300550
```

144

```
            C1=(PL+2.)/((PL+1.)*HI**(PL+2.))                            PS300560
            C2=HI*VRP+VR*DHDX(R,X)                                       PS300570
            C3=(PL+2.)*(VR-Q/(2.*HI))*DHDX(R,X)                          PS300580
            DADX=C1*(C2-C3)                                              PS300590
            RETURN                                                       PS300600
            END                                                          PS300610
C                                                                        PS300620
C-----FLOW COEFFICENT FOR THE Y-COMPONENT OF VELOCITY (VARIABLE UNITS)   PS300630
C                                                                        PS300640
            FUNCTION COEFI(R,X,OMEG,HO,PL,Q,X2,X4,XN,X1)                 PS300650
            AA= A(R,X,OMEG,HO,PL,Q,X2,X4,XN,X1)                          PS300660
            HI= H(R,HO,X)                                                PS300670
            C1= ((PL+1.)*AA*HI**PL)*DHDX(R,X)                            PS300680
            C2= DADX(R,X,Q,OMEG,HO,PL,X2,X4,XN,X1)*HI**(PL+1.)           PS300690
            C3= DVRXPP(OMEG,R,X,Q,HO,X2,X4,XN,X1)                        PS300700
            COEFI=C1+C2-C3                                               PS300710
            RETURN                                                       PS300720
            END                                                          PS300730
C                                                                        PS300740
C-----FUNCTION GIVING THE SURFACE X-VELOCITY OF THE SPLAT UNDER SLIPPING PS300750
C-----CONDITIONS IN TERMS OF THE SLIP COEFFICIENT AND EXPONENT(CM/S)     PS300760
C                                                                        PS300770
            FUNCTION VRXP(OMEG,R,X,Q,HO,X2,X4,XN,X1)                     PS300780
            SL=S(X,X2,X4,X1)                                             PS300790
            VR=VRX(OMEG,R,X)                                             PS300800
            H4=H(R,HO,X4)                                                PS300810
            VIN=Q/(2.*H4)                                                PS300820
            VRXP=(VR-VIN)*SL**XN + VIN                                   PS300830
            RETURN                                                       PS300840
             END                                                        PS300850
C                                                                        PS300860
C-----FUNCTION GIVING THE SLIPPED Y-VELOCITY IN THE SURFACE OF THE SPLAT PS300870
C-----(CM/S)                                                             PS300880
C                                                                        PS300890
            FUNCTION VRYP(OMEG,R,X,Q,HO,X2,X4,XN,X1)                     PS300900
            SL=S(X,X2,X4,X1)                                             PS300910
            VR=VRY(OMEG,R,X)                                             PS300920
            H4=H(R,HO,X4)                                                PS300930
            VRYP=VR*SL**XN                                               PS300940
            RETURN                                                       PS300950
            END                                                          PS300960
C                                                                        PS300970
C-----SLIP COEFFICENT (DIMENSIONLESS)                                    PS300980
C                                                                        PS300990
            FUNCTION S(X,X2,X4,X1)                                       PS301000
C           S=ABS((X4-X-.001)/(X4-X2-.001))                             PS301010
            S=ABS((X4-X-.001)/(X4+X1-0.001))                            PS301020
            RETURN                                                       PS301030
            END                                                          PS301040
C                                                                        PS301050
C-----DERIVATIVE OF THE SLIP COEFFICENT (1/CM)                           PS301060
C                                                                        PS301070
            FUNCTION DSDX(X2,X4,X1)                                      PS301080
            DSDX=-1./(X4-X2)                                            PS301090
C           DSDX=-1./(X4+X1)                                            PS301100
            RETURN                                                       PS301110
            END                                                          PS301120
C                                                                        PS301130
C-----FUNCTION GIVING THE X-DERIVATIVE OF THE SLIPPED VELOCITY (1/S)     PS301140
C                                                                        PS301150
            FUNCTION DVRXPP(OMEG,R,X,Q,HO,X2,X4,XN,X1)                   PS301160
            SL=S(X,X2,X4,X1)                                             PS301170
            VIN=Q/(2.*H(R,HO,X4))                                        PS301180
            VR=VRX(OMEG,R,X)                                             PS301190
            DVRXPP=((VR-VIN)*XN)*(SL**(XN-1.))*DSDX(X2,X4,X1)            PS301200
          1 +(SL**XN)*(DVRXDX(OMEG,R,X))                                PS301210
            RETURN                                                       PS301220
            END                                                          PS301230
```

145

```
      SUBROUTINE TDMA                                                    PS400010
C-------THIS ROUTINE USES A TWO-DIMENSIONAL VELOCITY FIELD TO            PS400020
C------COMPUTE THE CORRESPONDING TEMPERATURE FIELD.                      PS400030
C-------THE ROUTINE ASSUMES NO HEAT FLOW BOTH, ACROSS THE SYMMETRY       PS400040
C------PLANE (Y=0.0) AND THE LOWER HORIZONTAL PLANE (X=X3 OR X1) AS       PS400050
C------WELL AS PRESCRIBED TEMPERATURE AT THE UPPER HORIZONTAL BOUN-      PS400060
C------DARY (X=X4 OR X=X2),AND PRESCRIBED HEAT FLUX TO THE ROLLS.        PS400070
C-------THE CALCULATION PROCEEDS BY SOLVING THE SYSTEM OF NX             PS400080
C------EQUATIONS WITH NY UNKNOWNS EACH, OBTAINED FROM FINITE-DIFFEREN-   PS400090
C------CING OF THE HEAT FLOW EQUATION.THE METHOD IS ITERATIVE INASMUCH   PS400100
C------AN ASSUMED TEMPERATURE FIELD IS USED TO COMPUTE AN IMPROVED       PS400110
C------GUESS WHICH IN TURN IS USED TO COMPUTE AN EVEN BETTER GUESS.      PS400120
C------THE PROCEDURE IS REPEATED UNTIL SATISFACTORY CONVERGENCE IS       PS400130
C------REACHED.                                                          PS400140
C                                                                        PS400150
      COMMON/IND/R,HO,OMEG,Q,EMU,PL,TCL,TCS,RHO,CP                       PS400160
      COMMON/ROLL/TROLL,HTC,TCR,ALFR                                     PS400170
      COMMON/ZONE/X,X1,X2,X3,X4,DX,DT,XN,IVV                             PS400180
      COMMON/NODES/NX,NY,III                                             PS400190
      COMMON/VELO/VELX(12,6),VELY(12,6)                                  PS400200
      COMMON/TEMP/TA(12,6),T(12,6),CR(12,6),RE(12,6)                     PS400210
      COMMON/INTCOE/COO,C10,C20,CO12                                     PS400220
C                                                                        PS400230
C------THE FOLLOWING ARRAYS ARE NECESSARY FOR THE SOLUTION              PS400240
C------THE SYMBOLS ARE THE SAME AS IN S.PATANKAR, NUMERICAL             PS400250
C------HEAT TRANSFER AND FLUID FLOW, HEMISPHERE,WASHINGTON,1980,CH.5.   PS400260
C                                                                        PS400270
      DIMENSION A(12,6),B(12,6),C(12,6),D(12,6),P(12,6),Q(12,6)         PS400280
      DIMENSION DN(6),DS(6),DE(6),DW(6)                                  PS400290
      DIMENSION PEN(6),PES(6),PEE(6),PEW(6)                             PS400300
      DIMENSION AN1(6),AS1(6),AE1(6),AW1(6)                             PS400310
      DIMENSION AN2(6),AS2(6),AE2(6),AW2(6)                             PS400320
      DIMENSION COEN(6),COES(6),COEE(6),COEW(6)                         PS400330
      DIMENSION TG(12,6)                                                 PS400340
      NXN=NX-1                                                           PS400350
      NYN=NY-1                                                           PS400360
      TCL= 0.15                                                          PS400370
      TCS= 0.52                                                          PS400380
      CPL= 0.25                                                          PS400390
      CPS= 0.25                                                          PS400400
C                                                                        PS400410
C------THE FOLLOWING LOOP ONLY INITIALIZES THE TEMPERATURE FIELD        PS400420
C                                                                        PS400430
C      DO 1 I=1,NX                                                       PS400440
C          DO 2 J=1,NY                                                   PS400450
C          T(I,J)=TA(I,J)                                               PS400460
C2          CONTINUE                                                     PS400470
C1      CONTINUE                                                         PS400480
C                                                                        PS400490
C------THE FOLLOWING LOOP CONTROLS THE ITERATIONS                       PS400500
C                                                                        PS400510
C                              DO 3 III=1,800                            PS400520
                               COO=25.                                  PS400530
                               C10=0.                                   PS400540
                               C20=0.0                                  PS400550
```

```
C                                                                        PS400560
C------THE FOLLOWING LOOP ADVANCES THE SOLUTION IN THE X DIRECTION.      PS400570
C------THE COMPUTATION BEGINS AT I=2 BECAUSE AT I=1 THE TEMPERATURES     PS400580
C---L--ARE GIVEN AS BOUNDARY CONDITION BY THE POURING TEMPERATURE OR     PS400590
C------THE SOLIDUS TEMPERATURE,DEPENDING ON THE REGION OF COMPUTATION.   PS400600
C                                                                        PS400610
             DO 10 I=2,NXN                                               PS400620
CC           DTI=100.*(60./(2.*3.1416*OMEG))*(DX/SQRT(R*R-(X-DX)*(X-DX)))PS400630
C                                                                        PS400640
C----------THE NEXT LOOP  SETS THE INLET TEMPERATURE.                    PS400650
C                                                                        PS400660
             DO 15 J=1,NY                                                PS400670
             T(1,J)=TA(1,J)                                              PS400680
C            T(1,J)=TA(1,J) - 4.0*FLOAT(J) + 4.                          PS400690
15           CONTINUE                                                    PS400700
C                                                                        PS400710
C------WE BEGIN NOW THE CALCULATION OF THE COEFFICIENTS FOR THE HEAT     PS400720
C------FLOW EQUATION (DISCRETIZED).                                      PS400730
C----------THE NODES ALONG THE SYMMETRY LINE (Y=0.0) HAVE COEFFICIENTS   PS400740
C----------GIVEN BY THE SYMMETRICAL BOUNDARY CONDITION.                  PS400750
C                                                                        PS400760
             A(I,1)=1.                                                   PS400770
             B(I,1)=1.                                                   PS400780
             C(I,1)=0.                                                   PS400790
             D(I,1)=0.                                                   PS400800
C                                                                        PS400810
C----------CALCULATION OF THE COEFFICIENTS FOR GAUSS ELIMINATION         PS400820
C----------FOR THE NX NODES LYING ALONG THE SYMMETRY LINE(I,1)           PS400830
C                                                                        PS400840
             P(I,1)=B(I,1)/A(I,1)                                        PS400850
             Q(I,1)=D(I,1)/A(I,1)                                        PS400860
C                                                                        PS400870
C------WE CONTINUE NOW WITH THE SECONDARY LOOP WHICH ADVANCES THE CAL-   PS400880
C------CULATION OF THE COEFFICIENTS ALONG THE Y-DIRECTION.               PS400890
C                                                                        PS400900
                DO 20 J=2,NYN                                            PS400910
C                                                                        PS400920
C---------THE NEXT CONDITION IS REQUIRED TO MAINTAIN THE VALUES OF TC     PS400930
C---------AND CP THROUGHOUT THE CALCULATION.IT ENDS IN LABEL 5.          PS400940
C                                                                        PS400950
                IF (X.GE.X2) GO TO 4                                     PS400960
                TC= TCL                                                  PS400970
                CP= CPL                                                  PS400980
                GO TO 5                                                  PS400990
4               CONTINUE                                                 PS401000
                TC= TCS                                                  PS401010
                CP= CPS                                                  PS401020
5               CONTINUE                                                 PS401030
                HI=H(R,HO,X)                                             PS401040
                DDY=HI/(FLOAT(NYN))                                      PS401050
                IF(J.GE.NY) GO TO 21                                     PS401060
                JJ=J+1                                                   PS401070
                JJJ=J-1                                                  PS401080
C                                                                        PS401090
C------CALCULATION OF THE COEFFICIENTS FOR THE INTERNAL GRID POINTS.     PS401100
```

147

```
C---------COEFFICIENTS ON THE NORTH SIDE (Y+).                              PS401110
C                                                                          PS401120
              DN(J)=TC*DX/(CP*DDY)                                          PS401130
              PEN(J)=ABS(VELY(I,JJ)*DDY*RHO*CP/TC)                          PS401140
          AN1(J)=AMAX1(O.,((ABS(1.-O.1*PEN(J)))**4.)*(1.-O.1*PEN(J)))       PS401150
              AN2(J)=AMAX1(-RHO*DX*VELY(I,JJ),O.)                           PS401160
C                                                                          PS401170
C---------COEFFICIENTS ON THE SOUTH SIDE (Y-).                              PS401180
C                                                                          PS401190
              DS(J)=TC*DX/(CP*DDY)                                          PS401200
              PES(J)=ABS(VELY(I,JJJ)*DDY*RHO*CP/TC)                         PS401210
          AS1(J)=AMAX1(O.,((ABS(1.-O.1*PES(J)))**4.)*(1.-O.1*PES(J)))       PS401220
              AS2(J)=AMAX1(RHO*DX*VELY(I,JJJ),O.)                           PS401230
C                                                                          PS401240
C---------COEFFICIENTS ON THE EAST SIDE (X+).                               PS401250
C                                                                          PS401260
              DE(J)=TC*DDY/(CP*DX)                                          PS401270
              PEE(J)=ABS(VELX(I+1,J)*DX*RHO*CP/TC)                          PS401280
          AE1(J)=AMAX1(O.,((ABS(1.-O.1*PEE(J)))**4.)*(1.-O.1*PEE(J)))       PS401290
              AE2(J)=AMAX1(-RHO*DDY*VELX(I+1,J),O.)                         PS401300
C                                                                          PS401310
C---------COEFFICIENTS ON THE WEST SIDE (X-).                               PS401320
C                                                                          PS401330
              DW(J)=TC*DDY/(CP*DX)                                          PS401340
              PEW(J)=ABS(VELX(I-1,J)*DX*RHO*CP/TC)                          PS401350
          AW1(J)=AMAX1(O.,((ABS(1.-O.1*PEW(J)))**4.)*(1.-O.1*PEW(J)))       PS401360
              AW2(J)=AMAX1(RHO*DDY*VELX(I-1,J),O.)                          PS401370
C                                                                          PS401380
C--------CALCULATION OF GLOBAL COEFFICIENTS FOR N,S,E,AND W.                PS401390
C                                                                          PS401400
                      COEN(J)=DN(J)+AN1(J) + AN2(J)                         PS401410
                      COES(J)=DS(J)*AS1(J) + AS2(J)                         PS401420
                      COEE(J)=DE(J)*AE1(J) + AE2(J)                         PS401430
                      COEW(J)=DW(J)*AW1(J) + AW2(J)                         PS401440
                      AO=RHO*DX*DDY/DT                                      PS401450
C                                                                          PS401460
C-------CALCULATION OF THE MAIN COEFFICIENTS.                               PS401470
C                                                                          PS401480
              A(I,J)=COEN(J)+COES(J)+COEE(J)+COEW(J)+AO                     PS401490
              B(I,J)=COEN(J)                                                PS401500
              C(I,J)=COES(J)                                                PS401510
              D(I,J)=COEE(J)*TA(I+1,J)+COEW(J)*T(I-1,J)+AO*TA(I,J)          PS401520
C                                                                          PS401530
C-------CALCULATION OF THE COEFFICIENTS FOR THE GAUSS ELIMINATION           PS401540
C-------FOR THE INTERNAL NODES (I=2,NX-1;J=2,NY-1).                         PS401550
C                                                                          PS401560
              P(I,J)=B(I,J)/(A(I,J)-C(I,J)*P(I,JJJ))                        PS401570
              Q(I,J)=(D(I,J)+C(I,J)*Q(I,JJJ))/(A(I,J)-C(I,J)*P(I,JJJ))      PS401580
C                                                                          PS401590
  20                      CONTINUE                                          PS401600
C                                                                          PS401610
C-----------END OF INNER LOOP.                                              PS401620
C                                                                          PS401630
  21          CONTINUE                                                      PS401640
C                                                                          PS401650
```

148

```fortran
C                                                                       PS401660
C------THERMAL BOUNDARY CONDITION AT STRIP/ROLL INTERFACE.              PS401670
CC-----------------------INTRODUCTION OF IDEAL COOLING.                 PS401680
CC              IVV=I-1                                                  PS401690
CC              CALL IDEALC                                             PS401700
CC              A(I,NY)=TC/DDY + TCR/SQRT(3.1416*ALFR*DTI)              PS401710
CC              D(I,NY)=TCR*CO12/SQRT(3.1416*ALFR*DTI)                  PS401720
C                                                                       PS401730
C--------CALCULATION OF THE EFFECTIVE HEAT TRANSFER COEFFICIENT         PS401740
C                                                                       PS401750
               VR=VRX(OMEG,R,X)                                         PS401760
               VRP=VRXP(OMEG,R,X,Q,HO,X2,X4,XN,X1)                      PS401770
               HTCP=HTC*(VRP/VR)                                        PS401780
C                                                                       PS401790
C----------USE OF THE HEAT TRANSFER COEFFICIENT FOR BOUNDARY NODES      PS401800
C----------AT THE SPLAT/ROLL INTERFACE.                                 PS401810
C                                                                       PS401820
               A(I,NY)= TC/DDY  + HTCP                                  PS401830
               B(I,NY)=O.                                               PS401840
               C(I,NY)=TC/DDY                                           PS401850
               D(I,NY)= HTCP*TROLL                                      PS401860
C                                                                       PS401870
C------AT THIS STAGE, THE VALUES OF ALL THE COEFFICIENTS FOR THE NY     PS401880
C------Y-NODES LYING AT THE I-TH X-STEP,HAVE BEEN CALCULATED.           PS401890
C                                                                       PS401900
C-----EVALUATION OF THE N-TH COEFFICENT FOR THE  GAUSS ELIMINATION.     PS401910
C-----COEFFICIENT MAKE EQUAL TO THE TEMPERATURE OF NODE I,NY.           PS401920
C                                                                       PS401930
       Q(I,NY)=(D(I,NY)+C(I,NY)*Q(I,NYN))/(A(I,NY)-C(I,NY)*P(I,NYN))    PS401940
               T(I,NY)=Q(I,NY)                                          PS401950
C                                                                       PS401960
C-----THE FOLLOWING RECURSIVE NODE COMPUTES TEMPERATURES FOR NODES      PS401970
C-----LYING ALONG THE I-TH X-STEP, TRAVELING FROM THE SPLAT/ROLL        PS401980
C-----INTERFACE TOWARDS THE CENTER OF THE SPLAT.                        PS401990
C                                                                       PS402000
                         DO 30 K=1,NYN                                  PS402010
                         KK=NY-K                                        PS402020
                         KKK=NY+1-K                                     PS402030
             T(I,KK)=P(I,KK)*T(I,KKK) + Q(I,KK)                         PS402040
 30                      CONTINUE                                       PS402050
C                                                                       PS402060
C----------THE FOLLOWING LOOP COMPUTES THE RESIDUAL BETWEEN THE         PS402070
C----------FRESHLY CALCULATED TEMPERATURE FIELD AND THE ONE OBTAINED    PS402080
C----------FROM THE PREVIOUS ITERATION.                                 PS402090
C                                                                       PS402100
                         DO 35 KL=1,NY                                  PS402110
                         RE(I,KL)=(ABS(TA(I,KL)-T(I,KL)))/TA(I,KL)      PS402120
 35                      CONTINUE                                       PS402130
C                                                                       PS402140
C----------------THE NEXT LOOP CREATES A NEW (IMPROVED) GUESS FOR       PS402150
C----------------THE TEMPERATURE FIELD FROM THE FRESHLY CALCULATED.     PS402160
C                                                                       PS402170
                         DO 40 L=1,NY                                   PS402180
                         TA(I,L)=T(I,L)                                 PS402190
 40                      CONTINUE                                       PS402200
```

149

```
          IF(I.GE.NX) GO TO 60                                        PS402210
  10       CONTINUE                                                   PS402220
C                                                                     PS402230
C-------END OF MAIN (X) LOOP.AT THIS STAGE THE ENTIRE TEMPERATURE FIELDPS402240
C-------IS KNOWN EXCEPT THE VALUES FOR THE NY GRID POINTS LYING ALONG  PS402250
C-------THE NX-TH X-STEP.                                             PS402260
C                                                                     PS402270
  60       CONTINUE                                                   PS402280
C                                                                     PS402290
C--------THE NEXT LOOP USES THE BOUNDARY CONDITION OF ZERO HEAT FLOW   PS402300
C--------ALONG THE X-DIRECTION AND COMPLETES THE TEMPERATURE FIELD.    PS402310
C                                                                     PS402320
                         DO 80 LL=1,NY                                PS402330
C                         T(NX,LL)= 660.                              PS402340
C                         TA(NX,LL)= 660.                             PS402350
                          T(NX,LL)=T(NXN,LL)                          PS402360
                          TA(NX,LL)=TA(NXN,LL)                        PS402370
                          RE(NX,LL)=RE(NXN,LL)                        PS402380
  80                      CONTINUE                                    PS402390
              GO TO 700                                               PS402400
  81             CONTINUE                                             PS402410
C                                                                     PS402420
C----------THE NEXT LOOP SCANS THE ENTIRE TEMPERATURE FIELD COMPARING  PS402430
C----------THE FRESH VALUES WITH THOSE OBTAINED FROM THE PREVIOUS ITE- PS402440
C----------RATION AND LOOKS FOR THE LARGEST RESIDUAL.                 PS402450
C                                                                     PS402460
C                     RESMAX=0.0                                      PS402470
C                     DO 85 IV=1,NX                                   PS402480
C                      DO 90 JV=1,NY                                  PS402490
C                       IF(RESMAX.LT.RE(IV,JV)) RESMAX=RE(IV,JV)      PS402500
C                       RE(IV,JV)=0.0                                 PS402510
  90                    CONTINUE                                      PS402520
  85                    CONTINUE                                      PS402530
C                                                                     PS402540
C---------------SATISFACTION OF THE CRITERION FOR CONVERGENCE.        PS402550
C                                                                     PS402560
C                          IF(RESMAX.LT.0.0001) GO TO 69             PS402570
C3                                CONTINUE                            PS402580
C                                                                     PS402590
  69       CONTINUE                                                   PS402600
C69        X3=X                                                      PS402610
C                                                                     PS402620
C--------WRITING OF THE CONVERGED TEMPERATURE FIELD.                  PS402630
C                                                                     PS402640
           WRITE(6,100) ((T(I,J),J=1,NY),I=1,NX)                     PS402650
C                                                                     PS402660
C---------------CALCULATION OF COOLING RATE FIELD.                    PS402670
C                                                                     PS402680
                     DO 76 IK=2,NX                                    PS402690
                      IIK=IK-1                                        PS402700
                       DO 75 JK=1,NY                                  PS402710
                        TG(IK,JK)=(TA(IK,JK)-TA(IIK,JK))/DX           PS402720
                        CR(IK,JK)=ABS((TG(IK,JK))*(VELX(IK,JK)))      PS402730
  75                     CONTINUE                                     PS402740
  76                    CONTINUE                                      PS402750
C                                                                     PS402760
C----------WRITING THE FINAL COOLING RATE FIELD.                      PS402770
C                                                                     PS402780
           WRITE(6,100) ((CR(I,J),J=1,NY),I=1,NX)                    PS402790
           WRITE(6,66) RESMAX,III                                     PS402800
  66       FORMAT(//,25X,E12.5,3X,I3)                                 PS402810
 100       FORMAT(1X,6E12.5)                                         PS402820
 700          RETURN                                                  PS402830
              END                                                     PS402840
```

150

APPENDICES

2A.1.- A Comment on the Relationship Between the Size of

Microstructural Features and the Casting Parameters.

Many rapidly solidified samples have been observed to have

microstructures reminiscent of the well known cellular–dendritic

structures typical of more conventionally cast samples. The

main difference is that the size of these microstructural fea-

tures becomes smaller the larger the rate of heat extraction

from the sample. During the past few decades metallurgists have

been searching for appropriate correlations capable of represent-

ing the relationship between the microstructural features and

the solidification parameters. A convenient measure of the effect

of casting parameters on the material microstructure has been

found to be the so called dendrite arm spacing (i.e. the center

to center distance between neighboring dendrite arms). Both

primary and secondary dendrite arm spacings have been widely

used.

It is commonly believed that the dendrite arm spacing adjusts

itself to the prevailing growth conditions by reducing the

supercooling of the liquid lying between the dendrites to a

minimum value. The experimental results indicate that the prod-

uct of the temperature gradient in the liquid in front of the

solid-liquid interface, G_1 , and the growth velocity , R ,

correlates well with the measured arm spacings. The proposed

correlation has the following form ,

$$\lambda_s = B_1 \, (\, G_1 \, R \,)^{-n} \tag{1}$$

Note that , in Eqn(1), the product $G_1 \, R$ has the units of cooling rate (i.e. $^{\circ}C/s$) and in this sense it can be considered as an "effective" cooling rate just ahead of the solidification interface, i.e.

$$G_1 \, R = \dot{T}_e \tag{2}$$

Although the phenomenon of dendrite arm coarsening has been mentioned as one of the reasons for the occasional discrepancy found between Eqn(1) and actual measurements, this process is not believed to be very important during RS because of the small time intervals involved in the completion of the solidification. Moreover, in rapidly solidified melt spun samples, primary and secondary dendrite arm spacings are not easily recognized (Speck(1985)), and what one usually sees are cell-like structures which are very fine in the portion of the splat nearest to the wheel surface and which increase in size with increasing distance from this surface. It has also been suggested, (Kattamis(1981)), that the microstructural sizes measured in such samples be considered analogous to the secondary dendrite arm spacings observed in the more conventionally cast samples.

The rapid solidification of eutectic alloys by coupled eutectic growth produces a lamellar microstructure much finer than the one found in conventionally cast samples. In this case the inter-lamellar spacing is found to be given by

$$\lambda_s = B_3 (R)^{-1/2} \tag{3}$$

Equations (1) and (3) above can be used to predict the scale of the microstructure for a wide variety of alloys once the solidification conditions have been defined. The required values of the coefficients B_1 and B_3 for several alloy systems can be obtained from Table(1) below.

Table (2A.1.1).- Parameters for the Calculation of Cell-Secondary Dendrite Arm Spacings from the Solidification Conditions. See Eqns (1) and (3). From Jones(1982).

Alloy (wt%)	Cooling Rate Range (K/s)	B_1 (μm/(K/s)$^{-n}$)	B_3 ((μm)$^{3/2}$/s$^{1/2}$)	n (-)
Sn-15Pb	0.005 - 50	23	-	0.35
Al-4.5Cu	0.00002 - 300	41	-	0.39
Al-10.5Si	$400 - 1.2*10^5$	47	-	0.33
Cu-0.5Zr	$1 - 1*10^7$	160	-	0.40
Inconel 718	0.1 - 100	34	-	0.34
X-40 (Co-Cr)	0.1 - 200	40	-	0.27
Fe-20Mn	60 - 1400	150	-	0.25
Fe-25Ni	$0.001 - 1.7*10^6$	60	-	0.32
440 S.Steel	$15 - 1*10^5$	60	-	0.41
Maraging 300 Steel	0.1 - 1400	40	-	0.30
Ti- 2 to 30 Al,Fe,Ge,Mo or V	0.2 - 150	16 - 124	-	0.3 - 0.5

Table (2A.1.1).- (contd.)

Alloy (wt%)	Cooling Rate Range (K/s)	B_1 $(\mu m/(K/s)^{-n})$	B_3 $((\mu m)^{3/2}/s^{1/2})$	n (-)
Al-Al$_2$Cu	not given	–	10.5 – 11.8	–
Al–Zn	"	–	8.0	–
Bi–Zn	"	–	8.3	–
Cd–Zn	"	–	5.3	–
Pb–Ag	"	–	11.0	–
Pb–Cd	"	–	4.5	–
Sn–Ag	"	–	16.7	–
Sn–Cd	"	–	8.5	–
Sn–Pb	"	–	5.5	–
Sn–Zn	"	–	8.3	–

3A.1.-   The Governing Equations of Transport Phenomena.

Introduction

   The governing equations of transport phenomena simply express

well known facts about nature in mathematical symbols. These facts

are based on physics, specifically, Newton's laws and Thermodynamic

principles. There are two alternative ways of deriving the

governing equations for momentum, heat and mass transfer in

continua, namely;

(i) differential (shell) balances (e.g. Bird et al(1960) and

Szekely and Themelis(1971)). In these one uses the basic laws

of physics to establish mass, momentum and energy balances over

a small volume element inside the material under study. The

partial differential equations resulting from making the volume

of the element go to zero constitute the differential balances

for all points inside the domain.

(ii) The postulational approach (e.g. Slattery(1981) and Billington

and Tate(1981)). Here one starts from a small set of postulates

(also based on basic physics) and uses a mathematical result known

as the transport theorem to arrive to the governing equations.

These equations are general and valid for all materials and must

be specialized by introducing constitutive equations of material

behavior to arrive at the forms most useful for applications.

For the sake of completeness and since the postulational approach does not seem to have been widely known among metallurgists, we have decided to present here a brief summary of the method. After the derivation of the general equations for transport phenomena we will then discuss the boundary conditions most frequently found in fluid flow and heat and mass transfer problems. The section concludes with a comment on the special form the equations have for the case of the flow of thin liquid films and also the case of flows with negligible inertia. For details, however, the references given above should be consulted.

The Transport Theorem and the Postulates of Continuum Mechanics

The transport theorem is simply a mathematical identity which can be proved to be satisfied by any scalar, vector, or tensor valued function of time and position. We will restrict ourselves to the presentation of two of the most useful forms of the theorem.

If ϕ is a scalar, vector, or tensor and V is the volume of the material under study, the following is true,

$$d\left(\int_V \phi \, dV\right)/dt = \int_V \left(D\phi/Dt + \phi \, \mathrm{div} \, \underline{v}\right) dV \qquad (1)$$

and , if mass is conserved (i.e. if $\mathrm{div} \, \underline{v} = 0$),

$$d\left(\int_V \rho \, \phi \, dV\right)/dt = \int_V \left(\rho \, D\phi/Dt\right) dV \qquad (2)$$

The postulates of continuum mechanics are simply the summary of centuries of empirical observation of physical processes taking place in the world. They could be listed as follows;

a) the principle of conservation of mass: " The mass of a given body is independent of time". In symbols

$$d(\int_V \rho \ dV)/dt \ = \ 0 \tag{3}$$

b) The principle of conservation of momentum: "The rate of change of momentum of a body is equal to the sum of the forces acting on it", i.e.

$$d(\int_V \rho \ \underline{v} \ dV)/dt \ = \ \int_A \underline{T} \cdot \underline{n} \ dA \ + \ \int_V \rho \ \underline{f} \ dV \tag{4}$$

where $\underline{T} \cdot \underline{n}$ is the field of contact forces.

c) The principle of conservation of energy: "The rate of change of the total energy of a body is equal to the rate of work done on the body plus the rate of energy transmission to it", i.e.

$$d(\int_V \rho \ (U + \underline{v}^2/2) \ dV \ = \ \int_A \underline{v} \cdot (\underline{T} \cdot \underline{n}) \ dA \ + \ \int_V \rho \ (\underline{v} \cdot \underline{f}) \ dV \ +$$

$$+ \ \int_A h \ dA \ + \ \int_V \rho \ \dot{Q} \ dV \tag{5}$$

where the terms on the R.H.S. are , respectively, the rate of

158

work done by the contact forces, the rate of work done by the
external forces, the rate of energy transmission from the
enviroment to the body through its surface, and the rate of
energy generation inside the body.

Equations (3)-(5) are valid regardless of the size of the body,
thus , the relations valid for integrated quantities are also
valid for the quantities inside the integral signs. If one
uses now the transport theorem, the following forms of the
equations can be readily derived,

a) conservation of mass

$$\partial \rho / \partial t \; + \; \text{div}(\rho \; \underline{v}) \; = \; 0 \tag{6}$$

b) conservation of momentum

$$\rho \, \partial \underline{v} / \partial t \; + \; (\nabla \underline{v}) \cdot \underline{v} \; = \; \text{div} \; \underline{T} \; + \; \rho \underline{f} \tag{7}$$

and (c) conservation of energy,

$$\rho \, \partial U / \partial t \; + \; (\nabla U) \cdot \underline{v} \; = \; - \; \text{div} \; \underline{q} \; + \; \text{tr}(\underline{T} \cdot \nabla \underline{v}) \; +$$

$$+ \; \rho \, \dot{Q} \tag{8}$$

Since Eqns(6)-(8) apply regardless the material constitution
of the body in question,constitutive equations for material
behavior must now be introduced to account for the widely different
properties of various materials. The constitutive equations
are simply relationships between quantities in Eqns(6)-(8) which
make the transport problem well posed. Typically, the flux of
momentum $\underline{T}$, and the flux of energy, q , are related to the
intensity driving momentum transfer, $\nabla \underline{v}$, and to the intensity
driving heat flow, ∇u , respectively .

Constitutive Equations for Material Behavior

The constitutive equations are relationships between fluxes
and intensities which enable us to classify materials into various
groups based on similarities in their mechanical and thermal
behaviors. Several rules have been laid down for the construction
of appropriate constitutive equations. However, most of the most
useful ones are based on the results of a great deal of empirical
research. Here we restrict ourselves to presenting some of the
most widely used constitutive equations.

a) The Newtonian fluid : "The stress is a linear function of the
strain rate", i.e.

$$\underline{T} = - p \underline{I} + 2\mu((\nabla \underline{v}) + (\nabla \underline{v})^T)/2 \qquad (9)$$

b) The non-Newtonian, power law fluid-creeping solid,

$$\underline{\underline{T}} = -p \underline{\underline{I}} + 2 \eta ((\nabla \underline{v}) + (\nabla \underline{v})^T)/2 \tag{10}$$

where

$$\eta = S_{eff}/3 D_{eff} \tag{10a}$$

and

$$D_{eff} = B_{10} (S_{eff})^b \tag{10b}$$

where B_{10} and b are material properties and can be obtained for the case of creeping solids from the compilation by Frost and Ashby(1982). Moreover, since D_{eff} and S_{eff}, the effective deformation rate tensor and deviatoric stress tensor, are functions of the strain rate, $\underline{\underline{T}}$ in Eqn(10) is clearly a non linear function of the strain rate.

For heat transfer, the most widely used constitutive equation is Fourier's first law. This is,

$$\underline{q} = -K(u) \nabla u \tag{11}$$

The substitution of Eqns(9) and (11) into (6)-(8) leads to the forms of the governing equations which are the strating point for the calculations in this thesis. I.e.

a) the equation of continuity

$$\partial \rho / \partial t + \text{div}(\rho \underline{v}) = 0 \tag{12},$$

b) the equation of motion (Navier-Stokes),

$$\rho \partial \underline{v} / \partial t + (\nabla \underline{v}) \cdot \underline{v} = - \nabla p + \mu \, div(\nabla \underline{v}) + \rho \underline{f} \qquad (13)$$

and (c) the differential energy balance,

$$\rho \, \partial E / \partial t + (\nabla E) \cdot \underline{v} = \; div(K \nabla u) + tr((\underline{T} + p\underline{I}) \cdot \nabla \underline{v}) +$$

$$+ \rho \dot{Q} \qquad (14)$$

Equations (12)-(14) are the starting point of all of our calculations. However, before embarking oneself on the problem of solving these equations one has to look for suitable boundary conditions. Moreover, multicomponent systems are very common in practice and due account must be taken for them. So, in the next section we comment on the formulation of mass transfer problems in multicomponent systems and then we discuss the most commonly used boundary conditions for transport phenomena problems.

Multicomponent Systems: Mass Transfer

Although the presence of several components complicates the situation, relatively few additional ideas are required to formulate the governing equations for the case of multicomponent systems. Specifically, each of the component species in the

162

system can be regarded as a continuous medium with a variable mass density field. The model for the multicomponent mixture is then a superposition of all these continuous media.

A new vector field is also introduced to describe the rate of motion of each species in the system. Such quantity is called the mass flux vector $\underline{j}$. The mathematical indeterminancy resulting from the introduction of the mass flux vector has to be resolved by establishing constitutive relationships linking $\underline{j}$ with the corresponding intensities for mass transfer. This is reminiscent of the procedure followed before to transform Eqns(7) and (8) into (13) and (14). The simplest possible case is that of binary systems. In this case the constitutive equation is known as Fick's first law. For the binary system, the equation of continuity takes the following form,

$$\partial c / \partial t \; + \; (\nabla c) \cdot \underline{v} \; = \; div(D \, \nabla c) \; + \; r_c \tag{15}$$

Boundary Conditions for Momentum, Heat and Mass Transfer

For Eqns(12)-(15) to constitute a well posed problem, boundary and initial conditions representing the specific systems under study must be added. These conditions are nothing but restrictions on the values of the field variables or their fluxes, imposed by the actual physics of the problem, at some locations on the computational domain. We now describe some of the most widely used

boundary conditions for the solution of transport phenomena problems.

a) Boundary conditions for fluid flow problems.

(i) Continuity of tangential components of velocity at phase interfaces. This is the well known no-slip condition (Batchelor (1967)). In symbols, denoting by a subindex a, b the phases in question, we have

$$(\underline{v} \cdot \underline{t})_a = (\underline{v} \cdot \underline{t})_b \qquad (16).$$

(ii) Discontinuity of tangential components of velocity at phase interfaces. This condition, as opposed to the previous one, allows for some slip at the interface between phases in relative motion. It seems to be particularly useful when dealing with problems involving lines of contact (e.g. Dussan(1979)). In symbols, one possible way of expressing this, is

$$(\underline{v} \cdot \underline{t})_a = \mathcal{H} (\underline{v} \cdot \underline{t})_b \qquad (17).$$

(iii) Continuity of stress at phase interfaces. Both the tangential and the normal components of the stress acting on the phase interface must satisfy continuity relationships which involve stresses due to surface tension effects (Levich and Krylov(1969)). For an interface separating two Newtonian fluids,

the balance of tangential stresses is,

$$(\mu \, D_{ij} \, t_i \, n_j \,)_a = (\mu \, D_{ij} \, t_i \, n_j \,)_b + \nabla \sigma \cdot \underline{t} \qquad (18)$$

where $D_{ij} = ((\nabla \underline{v}) + (\nabla \underline{v})^T)/2$, and the usual summation convention of adding over repeated subscripts has been used.

And the balance of normal stresses is,

$$P_a - (\mu \, D_{ij} \, n_i \, n_j \,)_a = P_b - (\mu \, D_{ij} \, n_i \, n_j \,)_b +$$

$$+ \sigma \, (2 \, \mathcal{H}) \qquad (19).$$

b)   Boundary Conditions for Heat Transfer Problems.

(i)   Temperature specified at the interface (Dirichlet condition). In symbols

$$u_a = u_b \qquad (20).$$

(ii)   Heat flux specified at the surface (Neumann condition).Here,

$$(K \, \nabla u \,)_a \cdot \underline{n} = f(\underline{x},t) \qquad (21).$$

(iii) Heat flux at the surface specified by a heat transfer coefficient (Cauchy condition). In this case,

$$(K \nabla u) _a \cdot \underline{n} = - h (u - u_\infty) \qquad (22).$$

iv)   Continuity (or discontinuity) of the heat flux at the phase interface. This condition is also called ideal cooling (in the case of continuity) or the Stefan condition (in the case of moving boundary problems with a discontinuity). For ideal cooling , in symbols,

$$(K \nabla u)_a = (K \nabla u)_b \qquad (23).$$

When heat is released/absorbed at the phase interface due, for example to a change of phase (Stefan problem), this must be accounted for by adding a corresponding term to Eqn(23), (see Sec(3A.2) below). Additional discussion about the boundary conditions for heat transfer problems can be found in Luikov (1980).

c)   Boundary Conditions for Mass Transfer Problems.

i)   Concentration specified at the interface (Dirichlet condition),

$$C_a = C_b \qquad (24).$$

In many instances, the given concentration at the interface is the equilibrium value for the system under consideration.

ii) Mass flux specified at the surface (Neumann condition),

$$(D \; \nabla C)_a \cdot \underline{n} \;\; = \;\; g(\underline{x},t) \tag{25}$$

If there is generation/consumption of solute at the interface due to a reaction, g is given by chemical kinetics.

iii)   Mass flux at the surface specified by a mass transfer coefficient (Cauchy condition),

$$(D \; \nabla C)_a \cdot \underline{n} \;\; = \;\; k_m (C_a \; - \; C_\infty) \tag{26}.$$

iv)   Continuity (or discontinuity) of the mass flux at the surface or phase interface. When solute is generated at a phase interface due to a heterogeneous chemical reaction, the mass flux has a discontinuity at that interface. One example of this kind is the Stefan problem for alloy solidification (Sec(3A.2)). In symbols, this condition is then,

$$((D \; \nabla C)_a \; - \; (D \; \nabla C)_b) \cdot (\text{grad } F) \;\; = \;\; (C(F^-) - C(F^+))(\partial F/ \partial t)$$

$$\tag{27}$$

Very often, however, Eqn(23) is replaced by Eqn(25), requiring only the evaluation of the function g .

A Note on Flow in Thin Liquid Films and on Flows with Negligible Inertia

It can be expected that, when a fluid is in the form of a thin film, far less time will in general be required for the attainment of approximate equilibrium in the direction of the film thickness than in the direction of its length. Furthermore, the flow of liquids in thin films is an example of a system in which both viscous forces and surface tension effects play important roles. The governing equations for fluid flow can be considerably simplified for the case of flow of thin liquid films. This simplification comes about because of the following reasons: (i) Since the thickness of the film is small, all velocity derivatives across the film are large compared to those along its length, and (ii) the flow in thin liquid films can be safely assumed to be quasi-unidimensional.

If a coordinate system is chosen with the x- axis in the direction of the length of the film and the y- axis in the direction of its thickness, the Navier-Stokes equations become,

$$\partial v_x / \partial t + v_x \partial v_x / \partial x + v_y \partial v_x / \partial y = -(1/\rho) \partial p / \partial x +$$

$$+ (\mu/\rho) \partial^2 v_x / \partial y^2 + f_x \tag{28a}$$

and

$$\partial p / \partial y = 0 \tag{28b}$$

168

If one of the surfaces of the film is a free surface, the pressure there can be assumed equal to the capillary pressure and if the film is so thin that virtually the same pressure exists across its thickness, the first term on the R.H.S. of Eqn(28a) becomes,

$$- (1/\rho) \, dP_\sigma/dx = (\sigma/\rho) \, d^3H/dx^3 \qquad (29)$$

Now, since $v_y = \partial H/\partial t + v_x \partial H/\partial x$, the use of the equation of continuity, for steady state conditions, leads to,

$$\partial H/\partial x = -(1/v_x) \, \partial (\int v_x \, dy)/\partial x \qquad (30)$$

Equations (28)-(30) constitute the mathematical representation of the fluid motion which takes place inside thin liquid films.

It is well known that the presence of the non linear term $\underline{v} \cdot \nabla \underline{v}$ in the Navier-Stokes equations for the thin film makes the solution very difficult for all except the simplest flows. It is possible, however, to neglect this term in some cases. Although the term may not be really zero in these circumstances, it will be relatively small and the approximation can be justified. Furthermore, if steady state exists, the entire inertia term in the equations can be neglected when compared with either the pressure or the viscous forces. Flows such as these are known as flows with negligible inertia. The geometrical arrange-

ment characteristic of flows with negligible inertia is such that the thickness of the film must vary along its length and that the tendency of the motion must continually be to drag a supply of fluid from the thicker to the thinner portions of the film.

The formulation resulting from the use of the assumptions mentioned above is known as the theory of lubrication. In summary, the basic assumptions of the theory (e.g. Hamrock and Dowson(1981)) are,

i) the inertia and body forces are negligible compared with the pressure and viscous terms,

ii) there is a negligible variation of the pressure across the film thickness,

iii) the derivatives of the velocity in the direction of the thickness are much larger than the derivatives with respect to the film length,

iv) laminar flow conditions exist,

v)   the fluid properties are constant across the thickness, and

vi) there is no slip between fluid and solid boundaries.

In the most general case, the introduction of the assumptions of lubrication theory into Eqn(13) leads to

$$\nabla p = \mu \nabla^2 \underline{v} \qquad (31)$$

The introduction of suitable boundary conditions and the consideration of Eqn(12) lead to solutions of the general form,

$$\underline{v}/V_o = \underline{v}/V_o \ (x/L, \text{geometry of the B. C.'s }) \qquad (32)$$

if the boundary conditions involve $\underline{v}$ only. Here V_o is a

reference velocity, usually that of the moving substrate.

For additional information on lubrication theory one can

consult Batchelor or Schlichting(1979).

For the verification of approximations such as those of

lubrication theory it is frequently necessary to determine the

relative importance of the various terms in the governing

equations. For this purpose one can use a so called order of

magnitude analysis (see e.g. Schlichting). The final result

of such an analysis is in the form of certain quantities called

dimensionless numbers. These numbers are actually ratios de-

scribing the relative importance of the various terms in the

governing equations. The actual numerical values of these

ratios can be an useful first guide towards the understanding

of complex physical processes involving heat transfer and

fluid flow. Since RSP systems are characterized by these

features, in Table(1) below we list some of the dimensionless

numbers more frequently found to apply. For additional

details on the subject of dimensional analysis the reader can

consult the book by Szekely(1979).

Table (3A.1.1). - Dimensionless Numbers Useful in RSP.

Number	Formula		Meaning
Biot	$N_{Bi} = h\,z/k$	h = heat transfer coefficient z = reference length k = thermal conductivity of sample	$\dfrac{\text{internal thermal resistance}}{\text{outer surface thermal resistance}}$
Bond	$N_{Bo} = g(\rho - \rho_f)\,z/\sigma$	g = gravity ρ = density of sample ρ_f = density of fluid	$\dfrac{\text{gravitational force}}{\text{surface tension force}}$
Nusselt	$N_{Nu} = h\,z/k_f$	k = thermal conductivity of fluid	$\dfrac{\text{total heat transfer}}{\text{conductive heat transfer}}$
Mehrabian	$N_{Me} = R'_o\,L\,\rho/h$	R'_o = kinetic growth coefficient L = latent heat of fusion	$\dfrac{\text{energy released during recalescence}}{\text{energy extracted through outer surface}}$
Peclet	$N_{Pe} = C_p\,V_o\,z/k$		$\dfrac{\text{heat transfer by bulk motion}}{\text{heat transfer by conduction}}$

172

Table (3A.1.1).- (contd.)

Number	Formula	Meaning
Prandtl	$N_{Pr} = C_p \mu/k$	$\dfrac{\text{momentum diffusivity}}{\text{thermal diffusivity}}$
Reynolds (modified)	$N_{Re} = \rho\, z\, V\, (H/z)/\mu$	$\dfrac{\text{inertia force}}{\text{viscous force}}$
Stefan	$N_{St} = C_p(T_f - T_s)/L$	$\dfrac{\text{sensible heat}}{\text{latent heat}}$ T_s = surface temperature
Weber	$N_{We} = \rho\, z\, V_o^2 / \sigma$	$\dfrac{\text{inertia force}}{\text{surface tension force}}$
Weber-Reynolds	$N_{WR} = \mu\, V_o / \sigma$	$\dfrac{\text{viscous force}}{\text{surface tension force}}$

3A.2.-   The Formulation and Solution of Solidification Problems.

Introduction

The basic feature of solidification problems (also called
Stefan problems) is that they are represented by a parabolic
diffusion equation which has to be solved inside a region whose
boundaries are to be determined as part of the solution. In the
typical solidification (melting) problem, a substance has a
transformation temperature at which it changes phase with emission
or absorption of heat. The liberation or absorption of heat
takes place at the moving surface of separation between the two
phases. This surface of separation together with the temperature
field inside the two phases constitute the solution to the
solidification (melting) problem.

Stefan problems are at the core of casting metallurgy and good
reviews of the metallurgical aspects are available (e.g. Flemings(
1974)). Here we will concentrate on the mathematical aspects of the
subject by presenting the formulation of the governing equations
and the available techniques for their solution.

Formulation

The mathematical statement of the Stefan problem, in the absence
of fluid motions, consists of the following sets of equations:
i)   The heat equation

$$\partial u_i / \partial t = \text{div}(\alpha \text{ grad } u_i) + r_h \qquad (1) \quad ,$$

$$i = s, 1$$

ii) the heat balance at the moving boundary (Stefan condition),

$$\rho L \partial F / \partial t = (K \text{ grad } u)_s^1 \cdot \text{ grad } F \qquad (2)$$

where $F(\underline{x}, t) = 0$ is the phase change surface.

iii) Equilibrium phase change temperature at the interface

$$u_s = u_1 = u_f \qquad (3),$$

iv) appropriate boundary conditions on all other boundaries, which could be of Dirichlet, Neumann or Cauchy type.

v) Initial conditions.

Detailed reviews of the formulation of Stefan problems can be found in Tayler(1975) and in Crank(1984).

The problem represented by (i)-(v) above is nonlinear because of the moving boundary. The temperature field depends on the exact location of the boundary and this in turn depends on the temperature.

Exact, closed form solutions to the Stefan problem are known for only a small number of simple situations. In all cases these

solutions apply to one dimensional situations. The one dimensional Stefan problem is described by the following equations (see e.g. Carslaw and Jaeger(1959)),

$$\partial u_s / \partial t = \partial(\alpha_s(\partial u_s / \partial x))/ \partial x \qquad (4a)$$

$$\partial u_1 / \partial t = \partial(\alpha_1(\partial u_1 / \partial x))/ \partial x \qquad (4b)$$

$$K_s \partial u_s / \partial x - K_1 \partial u_1 / \partial x = \rho L \partial X / \partial t \qquad (4c)$$

and
$$u_s = u_1 = u_f \qquad (4d)$$

Closed Form Solutions

Only two exact solutions of Eqn(4) are available. These are the solution due to Neumann and the one due to Schwarz. Both are applicable only to infinite regions and under Dirichlet type boundary conditions. Schwarz's solution , however, incorporates the mold into the calculation.

a) Neumann's solution. If the problem represented by Eqns(4a)-(4d) is complemented by boundary and initial conditions such as

$$u(0,t) = u_1 < u_f \qquad (5a)$$
and

$$u(x,0) = u_2 > u_f \qquad (5b)$$

the solution is

$$u_s = u_1 + (u_f - u_1) \, \text{erf}(\, x/2(\alpha_s t)^{1/2} \,)/ \, \text{erf} \, \lambda \tag{6a}$$

$$u_1 = u_2 + (u_f - u_2) \, \text{erfc}(\, x/2(\alpha_1 t)^{1/2})/ \, \text{erfc}(\lambda(\alpha_s/\alpha_1)^{1/2}) \tag{6b}$$

$$X = 2\lambda(\alpha_s t)^{1/2} \tag{6c}$$

where the quantity λ is the root of

$$\exp(-\lambda^2)/\text{erf}\,\lambda \; - \; \frac{K_1 \, \alpha_s^{1/2} \, (u_2 - u_f) \, \exp(-\alpha_s \lambda^2/\alpha_1)}{K_s \, \alpha_1^{1/2} \, (u_f - u_1) \, \text{erfc}(\lambda(\alpha_s/\alpha_1)^{1/2})} \; =$$

$$= \lambda \, L \, \pi^{1/2}/ \, C_{p_s} \, (u_f - u_1) \tag{6d}$$

In Sec(5.2) above we have included a FORTRAN program called NEUMANN which computes the instantaneous moving boundary location X(t) and the temperature fields, $u_s(x,t)$, and $u_1(x,t)$ by means of Eqns(6a)-(6d).

b) Schwarz's solution- Here the chill is incorporated into the problem by imposing Dirichlet conditions at a point in the mold far away from the mold-casting interface. Figure(1) shows schematically how the two solutions differ.

MOLD   SOLID   LIQUID
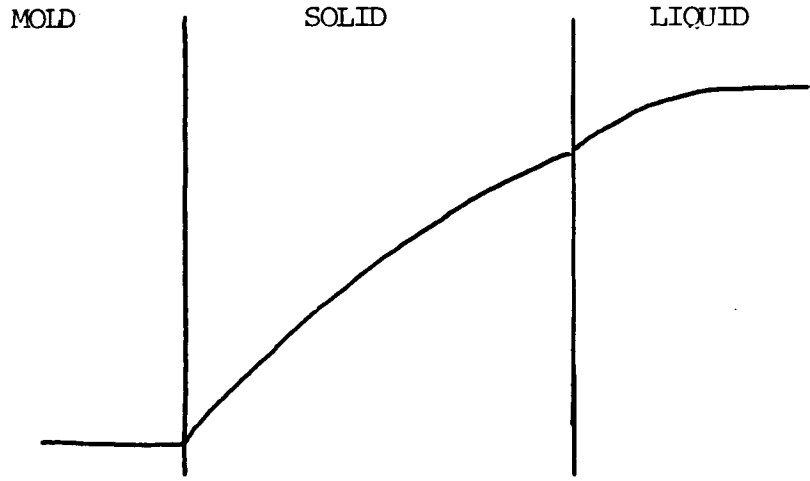
(a)
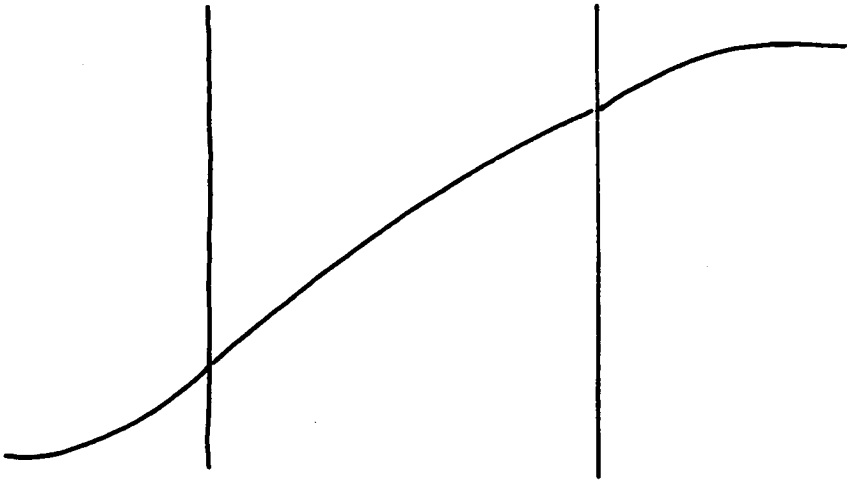
(b)

Fig (3A.2.1).-   Schematic comparison between (a) Neumann's and (b)
Schwarz's solutions of the classical Stefan problem,

Since now the mold is included in the calculation, the heat equation for the mold must be solved together with Eqns(4). For the mold we thus have

$$\partial u_m / \partial t = \partial (\alpha_m (\partial u_m / \partial x)) / \partial x \qquad (7a)$$

with the boundary condition

$$u_m \rightarrow u_1 < u_f , \quad \text{when} \quad x \rightarrow -\infty \qquad (7b).$$

The solution of the system of Eqns(4a)-(4d),(7a) and (7b) is

$$u_m = \frac{K_s \alpha_m^{1/2} (u_f - u_1)}{K_s \alpha_m^{1/2} + K_m \alpha_s^{1/2} \, \text{erf} \, \lambda} (1 + \text{erf}(x/2(\alpha_m t)^{1/2})) +$$

$$+ u_1 \qquad , \quad \text{for} \quad x < 0 \qquad (8a)$$

$$u_s = \frac{(u_f - u_1) (K_s \alpha_m^{1/2} + K_m \alpha_s^{1/2} \, \text{erf}(x/2(\alpha_s t)^{1/2}))}{K_s \alpha_m^{1/2} + K_m \alpha_m^{1/2} \, \text{erf} \, \lambda}$$

$$+ u_1 \qquad , \quad \text{for} \quad 0 < x < X \qquad (8b)$$

$$u_1 = \frac{(u_f - u_2) \, \text{erfc}(x/2(\alpha_1 t)^{1/2})}{\text{erfc}(\lambda (\alpha_s / \alpha_1)^{1/2})} + u_2 \quad , \quad \text{for} \quad x > X$$

$$\qquad (8c)$$

$$X = 2 \lambda (\alpha_s t)^{1/2} \qquad (8d)$$

where λ is the root of

$$\frac{K_m \, \alpha_s^{1/2} \, \exp(- \lambda^2)}{K_s \, \alpha_m^{1/2} + K_m \, \alpha_s^{1/2} \, \mathrm{erf} \, \lambda} +$$

$$+ \; \frac{K_l \, \alpha_s^{1/2} \, (u_2 - u_f) \, \exp(- \alpha_s \lambda^2 / \alpha_l)}{K_s \, \alpha_l^{1/2} \, (u_f - u_1) \, \mathrm{erfc}(\lambda \, (\alpha_s / \alpha_l)^{1/2})} \; = \; \frac{L \, \pi^{1/2} \, \lambda}{C_{p_s} (u_f - u_1)}$$

$$\tag{8e}$$

In Sec(5.3) we have included a program called SCHWARZ which computes the instantaneous position of the moving boundary and the temperature field according to Eqns(8).

c) The Case of Alloys. While pure substances solidify (melt) at a fixed temperature in normal circumstances, alloys change phase along a temperature range. This range is limited by the liquidus and solidus temperatures of the alloy, respectively, u_L and u_S . Moreover, during alloy solidification more or less severe solute redistribution processes take place. Here we restrict ourselves to the thermal problem which can be handled in a way analogous to Neumann's and Schwarz's solutions above if the following simplifying assumptions are introduced;

i) the heat of freezing is liberated uniformly over the melting range,

ii) the liquid is initially at the liquidus temperature, and

180

iii) inside the melting range a specific heat given by

$$C_{eff} = C_{p_1} + L/(u_L - u_S) \qquad (9),$$

is used.

It is now possible to write the solution to the alloy solid-ification problem according to either the Neumann or the Schwarz formulations. However, instead of Eqns(6d) and (8e) one should use

$$\frac{\exp((\alpha_s - \alpha_1)\lambda^2/\alpha_1)\ \mathrm{erfc}(\lambda(\alpha_s/\alpha_1)^{1/2})}{\mathrm{erf}\ \lambda} = \frac{(u_L - u_S)\ K_1\ \alpha_s^{1/2}}{(u_S - u_1)\ \alpha_1^{1/2}} \qquad (10),$$

or

$$\frac{K_m\ \alpha_s^{1/2}\ \exp((\alpha_s - \alpha_1)\lambda^2/\alpha_1)\ \mathrm{erfc}(\lambda(\alpha_s/\alpha_1)^{1/2})}{K_s\ \alpha_m^{1/2} + K_m\ \alpha_s^{1/2}\ \mathrm{erf}\ \lambda} = \frac{(u_L - u_S)\ K_1\ \alpha_s^{1/2}}{(u_S - u_1)\ K_s\ \alpha_1^{1/2}} \qquad (11).$$

These expressions were obtained by simply making $L = 0$ in Eqns(6d) and (8e) (since the latent heat is included in C_{eff}).

For actual computations one uses C_{eff} instead of C_1 and u_S instead of u_f in Eqns(6a)-(6c),(10) or (8a)-(8d),(11). The programs NEUMANN and SCHWARZ given in chapter 5 can be used to perform these calculations after the incorporation of these changes.

Additional analytic or semi analytic techniques have been used for the solution of Stefan problems in other geometries and with different boundary conditions. However, methods such as integral profile, series expansions and invariant embedding are limited to still relatively simple configurations. The availability of digital computers has led to the displacement of all these techniques by more convenient finite difference or finite element methods. The analytical solutions remain important, however, since they are used to verify the accuracy of numerical methods and sometimes to start the computational algorithms. The solution of most of the solidification problems found in practice will invariably require the use of numerical methods.

Numerical Methods for Solidification Problems

Since the advent of digital computers many complex solidification problems have been solved. Many numerical techniques have been proposed to handle the nonlinearities introduced by the moving boundary. No single "best" method seems to exist, however. Generally speaking all numerical methods subdivide the region of interest into small volume elements. Discrete forms of the

energy equation are then written for each element and the entire

set of resulting equations (for the whole system) is solved by

standard algebraic methods.

Broadly speaking, the numerical methods used for the solution

of Stefan problems can be classified according to the following

three criteria:

a) According to the treatment of the moving boundary. In this

case one has;

i) front tracking methods (Hsu et al(1981)). By careful readjust-

ment of the computational grid during the computation, the

precise location of the boundary is recorded for every time step.

The computational grid itself is redefined at each step on the

basis of the motion of the solidification interface.

ii) Fixed domain methods (Voller and Cross(1981)). The Stefan condi-

tion (Eqn(2)) is absorbed into the heat equation by introducing the

enthalpy. The resulting equation is then solved in a fixed grid.

The boundary can also be fixed, however by performing a coordinate

transformation using the solidification interface location as the

reference length of the transformation.

b) According to the discretization technique employed. Here we have:

i) finite difference methods (White(1983)). These are the easiest

to implement, however, special equation are required at the outer

boundaries in the case of irregular domains.

ii) Finite element methods (Ettouney and Brown(1983)). Here the

discretization equations is derived from a variational principle.

Since quadrilateral grids are not mandatory when using F.E., it is easier to fit the grid to the boundaries of irregular computational domains.

c) According to the procedure used to advance the solution in time. In this case we have;

i) explicit methods (Voller and Shadabi(1984)). The temperature at a given location depends only on the temperatures of neighboring points at the previous time step.

ii) Implicit methods (Elliott and Ockendon(1982)). The temperature depends on the temperatures of neighbouring points at the present time step.

iii) Semi-implicit methods. A combination of (i) and (ii) above.

Much more additional information about all these techniques and others can be found in the recent monograph by Crank .

When selecting a numerical method for a given problem, accuracy, ease in programming, stability and consistency are among the most important considerations. Since for the work reported in this thesis we used an explicit finite difference fixed domain method for the solidification calculations, this we will review in some detail. For the presentation we follow Elliott and Ockendon where the reader will find many details not covered in this brief review.

Fixed Domain Methods

a) Formulation. When solving problems with moving boundaries one

C-3

is usually interested on the properties of the phase chage boundary. Since heat is released or absorbed at the phase change temperature, this gives rise to discontinuities in the derivative of u across the interface. To deal with this lack of differentiability one introduces the concept of weak solutions. To describe weak solutions we start by noticing that Eqns(1) and (2) above representing the differential energy balance can be written in a different but equivalent form by using the enthalpy. From thermodynamics, the enthalpy is given as a monotonically increasing function of the temperature, i.e.

$$E = f(u) \qquad (12)$$

It can be shown that the original Stefan problem described by Eqns(1) and (2) can be reformulated in terms of Eqns(12) and (13),

$$\partial E/\partial t = div(K\ grad\ u) \qquad (13).$$

The classic solution to the Stefan problem thus being a pair of functions of time and position $\{u, F\}$ such that Eqns(12) and (13) , hold. The introduction of the enthalpy is useful for computational purposes since the location of the phase change surface is now implicit in the governing equations. Thus, instead of focusing on the pair $\{u, F\}$, we concentrate on $\{u, E\}$, with a considerable programming simplification. One can readily

verify that the formulation of the Stefan problem in terms of u and E is entirely equivalent to the original formulation in terms of u and F through the introduction of the concept of weak solutions.

A weak solution of the Stefan problem is defined as a pair of bounded integrable functions $\{u, E\}$ inside the domain of interest, such that Eqn(12) is satisfied and the integral identity (with Dirichlet data),

$$\int_t \int_\Omega (\rho\, \partial\phi/\partial t + u \nabla^2 \phi)\, d\underline{x}\, dt =$$

$$- \int_\Omega \rho\, E_0(\underline{x})\, \phi(\underline{x},0)\, d\underline{x} + \int_t \int_{\partial\Omega} g\, (\partial\phi/\partial n)\, d\underline{A}\, dt \quad (14)$$

where t is the time and $\underline{x}$ the space, holds for all test functions ϕ with continuous derivatives $\partial\phi/\partial t$, $\partial\phi/\partial x$, and $\partial^2 \phi/\partial x^2$, such that $\phi = 0$ on $\underline{x} = 0, 1$.

The two most important properties of such weak solutions are the following. Firstly, it can be proved that the weak solution exists and is unique. Second, certain difference schemes converge to the weak solution. These two properties are an essential requirement for any numerical technique to be useful. Most importantly, the consideration of weak solutions eliminates the first spatial derivative of u from the formulation making then unnecessary the separate consideration of solid and liquid regions in the computer code. The calculations are instead performed inside

the entire domain of interest using the same finite difference form and the location of the solidification interface is determined from the resulting temperature field. So, no complicated front tracking procedures are necessary and a rectangular grid can conveniently be used. More information about the mathematical aspects of weak solutions can be found in Atthey(1975).

b) Discretization of the weak formulation. Equation(13) must be put in a form suitable for computer calculations. This process is called discretization. Discretization can be done according to any of several more or less standard procedures. Finite differences and finite elements being two popular examples of discretization. Since for the calculations reported in this thesis a finite difference method was used, this we will describe. The main ideas, however, are independent of the discretization method used.

Assume first that the domain of interest is covered by a uniform, rectangular net. A finite difference approximation to Eqn(13) can be obtained by simply replacing spatial derivatives with central differences and the time derivative with a one sided difference (see e.g. Ames(1977)). The discrete problem thus consists of finding vectors $\underline{E}^{n+1}$ and $\underline{u}^{n+1}$, the values of the enthalpy and the temperature at the mesh points for the $n + 1$ th time step such that,

$$\underline{E}^{n+1} - \underline{E}^{n} + \underline{\underline{A}}\,\underline{u}^{n+\theta} = 0 \qquad (15)$$

where

$$\underline{u}^{n+} = \theta \, \underline{u}^{n+1} + (1 - \theta) \, \underline{u}^n \tag{16}$$

and such that

$$E_i^{n+1} \in f(u_i^{n+1}) \tag{17}.$$

Note that, in Eqn(15) the matrix $\underline{A}$ is the finite difference approximation to the Laplacian operator. Also note that the values of $\theta = 0$, $1/2$, and 1 , correspond, respectively to the explicit, Crank–Nicolson and implicit time discretizations. In particular, the explicit scheme has been found to be stable and convergent to the weak solution as long as the stability restriction

$$\alpha \, \Delta t / (\Delta x)^2 \leq 1/2 \tag{18}$$

is satisfied. The stability constraint, however, may lead to prohibitively small time steps when using fine grids. In this circumstances the added complexity of an implicit scheme may be warranted. Elliott and Ockendon have proposed a successive overrelaxation algorithm for the solution of the equations resulting from the implicit scheme and they have proved that their method is stable and convergent. The main reason for the adoption of the explicit scheme in this work was, however, the simplicity of its implementation.

c) Weak solutions for alloy solidification problems. Most materials of metallurgical interest are alloys and it is indeed fortunate that the enthalpy method can be readily extended to deal with alloy solidification problems. Since alloys do not solidify at a fixed temperature but along a melting range, the enthalpy-temperature curves for alloys do not show the jump characteristic of pure substances (see Fig(2)). The explicit finite difference scheme of the weak formulation for the alloy solidification problem is,

$$\underline{E}^{n+1} = \underline{E}^n - \underline{A}\,\underline{u}^n \tag{19}$$

with

$$u_i^{n+1} = \begin{cases} \alpha(E_i^{n+1} - E_f) + u_L & , \text{ for } E_i^{n+1} > E_f \\ (E_i^{n+1}/E_f)(u_L - u_S) + u_S & , \quad 0 \leq E_i^{n+1} \leq E_f \\ \alpha E_i^{n+1} + u_S & , \qquad E_i^{n+1} < 0 \end{cases}$$

$$\tag{20}$$

In this set of equations, however, one usually uses $u_i = K\,u_i$.

The computational procedure is as follows: Eqn(19) is used first to calculate $\underline{E}^{n+1}$ in the entire domain, then, Eqn(20) permits the calculation of the temperature field $\underline{u}^{n+1}$. This algorithm is stable and converges to the weak solution of the original problem as long as the stability constraint given by Eqn(18) is satisfied.

It must be said, however, that the alloy solidification problem also requires the calculation of the solute distribution resulting

E

u_f

u

(a)

E

u_S u_L

u
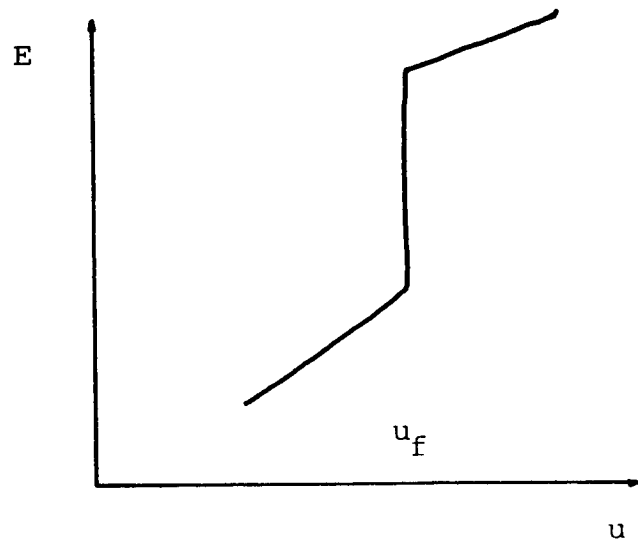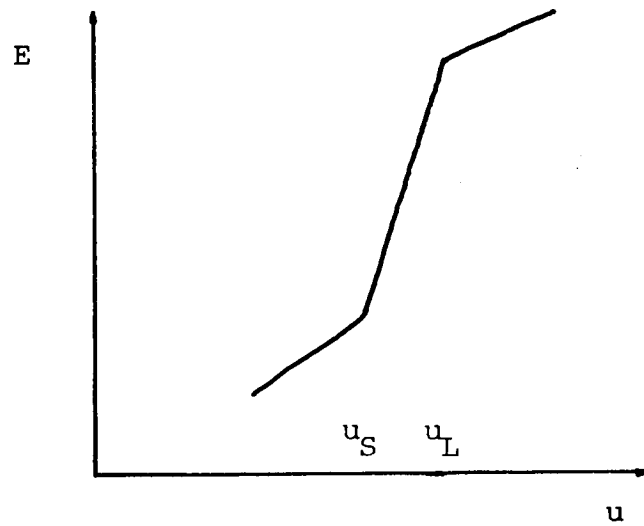
(b)

Fig (3A.2.2).- Schematic comparison of the enthalpy-temperature

curves for the cases of (a) a pure substance, and (b) an alloy.

190

from the difference in solubility of the impurity in the solid and liquid phases. Thus, a species transport problem has to be solved simultaneously with the heat equation. So besides solving Eqns(19) and (20) one also has to solve (see Sec(3A.1) and also Wilson et al (1984)),

$$\partial c_i / \partial t + (\nabla c_i) \cdot \underline{v} = \text{div}(D \text{ grad } c_i) + r_c \qquad (21)$$

$$i = s, 1$$

where c_i is the concentration of solute in the solid or liquid phases for the particular case of a binary alloy system. Moreover, a "jump" condition, analogous to the Stefan condition for heat transfer, must also be considered in the solution of the mass transfer problem, i.e.,

$$(C(F^-) - C(F^+))(\partial F / \partial t) = (D \text{ grad } C)_1^s \cdot \text{ grad } F$$

$$(22).$$

Furthermore, since the heat and mass transfer problems are coupled, one usually assumes thermodynamic equilibrium at the solidification interface, i.e.,

$$u(t, F^-) = u(t, F^+) = m_S C(t, F^-) + u_A$$

$$= m_L C(t, F^+) + u_A \qquad (23)$$

where u_A is the melting point of the pure solvent.

Wilson et al. have reformulated the alloy solidification problem in terms of weak solutions in an analogous way to the enthalpy formulation of the Stefan problem. They claim good results from the use of an explicit finite difference scheme to solve the coupled heat and mass transfer problem.

d) Solidification in the presence of fluid motion. This problem has been the subject of continued research for at least the last 30 years. The peculiar effects of fluid flow on the solidified material were recognized early on (e.g. Flemings(1956) and Roth and Schippers(1956)). The role of fluid motion in the dissipation of the melt superheat was also noticed (Adenis et al(1962)). Sahm(1982) has presented a comprehensive survey of the metallurgical effects of fluid motion during solidification.

The mathematical problem of phase change with fluid motion involves the solution of the fluid flow equations together with the energy balance incorporating a convective term. This is not a straightforward problem since the indetermination in the location of the solidification interface makes the flow problem into a non linear boundary value problem with unspecified boundaries. Thus, although the existence of a weak solution to the Stefan problem with convection due to Stokes' flow has been mathematically proved (Cannon et al(1983)), the actual numerical solution of specific problems is still the subject of active research. Most treatments to date have circounvented the flow problem.

192

Typically, a heat transfer coefficient is introduced at the phase change surface to account for the fluid motion (Larreq et al(1978)). Among the few reports of rigurous solutions most apply to simple geometries. Sparrow et al(1977) used a front tracking method to model melting inside a narrow cavity with natural convection. White(1982) used a fixed domain method to solve a somewhat similar problem. O'Neill(1983) and Argyris et al(1984) have used finite element analysis to model melting with fluid flow in cavities. Oreper and Szekely(1984) used a hopscotch fixed domain algorithm to describe melting and electromagnetic stirring inside welding pools.

Since the additional non linearities introduced by the flow equations will most likely complicate the solution of the Stefan problem, simplified versions of the general problem can be expected to be more easily solved. For example, the calculations by Miyazawa and Szekely (1979),(1981) and the ones reported in this thesis for the Stefan problem with fluid flow produced by an inertialess fluid, are a proof of this claim.

3A.3.- The Solution to the Fluid Flow Equations for the PFMS System.

For the schematic PFMS puddle shown in Fig(3.3.1.2) (and photographed in Plate(3.3.1.1)), the governing equations for fluid flow at steady state are;

the equation of motion

$$\mu \, d^2 V_x/dy^2 \quad = \quad dP/dx \qquad (1)$$

and the equation of continuity

$$Q \quad = \quad w \int_0^H V_x \, dy \qquad (2)$$

One can integrate Eqn(1) with respect to y for a fixed x-location to obtain an expression for V_x , i.e.

$$V_x \quad = \quad (1/2 \mu \,)(dP/dx) \, y^2 + K_1 \, y + K_2 \qquad (3)$$

Where the coefficients K_1 and K_2 depend on the particular boundary conditions used.

The boundary conditions on the top surface of the puddle change after the puddle detaches itself from the nozzle lip in the downstream direction. Because of this, the regions before and after the detachment point must be treated separately.

194

a) Points before detachment. In this region the appropriate

boundary conditions are:

i) the no-slip condition at the puddle nozzle interface, i.e.,

$$V_x = V_y = 0 \quad \text{at} \quad y = H \quad \text{(4a)}$$

and (ii) the continuity of velocity at the solidification

interface, i.e.,

$$V_x = V_{I_x} \;,\quad V_y = V_{I_y} \quad \text{on} \quad y = y_s \quad \text{(4b)}$$

where $\underline{V}_I$ is the (Eulerian) velocity of the interface.

Substitution of Eqns(4) into (3) and rearrangement leads to

$$V_x = A_o + A_1 y + A_2 y^2 \quad \text{(5a)}$$

where

$$A_o = (1/2\mu)(dP/dx) H y_s - V_{I_x}/((y_s/H) - 1) \quad \text{(5b)}$$

$$A_1 = V_{I_x}/(y_s - H) - (1/2\mu)(dP/dx)(y_s + H) \quad \text{(5c)}$$

and

$$A_2 = (1/2\mu)(dP/dx) \quad \text{(5d)}$$

We can readily see that the specification of five quantities, V_{I_x}, H, μ, dP/dx, and y_s allows the calculation of the velocity field. V_{I_x} ($\cong V_{r_x}$) and H ($\cong H_o$) are usually input data whereas y_s can be calculated from any of several solidification heat transfer models. dP/dx, on the other hand, has to be computed such that it satisfies the equation of continuity . At any given downstream location x, the total mass flow rate crossing through the entire puddle thickness is given by

$$Q = Q_s + Q_1 \qquad (6)$$

where Q_s and Q_1 are, respectively , the flow rates carried by the partially solidified ribbon and by the fluid film above it. Now, since the ribbon moves like a rigid body while the film is a Newtonian fluid, Q_s and Q_1 are given by,

$$Q_s = w \int_0^{y_s} V_{r_x} \, dy \qquad (7a)$$

and

$$Q_1 = w \int_{y_s}^{H} V_x \, dy \qquad (7b)$$

Performing the integrations of Eqn(7) and combining the result with Eqns(5) and (6) gives,

$$Q/w = V_{r_x} y_s + V_{r_x}/2(H - y_s) +$$

$$- (1/2\mu)(dP/dx)(H^3/6)(1 - 3(y_s/H) + 3(y_s/H)^2 - (y_s/H)^3) \quad (8)$$

whence

$$dP/dx = 12\mu \frac{(V_{r_x}/2(H - y_s)) + V_{r_x} y_s - Q/w}{H^3 (1 - 3(y_s/H) + 3(y_s/H)^2 - (y_s/H)^3)} \quad (9)$$

As expected, in the absence of solidification, Eqn(9) reduces
to the well known one dimensional form of Reynolds' equation of
lubrication theory (see e.g. Szekely(1979),p.115).

Equations (5) and (9) allow us to compute the velocity field
once the process parameters and the solidified thickness are
known.

Sometimes it is useful to present the results of flow calcu-
lations in terms of the stream function rather than the velocity.
A normalized stream function can be defined for our system as,

$$\psi = (w/Q) \int_0^y V_x \, dy \quad (10)$$

Substitution of Eqn(5) into (10) gives,

$$\psi = w (V_{r_x} y_s + (A_2/3)(y^3 - y_s^3) + (A_1/2)(y^2 - y_s^2) +$$

$$+ A_o(y - y_s))/ Q \quad (11)$$

b) Points after detachment. After detachment the no slip condition can not be applied to the top surface of the puddle. This is so because the fluid particles on this melt-gas interface are much more mobile than those on the melt-nozzle interface. For this case the proper boundary conditions are then, (see Sec(3A.1))

$$dV_x/dy = 0 \quad \text{on} \quad y = H \quad (12a)$$

and

$$V_x = V_{I_x} = V_{r_x} \quad \text{on} \quad y = y_s \quad (12b)$$

Equation (12a) simply represents the continuity of shear force across the melt-gas interface while Eqn(12b) is again the no slip condition applied to the solidification interface.

It must be noted that the precise location of the melt-gas interface (the free surface) is not known in advance but must be calculated simultaneously with the velocity. The calculation of H after detachment requires the consideration of the capillary effects due to the surface tension of the melt and the details are described in Sec(c) below. For the time being, we shall assume that such calculation has already been performed and that the function H(x) is known. Under these circumstances, the combination of Eqns(12) with Eqn(3) gives,

$$V_x = A_o + A_1 y + A_2 y^2 \quad (13a)$$

where

$$A_o = V_{r_x} - (1/2\mu)(dP/dx)(y_s^2 - 2y_sH) \tag{13b}$$

$$A_1 = -(1/2\mu)(dP/dx)(2H) \tag{13c}$$

and

$$A_2 = (1/2\mu)(dP/dx) \tag{13d}$$

Apart from the fact that the value of $H(x)$ must be obtained from a separate calculation, Eqns(13) are analogous to Eqn(5) for points upstream.

Since Eqns(6) and (7) are still valid after detachment, they can now be combined with Eqn(13) to obtain,

$$Q/w = V_{r_x} y_s + V_{r_x}(H - y_s) - (1/2\mu)(dP/dx)(2H^3/3)*$$

$$*(1 - 3(y_s/H) + 3(y_s/H)^2 - (y_s/H)^3) \tag{14}$$

and

$$dP/dx = 3\mu \frac{V_{r_x}(H - y_s) + V_{r_x} y_s - Q/w}{H^3(1 - 3(y_s/H) + 3(y_s/H)^2 - (y_s/H)^3)} \tag{15}$$

The corresponding expression for the stream function can now be derived. This turns out to be identical to Eqn(11) except that the coefficients A_o, A_1, and A_2 are now given by Eqns(13).

199

c) Calculation of the meniscus shape. The region around the free surface can be considered as constituted by three parts, namely (i) the melt, (ii) the gas phase, and (iii) the interface between them. In such a system the changes in free energy are related to the changes in the volume of the bulk phases as well as to the changes in the surface area of the interface. Denoting the free energy change by dF, we have that

$$dF = -\int (P_1 - P_2)\, dA\, dH_1 - \int \sigma\, (d^2H_1/dx^2)\, dA\, dH_1 \qquad (16)$$

Here, P_1 and P_2 are the pressures inside the bulk phases and dA is an element of area of the interface. For equilibrium, the free energy is a minimum, i.e. $dF = 0$, thus

$$P_1 - P_2 = -\sigma\, (d^2H_1/dx^2) \qquad (17)$$

The difference in pressure between two contiguous phases separated by an interface with surface tension σ is an important quantity in capillary hydrodynamics called the capillary pressure P_σ, i.e.

$$P_\sigma = -\sigma\, (d^2H_1/dx^2) \qquad (18)$$

As described in Sec(3A.1), the equation of motion for the thin film of melt contained between the meniscus and the solidification

200

interface, under the assumptions of lubrication theory, is

$$dP/dx \;=\; \mu \, d^2 V_x/dy^2 \qquad (19)$$

If the liquid layer is so thin that the pressure is essentially constant across its thickness, the substitution of Eqn(18) into Eqn(19) leads to,

$$\sigma \, (d^3 H_1/dx^3) \;+\; \mu \, (d^2 V_x/dy^2) \;=\; 0 \qquad (20)$$

Equation(20) can now be integrated with respect to y to obtain a closed form expression for V_x. This expression, in turn, can be combined with Eqns(6) and (7) above to produce an equation for the fluid film thickness H_1. This is

$$d^3 H_1/dx^3 \;-\; (3\mu/\sigma)((Q_1/wH_1^3) \;-\; V_{r_x}/H_1^2) \;=\; 0 \qquad (21)$$

Recall that here, as before, $H_1 = H - y_s$. Equation(21) is a third order non linear ordinary differential equation which can be used to compute the precise location of the meniscus. Closed form solution to Eqn(21) are known only for the asymptotic cases. Therefore, a numerical method is required to solve it for the conditions of our system. This we describe next.

To solve Eqn(21) using numerical methods we first transform it into an equivalent set of three first order equations, i.e.,

$$dH_1/dx = H_1' \tag{22a}$$

$$dH_1'/dx = H_1'' \tag{22b}$$

and

$$dH_1''/dx = (3\mu/\sigma)((Q_1/wH_1^3) - V_{r_x}/H_1^2) \tag{22c}$$

This system can be written in the abbreviated form

$$d\underline{H}_1/dx = \underline{f}(x) \tag{22d}$$

where $\underline{H}_1 = (H_1, H_1', H_1'')$ and $\underline{f}$ is the vector formed by the right hand sides of Eqns(22).

Although high order schemes may prove to be more accurate, for the calculations reported in this thesis we have used the simplest approximation method for initial value problems, namely Euler's forward method. As initial conditions for Eqn(22) we have the values of H_1, H_1', and H_1'' at the detachment point. The value of $H_1 = H_o - y_s$, depends on the solidified thickness at the point of detachment. The values of H_1' and H_1'', on the other hand, have been estimated from still frames of high speed movies of the puddle during PFMS. Our estimates, from the photos, were,

$$H_1' = -\tan\theta \qquad\qquad (23a)$$

and

$$H_1'' = 2/L_p \qquad\qquad (23b)$$

The discrete analogue of Eqn(22d) , obtained using Euler's method, is (see e.g. Dahlqvist and Björck(1974))

$$\underline{H}_1^{n+1} = \underline{H}_1^n + \Delta x\,\underline{f}(x) \qquad\qquad (24)$$

The calculation is then advanced step by step in the downstream direction. Starting from the values given by Eqns(23) , the repeated application of Eqn(24) allows the calculation of the location of the free surface. However, note that the solidified thickness must be calculated prior to solving Eqn(24) at each step to account for the solidification. It is here where the coupling between the flow problem and the solidification problem is made (see Sec(3.3.1)).

4A.1.-   A Comment on a Numerical Method for the Solution of Problems

Involving Transport Phenomena.

Introduction

When facing a problem involving transport processes it is always

advisable to look for suitable simplifying assumptions capable of

reducing the mathematical complexity of the problem. In many cases,

however, this is not possible and one must resort to numerical

methods for the solution of the governing partial differential

equations. The advent of powerful computers has contributed a great

deal to the development of the new field of numerical heat, mass,

and momentum transfer. Many procedures have been proposed to deal

with the equations of transport phenomena. Unfortunately, however,

only a few of them are in the form of commercially available,general

purpose computer programs. One of the most successful methods is

the one developed by Patankar and Spalding, among others, at the

Imperial College of London. The Patankar-Spalding (P-S) method solves

the equations of transport using implicit finite difference schemes

derived from a control volume formulation. In the next few pages we

present a brief description of some of the main features of this

method hoping to familiarize prospective users of the commercially

available version. For additional information the reader can

consult the presentations by Patankar(1980) and Spalding(1980).

The General Transport Equation

A careful look to the transport equations presented in Sec(3A.1) will reveal that they all have very much the same mathematical form. So, if instead of the physical variables velocity, temperature, and concentration we introduce the generalized transported variable ϕ , the differential balance, expressing the conservation of ϕ can be written as

$$\partial \phi / \partial t \;+\; (\nabla \phi) \cdot \underline{v} \;=\; \mathrm{div}(\Gamma \nabla \phi) \;+\; S \qquad (1)$$

where Γ is the diffusion coefficient for ϕ and S is the source term accounting for any absorption-release of ϕ inside the system.

The recognition of the mathematical similarity of the various conservation equations produces considerable simplification of the computational procedure since more or less the same method can be used to find $\underline{v}$, u, and C . It must be also recognized, however, that the solution of the fluid flow problem is more involved than that of the heat and mass transfer problems. The added complexity comes about because of three main reasons. First, the Navier-Stokes equations (Sec(3A.1)) are non linear. Second, four equations must be solved to determine the flow field, 3 for the velocity components and one for the pressure (continuity). Finally,

special techniques are required during the solution of the flow

equations to be ablo to obtain physically realistic solutions.

It is indeed fortunate that despite these complexities the P-S

algorithm retains its simplicity.

The basic idea of the numerical method is the replacement of

the governing equations by simple algebraic analogues which can

in turn be solved using a digital computer. The two main tasks are

then, first to devise a method for the derivation of the discrete

equations,and second to find a convenient method for their solution.

Discretization of the Governing Equations

To discretize the governing equations one starts by mentally

subdividing the region of interest into a number of small domains

called control volumes. The governing equations are then integrated

over the extent of such control volumes. Finally,one assumes a

local linear variation of the field variables inside every volume

element to arrive at the final set of algebraic equations repre-

senting the conservation principles inside the control volumes in

a discrete sense. The solution of this set of algebraic equations

is the (approximate) solution to the original problem.

Without going into details and for the sake of illustration we

now present the typical form of the resulting algebraic equations

for the control volume centered in P shown in Fig(1), as given

by Patankar for the case of unsteady two dimensional heat con-

duction with internal heat generation.
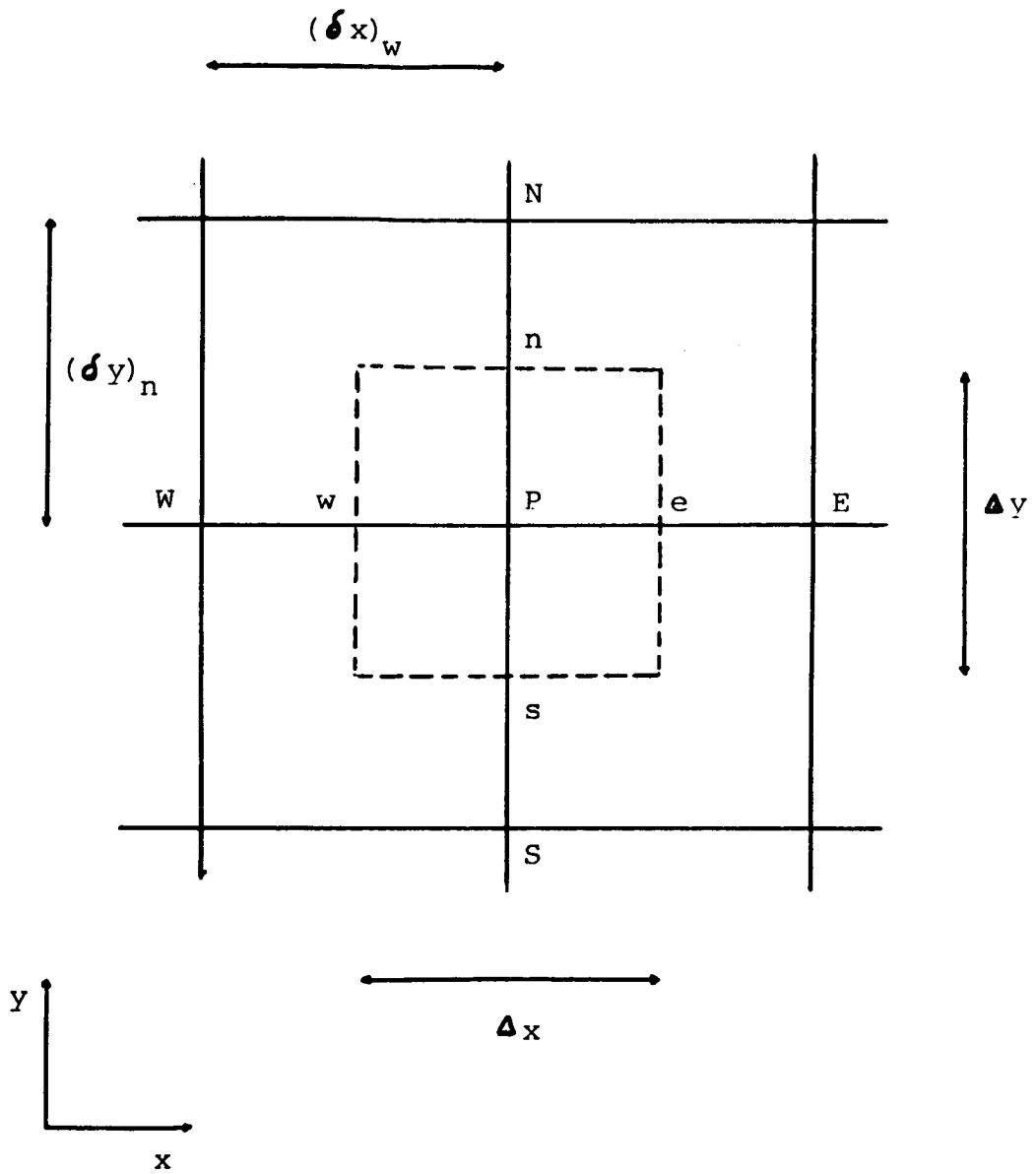
Fig (4A.1).- Control volume for the two dimensional case.

$$a_P \, u_P \; = \; a_E \, u_E \; + \; a_W \, u_W \; + \; a_N \, u_N \; + \; a_S \, u_S \; + \; b \qquad (2)$$

where

$$a_E \; = \; K_e \, \Delta y / (\delta x)_e \quad , \quad a_W \; = \; K_w \, \Delta y / (\delta x)_w \qquad (2a,b)$$

$$a_N \; = \; K_n \, \Delta x / (\delta y)_n \quad , \quad a_S \; = \; K_s \, \Delta x / (\delta y)_s \qquad (2c,d)$$

$$a_P^o \; = \; \rho \, c_p \, \Delta x \, \Delta y / \Delta t \qquad (2e)$$

$$b \; = \; S_C \, \Delta x \, \Delta y \; + \; a_P^o \, u_P^o \qquad (2f)$$

and

$$a_P \; = \; a_E \; + \; a_W \; + \; a_N \; + \; a_S \; + \; a_P^o \; - \; S_P \, \Delta x \, \Delta y \qquad (2g)$$

In Eqns(2), $\Delta x \, \Delta y *1$ is the volume of the control volume and Δt the time step . Moreover, the source term has been linearized, i.e. $S = S_C + S_P \, u_P$. Note that if the domain has been divided into N control volumes, the problem at this stage consists of solving a system of N algebraic equations with N unknowns (u_i , $i = 1, \ldots, N$).

The Effect of Fluid Motion

When the field variable being transported travels by convection as well as by diffusion the discretization equations must be slightly modified to account for the fact that convective transport takes place basically in the downstream direction of the flow . This procedure is called upwinding .

208

To deal with upwinding, Patankar proposes the so called "power law" scheme based on the results of comparison of the results obtained from it with the closed form solution of the one dimensional convection-diffusion equation. It is to the credit of the P-S method that the discretization equations remain basically unchanged after the introduction of upwinding, except for some changes in the actual values of the coefficients. So, for the two dimensional convection-diffusion problem the actual coefficients are; (see also Fig(2))

$$a_E = D_e A(|Pe_e|) + [[-F_e , 0]] \tag{3a}$$

$$a_W = D_w A(|Pe_w|) + [[F_w , 0]] \tag{3b}$$

$$a_N = D_n A(|Pe_n|) + [[-F_n , 0]] \tag{3c}$$

$$a_S = D_s A(|Pe_s|) + [[F_s , 0]] \tag{3d}$$

$$a_P^o = \rho_P^o C_p \Delta x \Delta y / \Delta t \tag{3e}$$

$$b = S_C \Delta x \Delta y + a_P^o u_P^o \tag{3f}$$

$$a_P = a_E + a_W + a_N + a_S + a_P^o - S_P \Delta x \Delta y \tag{3g}$$

where
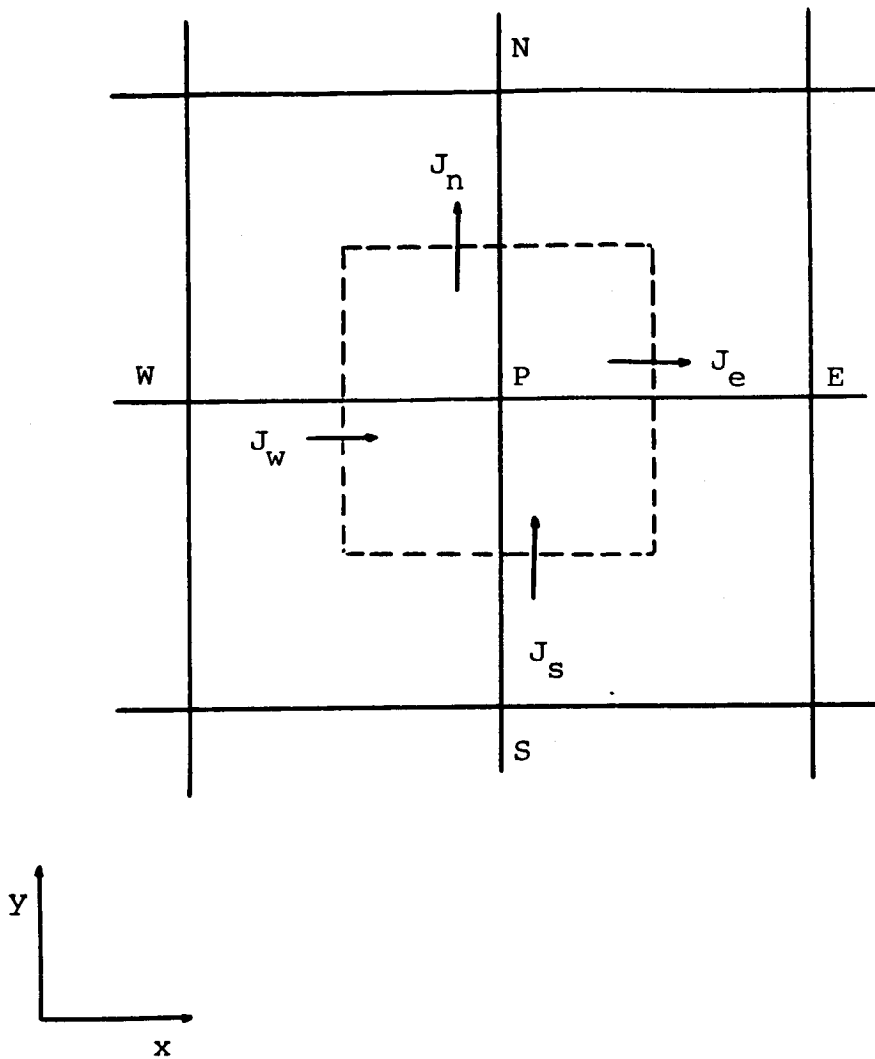
Fig (4A.<u>2</u>).- Control volume for the two dimensional case in the presence of convection. The fluxes J include both convection and diffusion.

$$D_e = K_e \Delta y / (\delta x)_e \qquad , \qquad D_w = K_w \Delta y / (\delta x)_w \qquad (3h,i)$$

$$D_n = K_n \Delta x / (\delta y)_n \qquad , \qquad D_s = K_s \Delta x / (\delta y)_s \qquad (3j,k)$$

$$A(|Pe|) = [[\ 0 \ , \ (\ 1 - 0.1|Pe| \ )^5 \ ]] \qquad (3l)$$

$$Pe_e = F_e / D_e \quad , \quad Pe_w = F_w / D_w \quad , \quad Pe_n = F_n / D_n \quad , \quad Pe_s = F_s / D_s$$

$$(3m,n,o,p)$$

and

$$F_e = (\rho v_x)_e \Delta y \qquad , \qquad F_w = (\rho v_x)_w \Delta y \qquad (3q,r)$$

$$F_n = (\rho v_y)_n \Delta x \qquad , \qquad F_s = (\rho v_y)_s \Delta x \qquad (3s,t)$$

In Eqns(3), the symbol   [[,   ]]   is a well known FORTRAN operation which simply selects the greater of the two quantities separated by the comma .

Note that even now the problem still consists of solving a system of as many equations as volume elements there are in the domain.

The Computation of the Flow Field

Many of the difficulties associated with solving the flow equations have been solved by the use of staggered grids of the type shown in Fig(3). The discrete equation for the pressure is derived by combining the discrete versions of the equations of
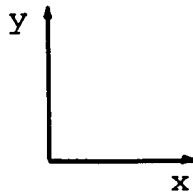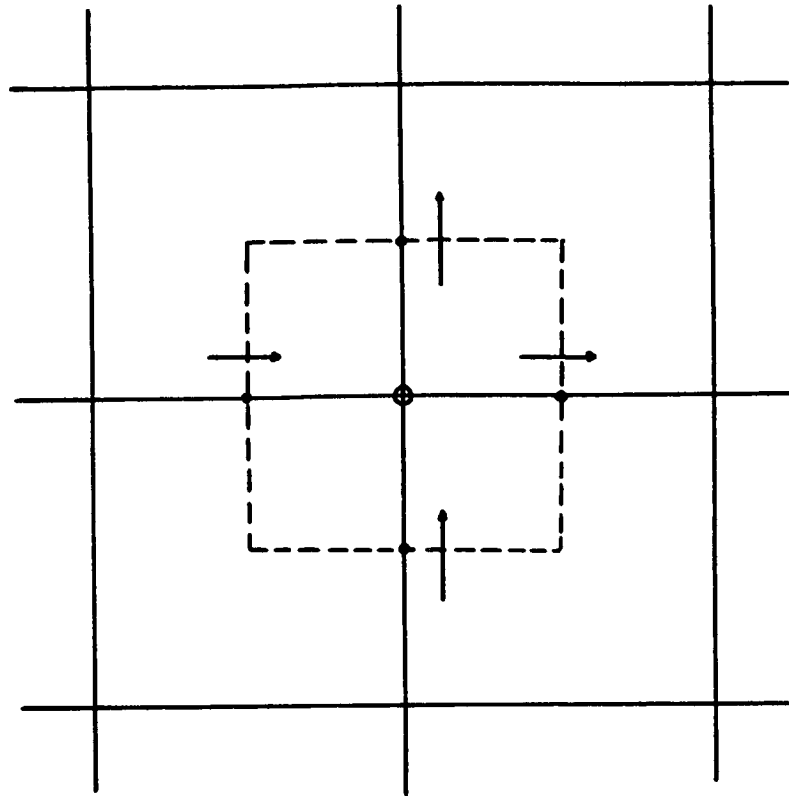
Fig (4A.$\underline{3}$).- Staggered locations for v_x and v_y. $\rightarrow$ = v_x ,

$\bullet\uparrow$ = v_y , $\bullet$ = all other variables .

continuity and motion. The resulting set of equations for the
general heat, mass, and momentum transfer problem consists of the
the following (in the case of N control volumes): (a) One set
of N equations for the pressure field, (b) three sets of   N
equations each for the three components of velocity, (c) one set
of N equations for the temperature field, and (d) as many sets
of N   equations each as chemical components there are in the
system.   In practice, many transport processes take place under
turbulent conditions and in this case additional conservation
equations (for turbulence quantities) must be introduced (from
corresponding turbulence models) to account for this. The references
given should be consulted for details in this regard.

The Solution of Systems of Algebraic Equations

From all the above it should be clear that once the discretiza-
tion procedure is finished the problem has been reduced to solving
sets of algebraic equations. These equations are not necessarily
linear. The method of solution, however, is the same regardless
of this fact. The method is a combination of direct and iterative
techniques and it is known as the Gauss-Seidel line by line
method.

In the Gauss-Seidel line by line method one starts by selecting
a direction for sweeping. Then , the equations for the grid points
lying on a line perpendicular to the sweeping direction are solved
simultaneously using a direct method (e.g. Gauss elimination). The

values used for the field variables of grid points on neighbouring lines are the latest ones available in the computer memory. Once this is done one moves forward to the next line of grid points along the sweeping direction and does the same thing. This operation is continued until the entire domain has been swept line by line. This concludes one sweep. However, since one uses guessed values for the field variables in order to start the computation, the sweeping operation must be repeated until the values of the variables stop changing appreciably from one sweep to the next. These final, converged values are considered the numerical solution of the original problem. In Sec(5.7) we have included a program constructed based on the P-S method and which is capable of computing heat transfer by conduction-convection for two dimensional situations . The flow field in this case, however, is not calculated numerically but from closed form expressions given by lubrication theory. Moreover, in Sec(5.6) we present a very simple program capable of solving systems of algebraic equations directly. This program can be used as the core of an algorithm based on the P-S method.

In practice, the need to solve many sets of equations simultaneously requires that some thought be put on the sequencing that must be followed. Patankar proposes the following series of steps as a general algorithm for the numerical solution of problems in fluid flow and heat and mass transfer:

a)   Guess the pressure field,

b)   solve the discrete Navier–Stokes equations to obtain a first estimate of the velocity field,

c)   correct the pressure by using the equation of continuity,

d)   compute again the velocities but this time use the corrected pressure,

e)   solve the discretization equations for all other field variables using the procedure described before. At the end of this step, one sweep for all field variables has been completed.

f)   Steps (b)-(e) are repeated again and again until the values of all the field variables in all the control volumes stop changing significantly from one cycle to the next.

Conclusion

The algorithm described above has been used extensively for the solution of transport phenomena problems in mechanical, chemical civil and metallurgical engineering. It offers the possibility of exploring the behavior of complicated systems with a relatively modest amount of effort. Instead of constructing his/her own program following the ideas presented above and described in detail in Patankar, the reader may choose to use the more convenient, commercially available versions. An improved understanding of RSP systems can be expected from the use of these ideas.

REFERENCES

Compendia on Rapid Solidification

Ashbrook, R.L. (ed); Rapid Solidification Technology Source Book, American Society for Metals, Ohio, 1983.

Beck, H. and H.J. Guntherodt (eds): Glassy Metals II , Springer-Verlag, Berlin, 1983.

Berkowitz, J. and R.O. Scattergood (eds): Chemistry and Physics of Rapidly Solidified Materials, TMS-AIME, New York, 1983.

Brela ; First International Conference on Metastable Metallic Alloys, in Fizika, 2(2)(1970).

Cantor, B. (ed); Rapidly Quenched Metals III, 2 Vols., The Metals Society, London, 1978.

Gilman, J.J. and H.J. Leamy (eds); Metallic Glasses, American Society of Metals, Ohio, 1978.

Grant, N.J. and B.C. Giessen (eds); Rapidly Quenched Metals II, MIT Press, Cambridge, 1976. Part 2 in Materials Science and Engineering, 23(2/3)(1976).

Güntherodt, H.-J. and H. Beck (eds); Glassy Metals I , Springer-Verlag, Berlin, 1981.

Hargitai, C. et al. (eds); Metallic Glasses: Science and Technology Kultura, Budapest, 1980.

Herman, H. (ed); Ultrarapid Quenching of Liquid Alloys, Academic Press, New York, 1981.

International Journal of Rapid Solidification, AB Academic Publishers U.K., 1985.

Jones, H. ; Rapid Solidification of Metals and Alloys, The Institution of Metallurgists, London, 1982.

Kear, B.H. et al. (eds); Rapidly Solidified Amorphous and Crystal-line Alloys, North-Holland, New York, 1982.

Kear, B.H. and B.C. Giessen (eds); Rapidly Solidified Metastable Materials, North-Holland, New York, 1984.

Liquid and Amorphous Metals; J. Physique, 41, Suppl. 8, (1980).

Masumoto, T. and K. Suzuki (eds); Rapidly Quenched Metals IV , 2 Vols., The Japan Institute of Metals, Sendai, 1982.

Mehrabian, R. et al. (eds); Rapid Solidification Processing I, Claitor's Publishing Division, Baton Rouge, 1978.

Mehrabian, R. et al. (eds); Rapid Solidification Processing II, Claitor's Publishing Division, Baton Rouge, 1980.

Mehrabian, R. (ed); Rapid Solidification Processing III, National Bureau of Standards, Washington, D.C., 1982.

Mottern, J. and W. Privott (eds); Spinning Wire from Molten Metal, AIChE Symp. Ser. No 180 , American Institute of Chemical Engineers, New York, 1978.

Murty, Y. and F. Mollard (eds); Continuous Casting of Small Cross Sections, TMS-AIME, New York, 1980.

Steeb, S. and H. Warlimont (eds); Rapidly Quenched Metals V , North-Holland, Amsterdam, 1985.

Suryanarayana, C.; Rapidly Quenched Metals: A Bibliography 1973-1979, IFI-Plenum, New York, 1980.

Tohoku University ; Structure and Properties of Amorphous Metals, Suppl. to Sci. Rep. Research Institute, Ser A, Tohoku, 1978.

General References

Adenis, J.P. et al.; J. Institute of Metals, 91(1962/3) 395-403.

Aldinger, F. et al., in Hausner,H.H. and P.V. Taubenblat (eds); Modern Developments in Powder Metallurgy, Vol 9, Metal Powder Industries Federation, Princeton, 1977, p. 141-151.

Ames, W.F.; Numerical Methods for Partial Differential Equations, 2nd ed., Academic Press, New York, 1977.

Anno, J.N.; The Mechanics of Liquid Jets, Lexington Books, Lexington 1977.

Anthony, T.R. and H.E. Cline; J. Appl. Phys., 48(9)(1977) 3888-94.

Anthony, T.R. and H.E. Cline; J. Appl. Phys., 49(2)(1978) 829-37.

Anthony, T.R. and H.E. Cline; J. Appl. Phys., 50(1)(1979) 245-54.

Apelian, D. et al.; International Metals Reviews, 28(5)(1983) 271-94.

Argyris, J.H. et al.; Computer Methods in Applied Mechanics and Engineering, 45(1984) 3-55.

Ashdown, C.; PhD Thesis, MIT, Cambridge, 1984.

Atthey, D.R., in Ockendon, J.R. and W.R. Hodgkins (eds); Moving Boundary Problems in Heat Flow and Diffusion, Clarendon, Oxford, 1975, p. 182-91.

Bass, M. (ed); Laser Materials Processing, North-Holland, Amsterdam, 1983.

Batchelor, G.K.; An Introduction to Fluid Dynamics, Cambridge U.P., Cambridge, 1967.

Beddow, J.K.; The Production of Metal Powders by Atomization, Heyden, London, 1978.

Billington, E.W. and A. Tate; The Physics of Deformation and Flow, McGraw Hill, New York, 1981.

Bird, R.B. et al.; Transport Phenomena, John Wiley & Sons, New York, 1960.

Bletry, J.; J. Phys., D: Appl. Phys., 6(1973) 256-75.

Boswell, P.G.; Metals Forum, 2(1)(1979) 40-54.

Bradley, D.; J. Phys., D: Appl. Phys., 6(1973) 2267-72.

Breinan, E.M. and B.H. Kear, in Bass, M. (ed), loc. cit..

Brody, H.D. and D. Apelian (eds); Modeling of Casting and Welding Processes, TMS-AIME, New York, 1982.

Cahn, J. et al. , in White, C.W. and P.S. Peercy (eds); Laser and Electron Beam Processing of Materials, Academic Press, New York, 1980, p. 89 .

Cannon, J.R. et al.; Comm. in Partial Differential Equations, 8(14) (1983) 1549-1604.

Carbonara, R.S. et al., in Masumoto, T. and K. Suzuki, loc. cit..

Carslaw, H.S and J.C. Jaeger; Conduction of Heat in Solids, 2nd ed., Clarendon, Oxford, 1959.

Champagne, B. and R. Angers; Powder Metallurgy International, $\underline{16}$ (3) (1984) 125-8.

Chan, C. et al., in Chen, M. et al. (eds); Transport Phenomena in Materials Processing, American Society of Mechanical Engineers, New York, 1983, 71-79.

Charter, S.J.B. et al.; J. Mater. Sci. (Lett.), $\underline{15}$(1980) 2658.

Chen, H.S and C.E. Miller; Mat. Res. Bull., $\underline{11}$(1976) 49-54.

Chen, H.S.; Rep. Prog. Phys., $\underline{43}$(1980) 353-432.

Chu, M.G.; PhD Thesis, MIT, Cambridge, 1983.

Clyne, T.W.; Metallurgical Transactions, $\underline{15B}$ (1984) 369-81.

Coriell, S.R. and R.F. Sekerka, in Mehrabian, R. et al(eds),(1980) loc. cit..

Crank, J.; The Mathematics of Diffusion, 2nd ed., Clarendon, Oxford 1975.

Crank, J.; Free and Moving Boundary Problems, Clarendon, Oxford, 1984.

Crowley, A.B.; IMA Journal of Applied Mathematics, $\underline{30}$(1983) 173-89.

Crowley, A.B.; Paper presented at the meeting on Problèmes a Frontières Libres, Maubuisson-Carcans, France, June 1984.

Dahlqvist, G. and Å. Bjorck; Numerical Methods, Prentice Hall, Englewood Cliffs, New Jersey, 1974.

Dantzig, J.A. and S.H. Davis; Materials Science and Engineering, $\underline{32}$ (1978) 199-209.

Dantzig, J.A. and J.T. Berry (eds); Modeling of Casting and Welding Processes II, TMS-AIME, New York, 1984.

Daugherty, T.S.; Journal of Metals, October 1964, 827-30.

Davies, H.A.; Physics and Chemistry of Glasses, $\underline{17}$(5)(1976) 159-73.

Davies, H.A.,in Cantor, B. (ed),(1978), loc. cit., p. 1-21.

Davies, H.A., in Mehrabian, R. et al. (eds)(1980), loc. cit., 153-64.

Davies, V. de L. and O. Westby; British Foundryman, 67(1974) 259.

den Decker, P. and A. Drevers, in Hargitai, C. et al.(eds), (1980),
loc. cit., p. 181.

· Domalavage, P.; PhD Thesis, MIT, Cambridge, 1980.

Dombrowski, N. and W.R. Johns; Chemical Engineering Science, 18
(1963), 203-14.

Dussan, E.B.V.; Ann. Rev. Fluid Mech., 11(1979) 371-400.

Duwez, P. and R.H. Willens; Transactions of the Metallurgical
Society of AIME, 227(1963) 362-65.

Elliott, C.M. and J.R. Ockendon; Weak and Variational Methods for
Moving Boundary Problems, Pitman, Boston, 1982.

El-Kaddah, N. et al., in Berkowitz, B.J. and R. Scattergood (eds),
(1983), loc. cit., p. 243-59.

Ettouney, H.M. and R.A. Brown; Journal of Computational Physics,
49(1983) 118-50.

Fiedler, H. et al.; Journal of Materials Science, 19(1984) 3229-35.

Flemings, M.C.; Solidification Processing, Mc Graw Hill, New York,
1974.

Flemings, M.C. et al.; Trans. AFS, 64(1956) 636-9.

Flemings, M.C., in Tien, J.K. and J.F. Elliott (eds); Metallurgical
Treatises, TMS-AIME, New York, 1981, p. 291.

Frost, H.J. and M.F. Ashby; Deformation Mechanism Maps, Pergamon,
Oxford, 1982.

Gill, W.N. et al.; Journal of Crystal Growth, 66(1984) 351-68.

Glickstein, M.R. et al., in Mehrabian, R. et al (eds)(1978), loc. cit.
p.46.

Grant, N.J.; Journal of Metals, 35(1)(1983) 20-27.

Grant, N.J., Rapid Solidification Science and Technology, Subject
3.70, MIT, Spring 1983 .

Hamrock, B.J. and D. Dowson; Ball Bearing Lubrication, John Wiley & Sons, New York, 1981.

Hildebrand, F.B.; Advanced Calculus for Applications, 2nd ed., Prentice Hall, Englewood Cliffs , New Jersey, 1976.

Hills, A.W.D.; Journal of the Iron and Steel Institute, 203(1965), 18-26.

Hinesley, C.P. and J.G. Morris; Metallurgical Transactions, 1(1970) 1476-8.

Hinze, J.O.; AIChE Journal, 1(3)(1955) 289-95.

Hirth, J.P.; Metallurgical Transactions, 9A(1978) 401-4.

Hocking, L.M.; Q. Jl. Mech. Appl. Math., 36(1)(1983) 55-69.

Hodkin, D.J. et al.; Powder Metallurgy, 16(32) (1973) 277-313.

Hsu, C.F. et al.; Int. J. Heat Mass Transfer, 24(8)(1981) 1335-43.

Huang, S.C. and H.C. Fiedler; Materials Science and Engineering, 51 (1981) 39-46.

Huang, S.C. and H.C. Fiedler; Metallurgical Transactions, 12A (1981) 1107-12.

Hubert, J.C. et al.; Z. Metallkde., 64(2)(1973) 835-43.

Jansen, C.H.; PhD Thesis, MIT, Cambridge, 1971.

Jech, R.W. et al.; Journal of Metals, 36(4)(1984) 41-45.

Jones, H.; Journal of Physics, D: Applied Phys., 4(1971) 1657.

Jones, H., Journal of Materials Science, 19(1984) 1043-76.

Katgerman, III, L.; Scripta Metallurgica, 14(1980) 861-64.

Kattamis, T., in Mukherjee, K. and J. Mazumder (eds); Lasers in Metallurgy, TMS-AIME, New York, 1981, p.1 .

Kavesh, S., in Gilman, J. and H. Leamy (eds),(1978), loc. cit., p. 36-73.

Kistler, S.F. and L.E. Scriven; International Journal for Numerical Methods in Fluids, 4(1984) 207-29.

Larrecq, M. et al.; Revue de Métallurgie, Juin 1978, 337-52.

Lawley, A.; The International Journal of Powder Metallurgy and Powder Technology, 13(3)(1977) 169-88.

Lebo, M.R.; PhD Thesis, MIT, Cambridge, 1971.

Levi, C. and R. Mehrabian; Metallurgical Transactions, 13A(1982), 221-34.

Levich, V.G.; Physicochemical Hydrodynamics, Prentice Hall, Englewood Cliffs, 1962, Ch. 7 and 12 .

Levich, V.G. and V.S. Krylov; Ann. Rev. Fluid Mech., 1(1969) 293-316.

Libera, M.R.; MS Thesis, MIT, Cambridge, 1983.

Liebermann, H.H. and C.D. Graham Jr.; IEEE Transactions on Magnetics MAG-12(6) (1976) 921-23.

Liebermann, H.H. et al.; Metallurgical Transactions, 14A(1983) 1817-23.

Liebermann, H.H. et al.; Metallurgical Transactions, 15B(1984) 155-61.

Luborsky, F.R.,(ed); Amorphous Metallic Alloys, Butterworth, London 1983.

Luikov, A.; Heat and Mass Transfer, MIR, Moscow, 1980.

Lynch, M.T.; MS Thesis, MIT, Cambridge, 1982.

Madejski, J.; Int. J. Heat Mass Transfer, 19(1976) 1009-13.

Manfre, G. et al.; Journal of Materials Science, 9(1974) 74-80.

Mawella, K.J.A.; Metal Science, 18(1984) 549-51.

Mehrabian, R.; International Metals Reviews, 27(4)(1982) 185-208.

Meyer, G.H.; Applied Mathematics and Computation, 4(1978) 283-306.

Miyazawa, K. and J. Szekely; Metallurgical Transactions, 10B(1979) 349-58.

Miyazawa, K. and J. Szekely; Metallurgical Transactions, 12A(1981) 1047-57.

Miyazawa, K. et al.; Trans. Japan Institute of Metals, 24(11)(1983) 781-88.

Murty, Y.V. and R.P.I. Adler; Journal of Materials Science, 17 (1982), 1945-54.

Narasimha, R. and J.A. Sekhar; Materials Letters, 2(5A)(1984) 407-410.

O'Neill, K., in Lewis, R.W. et al. (eds); Numerical Methods in Thermal Problems, Pineridge, Swansea, 1983, p.134.

Oreper, G. and J. Szekely; J. Fluid Mech., 147(1984) 53-79.

Patankar, S.V.; Numerical Heat Transfer and Fluid Flow, Hemisphere Washington, D.C., 1980.

Pietrokowsky, P.; Rev. Sci. Instr., 34(1963) 445-6.

Predecki, P. et al.; Trans. Met. Soc. AIME, 233(1965) 1581-6.

Predel, B.; Z. Metallkde., 69(1978) 773-6.

Pond, R.B. et al., in Hartley, C.S. et al (eds); New Trends in Materials Processing, American Society for Metals, Ohio, 1976.

Robertson, S.R. et al., in Mehrabian, R. et al. (eds)(1978)loc. cit..

Roth, W. and M. Schippers; Z. Metallkde., 47(2)(1956) 78-85.

Ruhl, R.C.; PhD Thesis, MIT, Cambridge, 1967.

Ruthardt, R. and E.G. Lierke, in Hausner, H. et al. (eds); Modern Developments in Powder Metallurgy, Vol 12, Metal Powder Industries Federation, Princeton, 1981, p. 105.

Sahm, P.R., in Zierep, J. and H. Oertel Jr. (eds); Convective Transport and Instability Phenomena, G. Braun, Karlsruhe, 1982, p. 515-56.

Savage, M.D.; J. Fluid Mech., 117(1982) 443-55.

Schlichting, H.; Boundary Layer Theory, 7th ed., Mc Graw Hill, New York, 1979.

Schmitt, H.; Powder Metallurgy International, 11(1979) 17-21,68-71.

Scott, M.G.; J. Materials Science, 9(1974) 1372.

Segal, H.; ME Thesis, MIT, Cambridge, 1983.

Shepelsky, N.V. and V.Z. Zhilkin; Poroshkovaya Metallurgiya, 82 (10)(1969) 44-51.

Singer, A.R.E. et al.; Powder Metallurgy, 23(2)(1980) 81-5.

Singer, A.R.E. and R.W. Evans; Metals Technology, 10(1983) 61-8.

Slattery, J.C.; Momentum, Energy and Mass Transfer in Continua, 2nd ed., Robert E. Krieger Pub. Co., Huntington, New York, 1981.

Sparrow, E.M. et al.; Journal of Heat Transfer, 99(1977) 520-26.

Speck, J.S.; MS Thesis, MIT, Cambridge, 1985.

Strachan, R.W.; PhD Thesis, MIT, Cambridge, 1967.

Sully, L.J.D.; AFS Transactions, 84(1976) 735-44.

Szekely, J. and N.J. Themelis; Rate Phenomena in Process Metallurgy John Wiley & Sons, New York, 1971.

Szekely, J.; Fluid Flow Phenomena in Metals Processing, Academic Press, New York, 1979.

Takeshita, K. and P.H. Shingu; Trans. Japan Institute of Metals, 24(5)(1983) 293-300.

Tallmadge, J.A., in Kuhn, H.A. and A. Lawley (eds); Powder Metallurgy Processing, Academic Press, New York, 1978, p.1 .

Tayler, A.B., in Ockendon, J.R. and W.R. Hodgkins (eds); Moving Boundary Problems in Heat Flow and Diffusion, Clarendon, Oxford, 1975, p. 120.

Timsit, R.S.; Appl. Phys. Lett., 40(5)(1982) 379-81 .

Uhlmann, D.R.; J. American Ceramic Society, 66(2)(1983) 95-100 .

Vincent, J. H. et al., in Murty, Y. and F.R. Mollard (eds) (1980) loc. cit., p. 103-16.

Vincent, J.H. et al., in Masumoto, T. and K. Suzuki (eds) (1982), loc. cit. .

Vincent, J.H. and H.A. Davies, in The Metals Society ; Solidification Technology in the Foundry and Casthouse, TMS, London, 1983.

Voller, V. and M. Cross; Int. J. Heat Mass Transfer, 24(1981) 545-56.

Voller, V. and L. Shadabi; Int. Comm. Heat Mass Transfer, 11(1984) 239-49.

White, R.E.; SIAM J. Numer. Anal., 19(6)(1982) 1129-57.

White, R.E.; Mathematics of Computation, 41(164)(1983) 337-347.

White, R.E.; SIAM J. Numer. Anal., 22(2)(1985) 205-244.

Williams, C.A. and H. Jones; Materials Science and Engineering, 19(1975) 293-7.

Wilson, D.G. et al.; International Journal for Numerical Methods in Engineering, 20(1984) 1067-84.

Zielinski, P.G. and D.G. Ast; Scripta Metallurgica, 17(1983) 291-4.

1. Report No. NASA CR-179551	2. Government Accession No.	3. Recipient's Catalog No.
4. Title and Subtitle The Mathematical Modeling of Rapid Solidification Processing		5. Report Date November 1986
		6. Performing Organization Code
7. Author(s) Ernesto Gutierrez-Miravete		8. Performing Organization Report No. None
		10. Work Unit No. 505-33-62
9. Performing Organization Name and Address Massachusetts Institute of Technology Department of Materials Science and Engineering Cambridge, Massachusetts 02139		11. Contract or Grant No. NAG3-365
		13. Type of Report and Period Covered Contractor Report Final
12. Sponsoring Agency Name and Address National Aeronautics and Space Administration Lewis Research Center Cleveland, Ohio 44135		14. Sponsoring Agency Code

15. Supplementary Notes

16. Abstract

The detailed formulation of and the results obtained from a continuum mechanics-based mathematical model of the planar flow melt spinning rapid solidification system are presented and discussed. The numerical algorithm proposed is capable of computing the cooling and freezing rates as well as the fluid flow and capillary phenomena which take place inside the molten puddle formed in the PFMS process. The fundamental equations of the theory of heat transfer with change of phase and those of the theory of lubrication and capillary hydrodynamics constitute the starting point of our formulation. Our results show, for the first time, several unexpected phenomena taking place inside the puddle; namely, recirculatory flows, stagnation points and fluid film thinning. The results also point towards the strong coupling existing between the flow phenomena and the heat transfer-solidification processes in this system. Comparison with available empirical evidence verifies the correctness of our approach. Furthermore, we have also included in this report several other items which should facilitate the extension of our methods to the study of other rapid solidification processing systems. For example, although we justifiably neglected the undercooling phenomenon in our calculations of the PFMS process, this cannot be done in various other RS systems. So we have described the basic ideas required to incorporate undercooling effects into our formulation. The basic starting point in this description has also been, however, the fundamental equations of continuum mechanics. This should help to understand the comprehensiveness of our approach. We have also included a description of the basic physical phenomena which take place in the various RSP systems proposed to date. The importance of fluid dynamics and the heat transfer-solidification phenomena are demonstrated. We believe that there remain many opportunities for useful modeling work in these systems. The main result expected from our work is a better understanding of the relationships between the processing variables and the structure and properties obtained in the products of RS. Needless to say, theoretical work of the type described here and experimental research must be combined in order to reach this end more quickly. Finally, for the convenience of the reader and also for the sake of completeness we have also included, (i) the FORTRAN listings of some of our most useful computer programs and (ii) a collection of appendices describing the basic equations used for the modeling. We hope that the research reported here illustrates the potential contribution mathematical methods can make to the understanding of the complex nature of RSP systems.

17. Key Words (Suggested by Author(s)) Melts spinning; Superalloys; Rapid solidification; Coarsening	18. Distribution Statement Unclassified – unlimited STAR Category 26		
19. Security Classif. (of this report) Unclassified	20. Security Classif. (of this page) Unclassified	21. No. of pages 238	22. Price* A11

*For sale by the National Technical Information Service, Springfield, Virginia 22161